COMPACTION OF SOIL BY A VIBRATORY ROLLER:

A THEORETICAL DESCRIPTION

by

David Towery

Thesis submitted to the Graduate Faculty of the

Virginia Polytechnic Institute and State University

in partial fulfillment of the requirements for the degree of

MASTER OF SCIENCE

in

Mechanical Engineering

APPROVED:

H. H. Robertshaw, Chairman

R. G. Leonard

R. G. Mitchiner

August, 1984

Blacksburg, Virginia

ACKNOWLEDGEMENTS

The author wishes to thank Dr. R. G. Leonard and Dr. R. G. Mitchiner for serving on his Advisory Committee. A special work of thanks is owed to Dr. Ryoichiro Minai of Kyoto University for his advice concerning some of the numerical difficulties encountered here.

The author is indebted to William Patten of the Building Construction Department for his unstinting efforts to inform the current work and educate its author in some rudiments of soil mechanics. It will be obvious to the reader of this work how heavily it relies on some of Bill's ideas. Any errors of presentation or interpretation are the author's own; any credit for successful application of theory to the practical problem of compaction must go in large part to Mr. Patten's patience and good advice.

Above all, thanks are due to Dr. H. H. Robertshaw for his instruction and guidance through both the author's undergraduate and graduate years at Tech.

Among all the sources of the gratitude that the author owes his wife Miho, the most immediately relevant are the illustrations and figures she provided for his work, which is dedicated in part to her and to our son, Walter; also to my parents, who had to wait too long for its beginnings, let alone its conclusion.

Finally, the author wishes to thank Ms. Eloise Lafon for the skillful typing that graces this work, and for her patience with its many revisions.

TABLE OF CONTENTS

TABLE OF CONTENTS (continued)

LIST OF FIGURES

LIST OF FIGURES (continued)

LIST OF FIGURES (continued)

LIST OF FIGURES (continued)

1. INTRODUCTION

This study models the compaction of soil by a vibratory roller compactor and examines changes to current designs that may provide more efficient compaction. The modeling of the soil differs from previous analyses of the compaction process through the use of two analytical methods. First, whereas previous theoretical models of the compactor-soil interaction have lumped the soil properties of stiffness and damping, the current model retains the distributed-parameter characterization of the soil mass. This is accomplished through a solution of the dynamic equations of a linearly elastic half-space, coupled with the lumped-parameter dynamics of the compactor, in order to obtain the compactor motion and the field of subsurface strains in the soil. Secondly, the strains and strain rates estimated from the linear model are used as inputs for nonlinear constitutive equations for soil that have been proposed by Patten (1). These relations describe the material damping in the medium and relate a fraction of the dissipated energy to the continuous evolution of residual stresses in the soil.

The theoretical model of the compaction process is used to estimate the effects of varying the frequency of vibration to match the evolutionary changes in soil properties during compaction. The effects of varying the static pre-load through redistribution of the compactor weight is also examined.

1.1 Purposes of Compaction

The preparation of a soil bed for the construction of building foundations, roadways, airport runways, and earthen dams requires that the native stiffness and strength of the soil be augmented by artifical techniques. Stiffening and strengthening of the subgrade can be accomplished by the addition of bonding agents that affect the adhesive properties of the soil particles (2). But the most commonly used and least costly technique for improving soil qualities is compaction, where the soil is densified by mechanical loadings.

Tamped-earth construction has been used since prehistoric times from Europe to the Far East (3,4). In the 1930's, it was realized that the application of a rapidly oscillating load could provide improvements in the properties of sand comparable to those obtained by static loads (5,6). More recently, vibratory compaction has been applied with some success to moderately cohesive soils (7,8).

The objectives of compaction, whether achieved by static loading or by vibration, are the increased strength and stiffness of the soil. Secondary beneficial effects include decreases in the permeability and subsequent swelling and shrinking of the medium (9). These are the observed effects of compaction, but some controversy still attends the relative importance of several processes occurring in the soil during compaction, all of which contribute to the ultimate stiffening.

In the first place, rapid acceleration of the particles of granular soil can produce a state of free-fall wherein the particles realign

themselves in a more closely-packed arrangement (5,6,7,10). Inasmuch as the mutual adhesion of clay particles can be broken down during vibration, this purely geometric alteration of the medium can occur in cohesive soils as well an in non-cohesive ones (5,11). The densification may be enhanced by the fracturing of angular grains, allowing closer fits among the particles (2).

But the strengthening and attendant densification of the soil is by no means accomplished only through this kinematic process. Brumund and Leonards (10) and Shatlova et al. (5) cite the importance of stresses induced in the medium by its repeated working.

These stresses are associated with plastic deformation of the soil solids themselves, so that some permanent densification results. Moreover, these stresses contribute directly to the stiffening of the medium in ways that are not causally related to the attendant deformation. The elastic moduli of soil in both shear (12) and compression (13) are strongly dependent on the confining pressure. Field measurements have shown that the residual stresses induced in the soil by compaction directly augment the confining pressure (6), providing a permanent stiffening.

The success of compaction is typically estimated by the increase in the soil density, or equivalently, in the reduction of air and water voids as a percentage of the total soil volume. But as Selig (9) points out, the objectives of compaction are stiffening and strengthening of the soil. Although densification is apparently correlated with these

and happens to be easier to measure, the correspondence is not exact and reference to density alone can be misleading.

The strength of the model proposed herein is that it directly predicts the increase in soil stiffness associated with the production of residual stress. Direct integration of the constitutive equations proposed by Patten (1) can predict both cumulative deformation and stress. At present, however, such an integration is feasible only for a lumped-parameter model of the soil. For reasons that will be made clear, the problem of a rolling compactor requires that the distributed-parameter characterization of the soil be retained. To this end, a linear model of the soil continuum that fails to predict permanent settlement is used in this study to estimate the displacement and strain amplitudes, so that ultimately only the residual stresses and not the geometric effects of compaction are obtained. We note again, however, that the ultimate aim of compaction is the enhancement of the soil's mechanical properties and not its densification.

1.2 Compactors

The dynamic loading for compactors is usually generated by rotating an eccentrically-mounted weight in a vertical plane, so that the vertical component of the centrifugal force varies sinusoidally with time (Fig. 1-1):

$$F_a(t) = m\, e\, \omega^2 \sin \omega t \qquad (1.1)$$

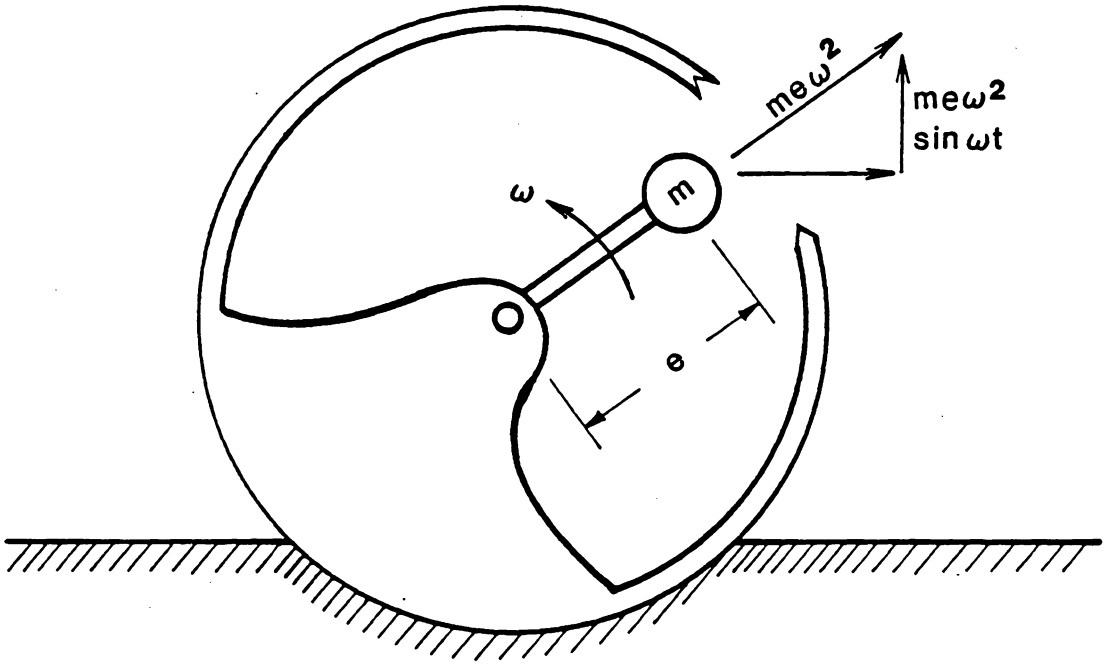

Fig. 1-1. Generation of a harmonic force by rotation of an eccentrically-mounted mass.

where

F_a is the generated force,

m is the mass of the eccentric,

e is the distance of the eccentric's center of mass from the axis of rotation

ω is the circular frequency of rotation.

This force is transmitted to a flat plate or a cylindrical drum resting on the earth.

The force transmitted from the compactor to the soil may be either smaller or larger than the generated force, depending on the frequency of excitation, the inertial and suspension properties of the compactor, and the stiffness of the soil. At some resonant frequency, the contact force will be maximized. This frequency has been taken by numerous authors (5,6,10,11,14) to be the optimal frequency of compaction, since it maximizes the energy transmitted to the soil. It is important to note that the resonant frequency is a property of the coupled dynamics of the compactor-soil system and is not an innate property of the soil alone. Thus, variations in compactor design can alter the location of the resonance peak.

The amplitude of the drum motion is also maximized at resonance. Depending on all of the factors mentioned above, and in addition on the relative magnitudes of the dynamic force and the static weight of the

compactor, the drum may (6) or may not (14) rise clear of the soil during compaction at resonance. The assumption made in this study is that contact is maintained over a cycle. It is argued in Section 5 that the violation of this hypothesis should not compromise the model's predictions of the amplitudes of the drum motion and soil strains.

The compactor modelled herein is the Ingersoll-Rand SP-56DD, a 20,700 lb (9387 kg) smooth-drum compactor with specifications given in Table A-1 and Fig. 3-1. The eccentric is driven by a hydrostatic motor at speeds of up to 30.4 Hz. The drum is connected to the yoke by 12 rubber vibration isolators loaded in shear. Large compactors are classed according to gross weight, but the distribution of weight over the frame is a design decision. Optimizing such a distribution with respect to compaction performance is therefore one object of this study.

1.3 Description of the Problem

Yoo and Selig (14) have noted that the interaction of a stationary compactor and the soil beneath it is quite different from the dynamics of a compactor travelling over the soil. Conceptually, the difference between the two processes resembles the distinction made in the study of heat-transfer and fluid-flow problems between "system" and "control volume" descriptions. In the first instance, one studies the evolution of the properties of some fixed quantity of matter. The soil beneath a stationary compactor may be compared to, say, the vapor in the cylinder of a reciprocating engine during a power or compression stroke (Fig. 1-

2(a)), in that the identity of the material being studied is fixed during the analysis.

By contrast, in the steady-state, steady-flow control-volume problem, a region of space through which the matter flows is analyzed. The identity of the matter inside the volume constantly changes, and so do the properties of an element of the material as it passes through the control volume. But the properties of the material entering or exiting the control volume remain unchanged over time. If we attach our control volume to the moving drum of the compactor, we note that the soil "entering" the volume always has the properties of the uncompacted medium, whereas the "exiting" soil has the properties of compacted earth. The analogy made in Fig. 1-2(b)) is to the flow of a gas through a compressor.

The behavior of the stationary compactor is thus obtained by integrating its transient response over time, as the compactor settles into the earth and the properties of the soil beneath it change with time. By contrast, the dynamics of the travelling compactor are characterized by their steady-state nature, with the compactor always acting upon a soil mass of unchanging properties -- loose and pliant at the leading edge of the contact area, dense and resilient at the trailing edge. The variation of soil properties experienced by the travelling compactor is therefore spatial rather than temporal, even though the physical processes occurring in the soil beneath it are identical to those experienced by the soil beneath the stationary compactor.

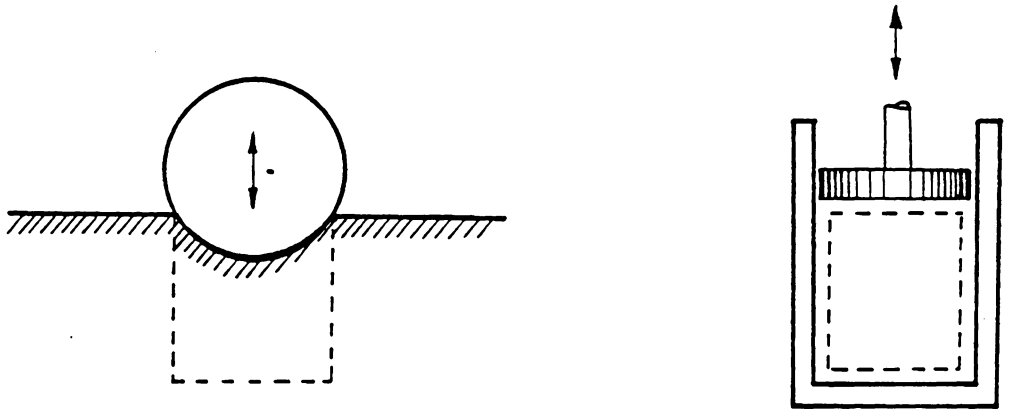

(a)

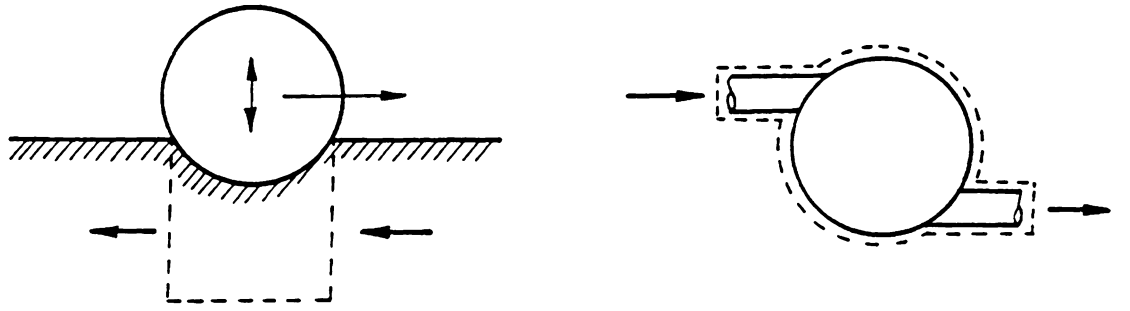

(b)

Fig. 1-2. System vs. control volume approaches to modelling vibratory compaction.

The instantaneous distribution of soil properties beneath the rolling compactor depicts soil elements in all stages of compaction and therefore illustrates the stress history that any particular soil element will undergo. The evolution of residual stresses and permanent settlement in soil is determined precisely by the stress history, i.e., the soil has a "memory" (13). In tracing the stress history of soil elements subjected to rolling compaction, we must therefore consider the spatial modulation of the stress field through which the element "moves." The steady-state characterization of the rolling compactor affords some theoretical simplification in treating the time dependence, but only at the cost of requiring that the spatial distribution of the soil properties be retained in the model. Previous studies (11,14) that have applied a lumped-parameter analysis to the moving compactor have been able to predict only the compactor dynamics, with no treatment of the evolution of the soil properties with time.

1.4 Overview of the Solution Method

The following steps are taken in modeling the soil and compactor:

(a) The compactor is treated as a two-degree of freedom lumped-parameter system: an effective frame inertia coupled to a drum inertia by a linear spring and a linear hysteretic damper (Section 3).

(b) The underlying soil is first treated as a conservative, linearly elastic, semi-infinite solid ("elastic half-space") acted on by a load distributed over a constant area and varying sinusoidally with

time (Section 4). This simplified treatment permits a solution for the coupled compactor-soil dynamics, as well as affording an estimate of the distribution of strains in the underlying soil (Section 5).

(c) The stress history of a soil element moving relative to the compactor is then traced. The elastic and plastic stresses in the soil are obtained from constitutive equations that relate the stresses to the strains and strain rates previously estimated. The effect of the accumulated stresses on the elastic moduli is then determined in terms of the growth of the soil's confining pressure, so that the alteration of soil properties for subsequent passes can be estimated.

The treatment afforded under (b) manifestly involves numerous oversimplifications of the properties of soils, each of which requires some defense. Specifically, the following simplifying (and erroneous) assumptions are made:

(1) The underlying soil mass is homogenous and its properties isotropic. The problem of compacting a shallow fill overlying a more dense layer is not accurately treated. Moreover, the inhomogeneity introduced by the compaction process itself (i.e., the difference in material properties at the leading and trailing edges) is ignored in the linear model.

(2) The soil is a conservative, continuous, linearly-elastic medium. In estimating the stran amplitudes, no cognizance is taken of material damping. The elastic half-space model does treat "geometric damping" (Section 4) which is typically the dominant mechanism of energy

dissipation in soil problems. To the extent that material damping is neglected in the linear model, the strain amplitudes are probably overestimated.

Other effects not considered under the assumptions of continuity and linear elasticity are the effects of granular rearrangement and the localized plastic failure of soil immediately beneath the drum (16).

(3) The soil and drum remain in contact over a cycle, and during a cycle the variation in contact area can be ignored by treating an "average" contact area equal to that resulting from the compactor's deadweight. More generally, the assumption is made that the drum displacement and soil strains are simple harmonic functions of time.

These assumptions, their justifications, and their attendant errors are discussed more extensively in Sections 4 and 5. A second aspect of the modeling that requires some defense is the compatibility of the constitutive relations in parts (b) and (c) above. To what extent is it meaningful to use an estimate of soil properties obtained from one set of constitutive relations (i.e., strains estimated by linear elasticity theory) in generating other properties from other relations (i.e., residual stresses obtained from the nonlinear constitutive equations)? The author freely admits the inelegance of coupling the two methods, but notes the frequency in engineering practice of just such "contradictory" patching-together of different models. In the study of fluids, for instance, one set of assumptions is invoked in treating a viscous boundary layer, while a whole other set of assumptions is introduced in

treating predominantly inviscid behavior in the region beyond the boundary layer. In Hertz's classic solution for contact stresses, apparently contradictory assumptions are invoked at different stages of the solution (17). Ultimately, the appropriateness of using the strains offered by the simpler theory rests solely on whether the estimate is a good approximation to the actual strains in the soil, regardless of whether the constitutive equations in the two stages of the solution have identical algebraic forms. In Section 4, the argument is made that the estimates of elastic strains made by the linear theory are acceptable.

1.5 Model Summary

Section 2 of this work reviews the previous efforts to model and measure soil vibrations and the compaction process. Section 3 develops the lumped-parameter model of the compactor. In Section 4 the integral equations for a linear elastic half-space are developed, and their suitability to the current problem is discussed. In Section 5, the equations describing the coupled dynamics of the soil and compactor are assembled. Section 6 introduces the nonlinear, nonconservative constitutive relations by which the growth of residual stresses in the soil is described. The results of model simulations for various frequencies and compactor weight distributions are described in Section 7, together with a proposed optimization strategy for varying the compactor frequency with each successive pass of the compactor. Conclusions and recommenda-

tions are made in Section 8, both for the compaction process and for the further development of the model.

Model inputs are summarized in Appendix A and numerical methods are detailed in Appendix B. A program listing showing the model implementation is given in Appendix C.

2. REVIEW OF PREVIOUS INVESTIGATIONS IN SOIL VIBRATIONS

This section reviews previous efforts to model or measure the compaction process and summarizes some of the findings in soils research that bear on the compactor problem. Some special attention is paid to the historical efforts to model the dynamics of soil as those of an elastic medium, since much of the current study is based on such a model.

2.1 Experimental Treatments of Compaction

Converse (36) was one of the earliest investigators to note the efficiency of compacting sand at resonance. Working with a circular-plate stationary vibrator, he developed empirical formulas for determining the frequency of resonance based on the compactor weight, the plate diameter, and the soil density and elastic modulus.

In 1953 Whiffin (15) sought to measure the dynamic pressures generated in silty clay by rolling compactors. Because of its cohesion, the soil was capable of sustaining tensile as well as compressive stresses during vibration. The largest stresses and densities occured at the shallowest depth of measurement (1 ft, 0.3 m). This is in contrast with observations made by other investigators working with sand, which will not support tensile stresses and which, at shallower depths, is actually loosened by vibration.

In 1957 Converse (11) measured displacement amplitudes and phase angles to determine parameters for a linear single-degree of freedom

model of the compaction process for cohesive soils. Both the measurements and the model confirmed that compaction at resonance maximizes the rate of compaction.

Lewis (8) conducted tests on several soil types using both vibratory plate and roller compactors. The greatest compaction was achieved at the soil surface, even for granular soils. Compaction of soils at resonance was found to offer some slight improvement over operation at other frequencies. For sand the resonance condition occurred at 38 Hz; for clay, at about 35 Hz. For some reason a mixture of sand and clay produced the lowest frequency of resonance, at about 32 Hz.

An exhaustive experimental study of compaction of sand using a vibratory roller was undertaken by D'Appolonia et al. (6) in 1967. Measurements of density, acceleration, and in situ stress were made at various depths in the sand for up to 50 passes by the compactors. The investigators also measured drum displacements and accelerations. Their results, in contrast to those of Lewis, showed that the greatest densification occurred at depths of 2 ft (0.6 m) for a 12.5-kip (5700 kg) drum. The acceleration measurements verified that the sand particles at this depth were in a state of free-fall for part of each cycle. At shallower depths, the sand was not compacted and was in fact somewhat loosened by the vibration. Measurements were also made of the horizontal stresses remaining in the soil following each pass of the compactor. These were noted to be substantially larger than the at-rest pressures generated by the weight of the soil column. Moreover, the

induced stresses normal to the path of the roller were far larger than the stresses parallel to the path, indicating that some anisotropy in the applied stresses was carried over in the induced state of residual stress.

Moorhouse and Baker (37) studied the compaction of a 10 ft (3 m) lift of sand and found the greatest compaction occurring at nearly 4 ft (1.2 m) below the surface. The compactor employed in this study had a drum weighing 25.5 kips (11,600 kg), twice that of the compactor used by D'Appolonia.

Brumund and Leonards (10) undertook laboratory experiments that related the settlement of vibrating sand to the energy transmitted to it by the applied dynamic force. They observed a linear relationship between settlement and transmitted energy and a logarithmic relation between densification and transmitted energy. They emphasized the importance of irrecoverable shear strains induced in the sand in accounting for the amount of subsidence.

Several studies were undertaken by Selig and Yoo in the 1970's. In 1977 (7) they introduced a simple two-degree-of-freedom model of a compactor that treated the frame and drum as lumped inertias and the soil as a lumped stiffness and viscous damper. The model and its predictions were more fully described in a later publication (14). The stiffness and damping parameters for soil were obtained from direct measurements of the compactor, rather than from elastic theory. Although such direct measurements are highly desirable for a medium as

complex as soil, the authors make the curious asertion that the elastic theory is more germaine to the problem of a vibrating foundation than to that of a moving compactor. Inasmuch as elastic theory fails to predict residual settlement, which is more marked under a stationary vibrator than a travelling one, it would seem to the author that elastic theory is more applicable for moving compactors.

2.2 Models of Soil Vibration Based on the Theory of Elasticity

Problems involving periodic loading of a semi-infinite solid can be classified by several typologies. First, there are the assumptions made about the constitutive properties of the solid, whether they are elastic or viscoelastic, isotropic or anisotropic, homogeneous or varying with depth, etc. Most of the analytical treatments to date have assumed the simplest case of a homogeneous, isotropic, linearly elastic medium, and inasmuch as that is the soil model employed in this study, the discussion below is restricted to such analyses.

A second typology by which the various works may be classified lies in the geometry of the loading. The earliest treatment by Lamb (18) in 1904 dealt with point and line loads. The distributed loading of a circular plate resting on the half-space, perhaps the most frequently considered problem, has been analyzed by Reissner (19), Sung (20), Quinlan (21), and Arnold, Bycroft, and Warren (22). All of these problems are simplified by the radial symmetry of the loading, which permits a two-dimensional (r,z) description of the spatial dependence.

In 1962, Kobori published the first results for the loading of rectangular regions (28). An expanded treatment was given by Thomson and Kobori the following year (23). The lack of radial symmetry in this problem requires that the solutions be couched in terms of double integrals with infinite limits of integration. In addition to demonstrating how such a complication can be overcome, Thomson and Kobori introduced a numerical technique for the direct evaluation of the integrals, which previously were treated by demanding and intricate contour integrations in the complex plane.

A third typology by which the various authors may be grouped is the treatment they accord to the stiffness of the plate bearing on the half-space surface, which affects the assumptions they make about the distribution of the contact stress beneath it. Reissner and Kobori both assumed a uniform distribution of the contact stress. Such a result is only obtained from uniform loading of a perfectly flexible plate. If the plate possesses flexural rigidity, the contact pressure is redistributed according to the relative stiffnesses of the plate and the underlying medium. The difficulty in solving such a problem is that it has mixed boundary conditions: on the unloaded part of the half-space surface, the stresses and tractions are specified to be zero, whereas on the loaded region the displacements are prescribed by the flexural stiffness of the plate. The transform method used to solve such a problem requires that the boundary conditions be specified as integrals over the entire surface of the half-space. The mixed conditions imposed

by plate rigidity therefore lead to a problem of dual integral equations.

In their studies of circular plates, Sung and Quinlan skirted the problem by assuming various distributions of the contact stress: uniform, parabolic, and a distribution proportional to that produced by static loading. None of these distributions accords with the actual contact pressures developed under dynamic loading, although the static distribution gives an approximation for very low frequencies.

The first direct solutions for rigid plates were made for simple geometries that afford a two-dimensional treatment of the spatial dependency. In 1965 Awojobi and Grootenhuis (29) considered the circular plate; in 1967, Karasudhi et al. solved the plane-strain problem of a rigid, infinitely long strip resting on the half-space (30). In both cases the authors were able to reduce the set of dual integral equations to a single integral amenable to evaluation by contour integration.

The more demanding problem of rigid rectangular plates required a more practical approach. Since the first solution by Elorduy, Nieto, and Szekely (31) in 1967, the favored technique for attacking non-radially symmetric geometries has been to divide the contact area into elemental regions, each of whose loads is of an assumed distribution but of unknown magnitude. Superposition is invoked, and the magnitudes of the elemental loads are adjusted to yield the correct force-displacement characteristics corresponding to the rigidity of the plate. To this end, Elorduy et al. considered approximations to the response functions

of the half-space to elemental point loads. Wong and Luco (32) obtained a superior approximation by considering rectangular elements with uniformly distributed loads, using the methods of Thomson and Kobori to obtain the elemental response functions. Such an approach is computationally quite burdensome, however, since the response function for each pair of elements is expressed as a double integral. Kitamura and Sakurai (33) introduced a low-frequency approximation for the elemental response functions that avoids integration altogether; Adeli et al. (34) took the intermediate approach of treating rectangular elements whose response functions are approximated by those of circular elements of equal area. Most recently, Whittaker has used elemental point loads to study the response of the half-space to loaded plates of intermediate rigidity (35).

The approach taken in this study is essentially that of Wong and Luco, modified for the simpler problem of plane strain. That is, we approximate the contact area between the drum and the soil as an infinitely long rigid plate subject to a periodic load. The contact area is decomposed into elemental strips, under each of which the contact stress is assumed uniform but of undetermined magnitude. The response of each strip to a unit loading of every other strip (and of itself) is obtained, so that an overall compliance matrix is generated relating the elemental displacements to the elemental loads. By requiring that the loaded areas experience uniform displacement (corresponding to the motion of a rigid drum) we achieve results identical to those of Karasudhi albeit by a wholly different approach.

3. COMPACTOR MODEL

Vibratory-drum compactors range in weight from 1000 lb (500 kg) walk-behind models to 35,000 lb (16,000 kg) machinery used in compacting rock fills. The roller modeled here is Ingersoll-Rand's SP56-DD, a 20,700 lb (9400 kg) smooth-drum compactor used on granular soils. Its dimensions are shown in Fig. 3-1 and other data is given in Table A-1.

The two-degree-of-freedom model of the compactor, shown in Fig. 3-2(a), is essentially that used by Yoo and Selig (14), except that the suspension damping is taken to be structural rather than viscous. The suspension connecting the drum to the yoke is comprised of twelve rubber isolators loaded in shear and acting in parallel. The linearized force-displacement characteristic for such mounts is given as a complex stiffness, wherein the damping in steady-state vibration is related to the amplitude of the deflection rather than the velocity:

$$F_k(\omega) = [K_1 + jK_2]\ [w_F(\omega) - w_D(\omega)]$$

where

$F_k e^{j\omega t}$ is the force transmitted from the frame to the drum,

$w_F e^{j\omega t}$ is the frame displacement,

$w_D e^{j\omega t}$ is the drum displacement.

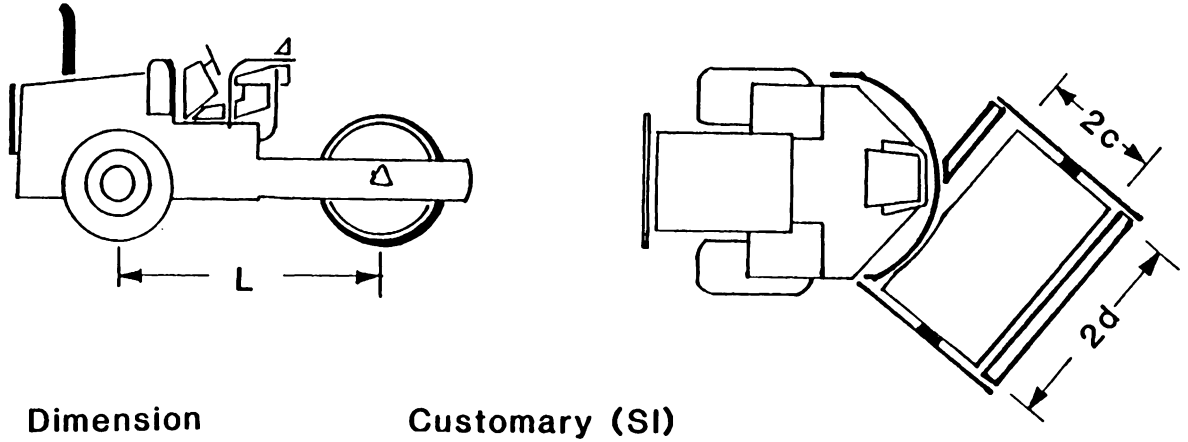

Dimension	Customary (SI)
L	10' 7" (3.22m)
2c	56" (1.42m)
2d	84" (2.13m)

Fig. 3-1. Ingersoll-Rand SP-56DD compactor.

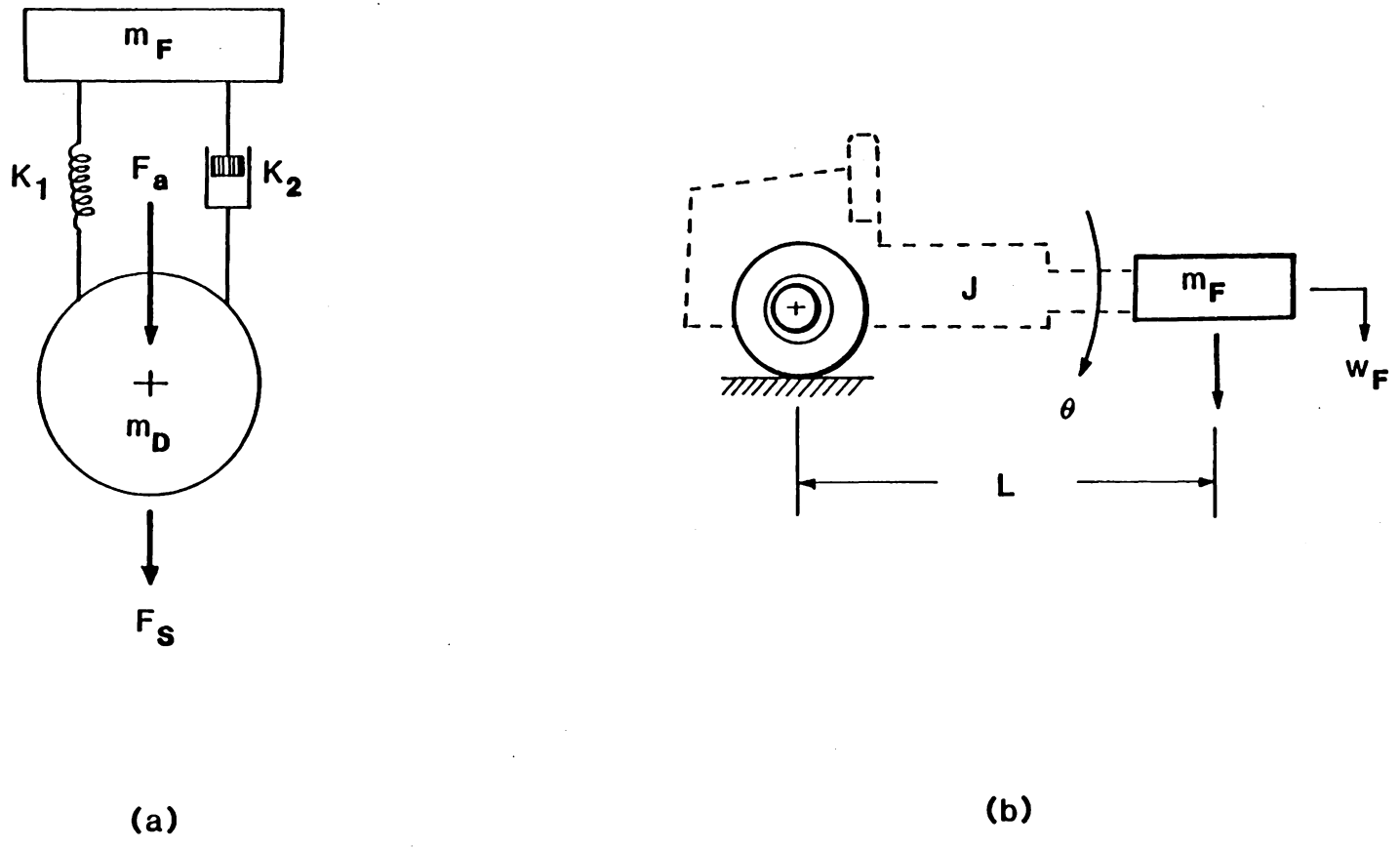

Fig. 3-2. Lumped-parameter model of compactor.

All displacements and forces are taken as positive downwards. Manufacturer's data (38) provides an overall estimate of the complex stiffness as

$$K_1 = 24060 \text{ lb/in. } (4210 \text{ kN/m})$$

$$K_2 = 3850 \text{ lb/in. } (674 \text{ kN/m}).$$

The lumped drum inertia is just the mass of the drum. (Rotational effects are not considered.) Estimating the effective frame inertia, however, is less straightforward. Yoo and Selig assume that the rubber tires of the tractor act as a static pivot about which the frame executes small-amplitude angular oscillations (Fig. 3-2(b)). Taking moments about the pivot,

$$J\ddot{\theta} = F_k L,$$

where J is the mass moment of inertia of the frame about the tires and L is the wheelbase. Using the small-angle approximation $\theta \approx (w_F/L)$,

$$\left(\frac{J}{L^2}\right) \ddot{w}_F = F_k$$

so that the effective frame inertia in Fig. 3-2(a) is

$$m_F = \frac{J}{L^2}.$$

The spatial distribution of the frame mass is needed to calculate J and was not available to the author. However, various assumptions about the distribution lead to estimates for the effective mass as 20 to 30 percent of the total frame mass. (Yoo and Selig's estimate was 30 percent.) Since estimating the optimal mass distribution is one of the aims of this study, an exact value is not required. A nominal value of 25 percent (2980 lb = 1350 kg) was assumed when examining the effects of other variables.

In Fig. 3-2(a), the model is shown acted upon by the generated dynamic force

$$F_a(\omega)e^{j\omega t} = (m\ e\ \omega^2)\ e^{j\omega t}$$

and the soil reaction

$$F_s(\omega)\ e^{j\omega t} = (F_s{}^R + F_s{}^I)\ e^{j\omega t}.$$

The steady-state soil reaction is assumed to be harmonic at the driving frequency but of undetermined magnitude and phase. (The validity of this assumption is examined in Section 5.) The steady-state equations of motion are:

$$m_F(j\omega)^2\ w_F = (K_1 + jK_2)\ (w_D - w_F) \qquad (3.0\text{-}1)$$

$$m_D(j\omega)^2 w = (K_1 + jK_2)(w_F - w_D) + F_a + F_s$$

where the coefficient $e^{j\omega t}$ is understood to multiply all displacements and forces.

Eliminating the frame displacement from these equations allows us to write

$$\frac{w_D}{F_a + F_s} = -\frac{1}{\omega^2} \frac{m_F\omega^2 - (K_1 + jK_2)}{m_D m_F \omega^2 - (K_1 + jK_2)(m_D + m_F)} .$$

The amplitude of the complex frequency-response function is shown in Fig. 3-3. Note that the input treated is the resultant of the driving force and the soil reaction. Although the applied force is a pure sinusoid, the soil reaction will probably contain harmonics at higher frequencies because of the intermittent contact at the leading and trailing edges of contact and because of nonlinearities in the soil properties. Note, however, that the response to frequencies higher than 10 Hz falls off at a rate of 40 dB/decade. It will be shown in Section 7 that efficient compaction requires operation at frequencies well above the cut-off frequency in Fig. 3-3. Therefore, any higher harmonics introduced by the clipping of the contact area will be selectively attenuated, providing some measure of confidence in the linear approximation introduced in the following sections.

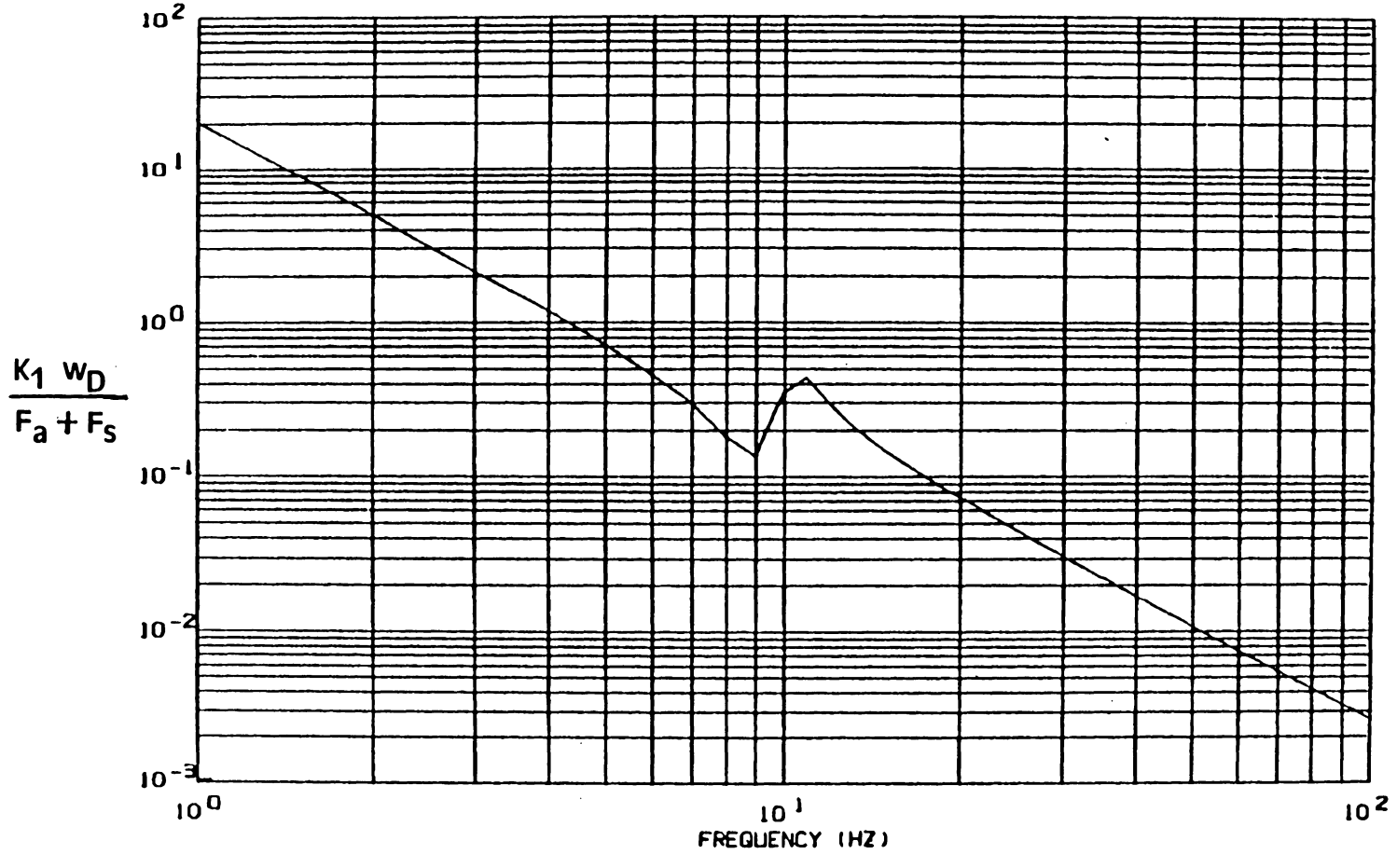

Fig. 3-3. Frequency response of drum to harmonic forces.

4. THE LINEAR ELASTIC MODEL

In this section the solutions of the dynamic equations for a linearly-elastic body are obtained. The boundary conditions appropriate for a surface-loaded half-space and a finite elastic layer on a rigid base are introduced, and the formal solutions to these problems are expressed as Fourier integrals. The reduction of the integral solutions for a half-space to the special case of plane strain is then made.

The plausibility of the linear model for the study of soil vibrations is then discussed. The selection of appropriate elastic moduli for soil is also treated.

4.1 Transformation of the Dynamic Equations for an Elastic Body

This section develops the integral relations for an elastic body subject to harmonic excitation. The treatment given here is essentially that of Thomson and Kobori (23), but numerous authors (18,20,21,22,23) have supplied other derivations.

Timoshenko and Goodier (17) developed the dynamic equations for an elastic body. These can be expressed concisely in vector notation:

$$(\lambda+G) < \frac{\partial \Delta}{\partial x} , \frac{\partial \Delta}{\partial y} , \frac{\partial \Delta}{\partial z} > + (G\nabla^2 - \rho \frac{\partial^2}{\partial t^2}) <u,v,w> = 0 \quad . \qquad (4.1\text{-}1)$$

In the foregoing, ρ is the material density and G and λ are Lame's constants, related to Young's modulus E and Poisson's ratio ν by

$$\lambda = \frac{\nu E}{(1 + \nu)(1 - 2\nu)}$$

$$G = \frac{E}{2(1 + \nu)} = \text{shear modulus.}$$

Δ is the volume dilation, expressed in terms of the coordinate strains

$$\Delta = \varepsilon_x + \varepsilon_y + \varepsilon_z = \frac{\partial u}{\partial x} + \frac{\partial v}{\partial y} + \frac{\partial w}{\partial z} .$$

∇^2 is the Laplacian operator:

$$\nabla^2 = \frac{\partial^2}{\partial x^2} + \frac{\partial^2}{\partial y^2} + \frac{\partial^2}{\partial z^2} .$$

Finally, $\langle \bullet, \bullet, \bullet \rangle$ denotes a vector, and u, v, and w are the displacements in the x, y, and z directions, respectively.

If we consider the steady-state vibration of the body subject to a harmonic force, we can write, for example,

$$u(x,y,z,t) = \hat{u}(x,y,z)\, e^{j\omega t}$$

$$\frac{\partial}{\partial t} u(x,y,z,t) = j\omega \hat{u}(x,z,z,)\, e^{j\omega t}$$

$$\frac{\partial^2}{\partial t^2} u(x,y,z,t) = - \omega^2 \hat{u}(x,y,z)\, e^{j\omega t}$$

etc. Henceforth, the circumflex (^) will be dispensed with and the factor $e^{j\omega t}$ will be understood to multiply all time-varying properties (displacements, forces, stresses, and strains).

Then Eq. 4.1-1 may be rewritten:

$$(\lambda + G) \left\langle \frac{\partial \Delta}{\partial x}, \frac{\partial \Delta}{\partial y}, \frac{\partial \Delta}{\partial z} \right\rangle + (G\nabla^2 + \rho\omega^2) \langle u,v,w \rangle = 0 \ . \qquad (4.1\text{-}2)$$

Equations 4.1-2 can be treated as the superposition of a volume dilation and a rotational distortion (17). That is, we write

$$u(x,y,z) = u_D(x,y,z) + u_S(x,y,z),$$

etc. Timoshenko and Goodier show that, for dilation without distortion, Eq. 4.1-2 reduces to

$$(\nabla^2 + h^2) \Delta = 0 \qquad (4.1\text{-}3)$$

where

$$\Delta = \frac{\partial}{\partial x} (u_D) + \frac{\partial}{\partial y} (v_D) + \frac{\partial}{\partial z} (w_D)$$

$$h = \frac{\omega}{C_D}$$

$$C_D = \left(\frac{\lambda + 2G}{\rho}\right)^{1/2} = \text{dilational wave velocity.}$$

Conversely, for distortion without dilation, we require

$$\Delta(x,y,z) \equiv o$$

$$\frac{\partial \Delta}{\partial x} = \frac{\partial \Delta}{\partial y} = \frac{\partial \Delta}{\partial z} \equiv 0.$$

Then Eq. 4.1-2 reduces to

$$(G\,\nabla^2 + \rho\omega^2) < u_S,\ v_S,\ w_S > = 0. \qquad (4.1\text{-}4)$$

We note that the dilation given by Eq. 4.1-3 satisfies Eq. 4.1-2 in addition to the constraints of irrotation. Writing Eq. 4.1-2 for the dilation alone and adding the expressions of Eq. 4.1-4 gives

$$\begin{array}{l} (\lambda + G)\left\langle \frac{\partial \Delta}{\partial x},\ \frac{\partial \Delta}{\partial y},\ \frac{\partial \Delta}{\partial z} \right\rangle + (G\nabla^2 + \rho\omega^2)\langle u_D, v_D, w_D \rangle = 0 \\ \qquad\qquad 0 \qquad\quad + (G\nabla^2 + \rho\omega^2)\langle u_S, v_S, w_S \rangle = 0 \\ \hline (\lambda+G)\left\langle \frac{\partial \Delta}{\partial x},\ \frac{\partial \Delta}{\partial y},\ \frac{\partial \Delta}{\partial z} \right\rangle + (G\nabla^2 + \rho\omega^2)\langle u_C+u_S, v_D+v_S, w_D+w_S \rangle = 0 \end{array}$$

which is just the original dynamic equation. Thus, although the expression for the dilation in Eq. 4.1-3 was obtained by assuming irrotationality, it is evidently valid for dilation in the presence of distortion as well. If Eq. 4.1-3 is solved for the dilation, the results may be directly inserted into the more general expression of Eq. 4.1-2.

At this point, we introduce the double Fourier transform. A single Fourier-transform pair is given by

$$\tilde{f}(\beta) = \mathcal{F}\{f(x)\} = \frac{1}{\sqrt{2\pi}} \int_{-\infty}^{\infty} f(x)\, e^{-j\beta x} dx$$

$$f(x) = \mathcal{F}^{-1}\{\tilde{f}(\beta)\} = \frac{1}{\sqrt{2\pi}} \int_{-\infty}^{\infty} \tilde{f}(\beta)\, e^{j\beta x} d\beta.$$

In reducing Eq. 4.1-3 to an ordinary differential equation, we transform over both horizontal coordinates, using the double Fourier transform:

$$\tilde{f}(\beta,\gamma) = \mathcal{F}^{2}\{f(x,y)\} = \frac{1}{2\pi} \int_{-\infty}^{\infty}\int_{-\infty}^{\infty} f(x,y)\, e^{-j(\beta x+\gamma y)} dxdy$$

$$f(x,y) = \mathcal{F}^{-2}\{\tilde{f}(\beta,\gamma)\} = \frac{1}{2\pi} \int_{-\infty}^{\infty}\int_{-\infty}^{\infty} \tilde{f}(\beta,\gamma)\, e^{j(\beta x+\gamma y)}\, d\beta d\gamma.$$

Here, β and γ are wave numbers along the x and y coordinates, corresponding to the frequency parameter ω in a time-series transform. Transforms in the (β,γ) space will be represented by tilde ($\sim$) overscore.

Just as ordinary differentiation is transformed in the single-transform case to multiplication by $j\beta$ (or in a time series, by $j\omega$), we have, for partial differentiation,

$$\mathcal{F}^{2}\left\{\frac{\partial}{\partial x} f(x,y)\right\} = j\beta\mathcal{F}^{2}\{f(x,y)\} = j\beta\tilde{f}(\beta,\gamma)$$

$$\mathcal{F}^2\{\frac{\partial}{\partial y} f(x,y)\} = j\gamma\mathcal{F}^2\{f(x,y)\} = j\gamma\tilde{f}(\beta,\gamma).$$

Equation 4.1-3, transformed, becomes

$$[\frac{d^2}{dz^2} - (\beta^2 + \gamma^2 - h^2)]\,\tilde{\Delta} = 0 \qquad (4.1\text{-}5)$$

where β and γ are treated as parameters independent of z. Note that β and γ may vary over $(-\infty, \infty)$, so that a comprehensive solution to Eq. 4.1-5 requires that we define a complex variable

$$\alpha_1 = \sqrt{\beta^2 + \gamma^2 - h^2}\ .$$

To ensure single-valued functions, we take α_1 as positive real or positive imaginary. We can then write the transform solution as

$$\tilde{\Delta}(z;\ \beta,\gamma) = A_1 e^{-\alpha_1 z} + A_2 e^{\alpha_1 z} \qquad (4.1\text{-}6)$$

with the coefficients A_1 and A_2 to be determined. Note that, since the solution has been obtained in a transform space, the values of these coefficients are parameterized in terms of the transform variables β and γ. The boundary conditions necessary for their evaluation must therefore be imposed in the transform space, since the Fourier transforms may not be inverted without knowledge of the dependence of A_1 and A_2 on β and γ.

We therefore transform the whole of Eq. 4.1-2 before substituting for the dilation. Doing so leads ultimately to

$$\left[\frac{d^2}{dz^2} - \alpha_2^2\right] < \tilde{u},\tilde{v},\tilde{w} > = \left(\frac{k^2}{h^2} - 1\right) \{<j\beta, j\gamma, -\alpha_1 > A_1 e^{-\alpha_1 z}$$

$$+ < j\beta, j\gamma, \alpha, > A_1 e^{\alpha_1 z} \} \qquad (4.1\text{-}7)$$

where

$$\alpha_2 = \sqrt{\beta^2 + \gamma^2 - k^2}$$

$$k = \frac{\omega}{C_S}$$

$$C_S = \left(\frac{G}{\rho}\right)^{1/2} = \text{shear wave velocity} .$$

The solution of Eq. 4.1-7 is given in terms of unevaluated coefficients A_1, A_2, B_1, B_2, C_1, C_2, D_1, and D_2 as

$$< \tilde{u},\tilde{v},\tilde{w} > = -\frac{A_1}{h^2} < j\beta, j\gamma, -\alpha_1 > e^{-\alpha_1 z} - \frac{A_2}{h^2} <j\beta, j\gamma, \alpha_1> e^{\alpha_1 z}$$

$$+ < B_1, C_1, D_1 > e^{-\alpha_2 z} + < B_2, C_2, D_2 > e^{\alpha_2 z} . \qquad (4.1\text{-}8)$$

We note that the expression for the dilation in Eq. 4.1-6 can be used to eliminate two of the coefficients, yielding

$$D_1 = \frac{j}{\alpha_2}(\beta B_1 + \gamma C_1)$$

$$D_2 = \frac{j}{\alpha_2}(\beta B_2 + \gamma C_2) \; . \tag{4.1-9}$$

4.2 Imposition of the Boundary Conditions

In this section we apply the boundary conditions for both an elastic half-space and an elastic layer of finite depth supported by a rigid, smooth base.

In the half-space defined by $z \geq 0$, we require that the effects of a load on the plane $z = 0$ vanish as $z \to \infty$. Since the quantities α_1 and α_2 have been taken as positive real for some values of β and γ, we must have

$$A_2 = B_2 = C_2 = D_2 = 0 \; .$$

The applied load is assumed to be normal to the bounding plane and distributed over some region A_C, and the surface tractions are assumed zero. Then

$$\sigma_z(x,y,0) = \begin{cases} -S(x,y) & \text{for } (x,y) \in A_C \\ 0 & \text{for } (x,y) \in A_C \end{cases}$$

$$\tau_{xz}(x,y,0) = 0$$

$$\tau_{yz}(x,y,0) = 0$$

where the distributed load S(x,y) is directed along the positive z axis and the normal stress σ_z is negative in compression (i.e., when S is positive). In terms of the displacements,

$$\sigma_z(x,y,o) = (\lambda\Delta + 2G\frac{\partial w}{\partial z})\Big|_{z=o}$$
$$\tau_{xz}(x,y,o) = G(\frac{\partial w}{\partial x} + \frac{\partial u}{\partial z})\Big|_{z=o}$$
$$\tau_{yz}(x,y,o) = G(\frac{\partial w}{\partial y} + \frac{\partial v}{\partial z})\Big|_{z=o}$$

These conditions can be transformed to yield three equations in the four remaining unknowns A_1, B_1, C_1, and D_1. Equation 4.1-9 provides the remaining relation needed to evaluate the coefficients. The formal solution of these equations yields, for the elastic half-space,

$$\langle \tilde{u},\tilde{v},\tilde{w} \rangle = \frac{\tilde{S}(\beta,\gamma)}{GF(\beta,\gamma)} \{[2(\beta^2 + \gamma^2) - k^2]\langle j\beta, j\gamma, -\alpha_1 \rangle e^{-\alpha_1 z}$$
$$-2\alpha_1\alpha_2 \langle j\beta, j\gamma, -\frac{\beta^2+\gamma^2}{\alpha_2} \rangle e^{-\alpha_2 z}\} \qquad (4.2\text{-}1)$$

where

$$\tilde{S}(\beta,\gamma) = \frac{1}{2\pi} \iint_{A_C} S(x,y)\, e^{-j(\beta x + \gamma y)}\, dxdy$$

$$F(\beta,\gamma) = [2(\beta^2 + \gamma^2) - k^2]^2 - 4\alpha_1\alpha_2(\beta^2 + \gamma^2) .$$

Inverting these transforms leads to expressions like

$$w(x,y,0) = \frac{1}{2\pi} \int_{-\infty}^{\infty} \int_{-\infty}^{\infty} \frac{\alpha_1 k^2}{G} \frac{\tilde{S}(\beta,\gamma)}{F(\beta,\gamma)} e^{j(\beta x + \gamma y)} d\beta d\gamma$$

for example.

Several difficulties are presented in the evaluation of such integrals. In the first case, there are four infinite limits of integration. For the special cases of point loads or radially symmetric loading on a circular region, or for loading on an infinitely long line or strip (plane strain), the double integrals reduce to single integrals. For the more unwieldy problems of non-axisymmetric loads (e.g., rectangular regions of loading), Thomson and Kobori introduce polar coordinates, writing

$$\beta = r \cos \theta$$

$$\gamma = r \sin \theta$$

$$w(x,y,0) = \frac{1}{2\pi} \int_{0}^{2\pi} \int_{0}^{\infty} \frac{k^2}{G} \frac{\sqrt{r^2 - h^2}}{F(r)} \hat{S}(r,\theta) e^{j(xr\cos\theta + yr\sin\theta)} r dr d\theta \qquad (4.2\text{-}2)$$

$$F(r) = [2r^2 - k^2]^2 - 4r^2(r^2 - h^2)^{1/2} (r^2 - k^2)^{1/2}$$

$$\hat{S}(r,\theta) = \tilde{S}(\beta,\gamma).$$

Thus, the number of infinite limits is reduced to one.

A second and more difficult problem is posed by the denominator F(r), which contributes two branch-point singularities and a simple pole. The customary method of evaluating such integrals is to treat the real variable r as complex and perform a contour integration in the complex plane, taking care not to cross the branch barriers. Ewing, Jardetsky, and Press show that the branch lines are hyberbolas in the second and fourth quadrants of the r-plane (25). Thomson and Kobori introduced a more straightforward approach, discussed below, that permits direct integration along the real axis past the singularities.

Before describing the techniques used for evaluating the integrals, we present the related results for a finite layer and for the specialization of the half-space results to the case of plane strain. Each of these cases has some practical bearing on the modelling of a vibratory roller compactor. Whereas the former affords enormous complications, the latter provides some simplification of the numerical problem.

Compaction is frequently accomplished by laying a thin fill of sand on the subgrade, rolling it, and then repeating the operation several times. The underlying layers are therefore stiffer than the upper ones. A better approximation to such operations is obtained by considering the response of a surface-loaded elastic layer of thickness H supported by a rigid, smooth base. Instead of requiring all effects to vanish at infinite depths, we impose instead the conditions

$$w(x,y,H) = 0$$
$$\tau_{xz}(x,y,H) = 0$$
$$\tau_{yz}(x,y,H) = 0 \ .$$

These conditions lead to the following expressions, for use with Eq. 4.1-8:

$$< A_1, A_2 > = F_1(\beta,\gamma) < e^{\alpha_1 H}, e^{-\alpha_1 H} >$$
$$< B_1, B_2 > = F_2(\beta,\gamma) < e^{\alpha_2 H}, e^{-\alpha_2 H} >$$
$$< C_1, C_2 > = F_3(\beta,\gamma) < e^{\alpha_2 H}, e^{-\alpha_2 H} >$$
$$< D_1, D_2 > = F_4(\beta,\gamma) < e^{\alpha_2 H}, e^{-\alpha_2 H} >$$

$$F_1(\beta,\gamma) = -\frac{\tilde{S}(\beta,\gamma)}{G\, F_o(\beta,\gamma)} \frac{h^2}{2} (\alpha_2^2 + \beta^2 + \gamma^2) \sinh \alpha_2 H$$

$$F_2(\beta,\gamma) = -\frac{\tilde{S}(\beta,\gamma)}{G\, F_o(\beta,\gamma)} j\ \alpha_1 \alpha_2 \beta \sinh \alpha_1 H$$

$$F_3(\beta,\gamma) = -\frac{\tilde{S}(\beta,\gamma)}{G\, F_o(\beta,\gamma)} j\ \alpha_1 \alpha_2 \gamma \sinh \alpha_1 H$$

$$F_4(\beta,\gamma) = \frac{\tilde{S}(\beta,\gamma)}{G\, F_o(\beta,\gamma)} \alpha_1 (\beta^2 + \gamma^2) \sinh \alpha_1 H$$

$$F_o(\beta,\gamma) = \left[2(\beta^2 + \gamma^2) - k^2\right]^2 \cosh \alpha_1 H \sinh \alpha_2 H$$

$$- 4\, \alpha_1 \alpha_2 (\beta^2 + \gamma^2) \cosh \alpha_2 H \sinh \alpha_1 H$$

The resemblance of the denominator $F_o(\beta,\gamma)$, to the Rayleigh function $F(\beta,\gamma)$ is noted. But whereas $F(\beta,\gamma)$ is algebraic and contributes a single pole, $F_o(\beta,\gamma)$ is transcendental. Ewing et al. (25) offer us scant comfort in their reassurances that the number of zeroes of $F_o(\beta,\gamma)$ is finite. The integration of these relations, while undoubtedly relevant to the problem at hand, was not undertaken by the author.

A second geometry of interest to the rolling compactor is that associated with plane strain. For harmonic loading of a rectangular region on the surface of a half-space, a plane-strain approximation (corresponding to the loading of an infinite strip) yields errors on the order of 10 percent when the length-to-width ratio of the rectangle is 10:1. Computational time is reduced by approximately 90 percent, since the transforms and their inversions are now accomplished with single integrals. By techniques similar to those of the last section, we can arrive at the following expressions for the case of plane strain in an elastic half-space, where the infinite dimension of the loaded area is parallel to the y axis and the z axis is positive downwards.

$$< \tilde{u},\tilde{w} > = \frac{\tilde{S}}{G\,F(\beta)} \{(2\beta^2 - k^2) < j\beta, -\alpha_1 > e^{-\alpha_1 z}$$

$$- 2\,j\alpha_1\alpha_2\beta < j, -\frac{\beta}{\alpha_2} > e^{-\alpha_2 z} \}\,,$$

$$F(\beta) = (2\beta^2 - k^2)^2 - 4\beta^2\alpha_1\alpha_2,$$

$$\alpha_1 = \sqrt{\beta^2 - h^2} \ ,$$

$$\alpha_2 = \sqrt{\beta^2 - k^2} \ ,$$

$$\tilde{S}(\beta) = \frac{1}{\sqrt{2\pi}} \int_{-c}^{c} S(x)\, e^{-j\beta x} dx$$

where 2c is the finite dimension of the loaded area. Of special interest to us are the resulting expressions,

$$w(x,o) = \frac{1}{\sqrt{2\pi}} \int_{-\infty}^{\infty} \frac{\alpha_1 k^2 \tilde{S}(\beta)}{G\, F(\beta)} e^{j\beta x} d\beta \qquad (4.2\text{-}3)$$

and

$$\varepsilon_z(x,z) = \frac{1}{\sqrt{2\pi}} \int_{-\infty}^{\infty} \frac{\tilde{S}(\beta)}{G\, F(\beta)} \{(2\beta^2 - k^2)\ \alpha_1^2\, e^{-\alpha_1 z}$$

$$-2\alpha_1 \alpha_2 \beta^2\, e^{-\alpha_2 z}\}\, e^{j\beta x} d\beta \ . \qquad (4.2\text{-}4)$$

4.3 Evaluation of the Integrals

The principal contribution of Thomson and Kobori in (17) is a direct method for the evaluation of integrals like those of 4.2-2, 4.2-3, and 4.2-4. Consider an integral of the form

$$I_1 = \int_a^b \frac{H(\beta)}{F(\beta)}\, d\beta$$

$$F(\beta) = 0, \quad \beta_o \text{ real}$$

The integrand, as written, is an integral over the real β axis. Unfortunately, the pole contributed by the denominator lies in the path of integration. One workable approach to the problem is a tedious contour integration along a path encircling the pole. The branch barriers, however, require that a convoluted path be taken to maintain analyticity (25).

Thomson and Kobori consider, instead, a path along the real axis. In the vicinity of the pole an excursion is made on a semicircular arc of radius R (Fig. 4-1). The integral over this path is given as

$$I_2 = \int_c \frac{H(\beta)}{F(\beta)}\, d\beta$$

$$= \int_a^{\beta_o - R} \frac{H(\beta)}{F(\beta)}\, d\beta + \int_\Gamma \frac{H(\beta)}{F(\beta)}\, d\beta + \int_{\beta_o + R}^{b} \frac{H(\beta)}{F(\beta)}\, d\beta$$

where β_o is the pole and Γ is the semicircular arc. The value of the first integral is obtained in the limit by letting $R \to 0$:

$$I_1 = \lim_{R \to 0} I_2$$

The integral over the segment Γ, in the limit, goes to $-j\pi \text{Res}(\beta_o)$, according to Hildebrand (25). The remaining terms define the Cauchy principal value of the integral:

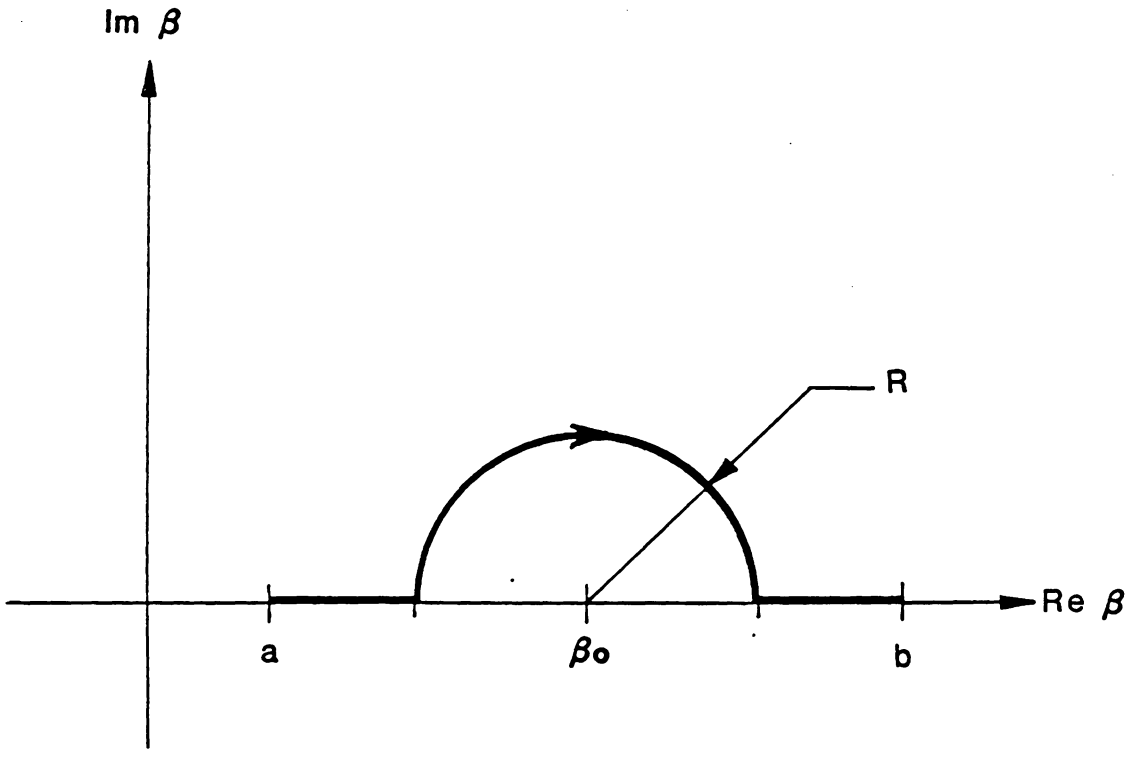

Fig. 4-1. Path of integration around a singularity.

$$P \int_a^b \frac{H(\beta)}{F(\beta)}\, d\beta \triangleq \lim_{R\to 0} \left\{ \int_a^{\beta_o - R} \frac{H(\beta)}{F(\beta)}\, d\beta + \int_{\beta_o + R}^b \frac{H(\beta)}{F(\beta)}\, d\beta \right\} .$$

Thus, we write

$$\int_a^b \frac{H(\beta)}{F(\beta)}\, d\beta = P \int_a^b \frac{H(\beta)}{F(\beta)}\, d\beta - j\pi\, \mathrm{Res}(\beta_o),$$

$$\mathrm{Res}(\beta_o) = \frac{H(\beta)}{F'(\beta)} \quad . \tag{4.3-1}$$

As described so far, the approach is not new. The problem of evaluating the improper integral has been reduced to the evaluation of its principal value. The contribution of Thomson and Kobori is in their application of a technique developed by Longman (26) for obtaining the principal value. We first translate the origin of the β axis to the singularity, writing, say,

$$\frac{H(\beta)}{F(\beta)} = f(\beta - \beta_o) \equiv f(\xi).$$

We then consider an interval symmetric about β_o and express the integrand as the sum of even and odd components:

$$f(\xi) = \frac{1}{2}\,[f(\xi) + f(-\xi)] + \frac{1}{2}\,[f(\xi) - f(-\xi)].$$

The integral of the odd component on the symmetric interval vanishes, whereas the integral of the even component is just twice the integral over one half of the interval:

$$\int_{-a}^{a} \frac{1}{2}\left[f(\xi) + f(-\xi)\right] d\xi = 2 \int_{o}^{a} \frac{1}{2}\left[f(\xi) + f(-\xi)\right] d\xi.$$

Thus, the problem of obtaining the Cauchy principal value is in turn reduced to one of evaluating the integral of a function unbounded at one limit, for which methods are known (27).

The subtraction of the residue term in 4.3-1 has an interesting interpretation attributed to Lamb (18) but developed more fully by Quinlan (21). As improper integrals, expressions like those of Eq. 4.2-2 and 4.2-3 have some indeterminateness. As formal solutions to the problem posed, they satisfy the dynamic equations and the prescribed boundary conditions, but they admit the possibility of waves propagating inwards from infinity to the source. Physically, such a possibility is obviated by material damping in the medium, but no such damping has been incorporated in our model thus far. By subtracting half of the residue at the pole, we are eliminating the energy associated with incoming waves, enforcing a Sommerfeld radiation condition (25). The physical significance of the pole is that it is associated with a (non-existent) resonance condition of standing waves in the horizontal planes in which we executed our transforms. These standing waves are the superposition of outgoing and incoming waves, and their presence in our solution is avoided by removing half the energy contributed by the Rayleigh pole.

A more complete description of the procedures followed in evaluating the integrals of Eqs. 4.2-3 and 4.2-4 is given in Appendix B.

4.4 Applicability of the Linear Model

The foregoing development rests on the assumption that the soil mass is homogeneous and of semi-infinite extent and that it possesses the properties of isotropic linear elasticity. All of these assumptions are contradicted to some degree by real soil and pose some restrictions on the applicability of the model.

In the first place, the linear-elastic constitutive relations are conservative, whereas soil is a dissipative medium. Figure 4-2 compares the stress-strain relations under cyclic loading of actual soil to the idealized behavior assumed so far. Two important features are absent from the linear model. The first is the characteristic hysteresis loop, where the stress path taken during unloading differs from the path during loading. Since the linear model is conservative, the stress state it predicts is a single-valued function of the strain alone. The second feature lacking is the permanent settlement associated with repeated loading, which progressively translates the points of the hysteresis loop to the right on the stress-strain diagram.

Although the most visible effect of compaction is the permanent deformation of the soil, the usefulness of the linear model is less restricted than it may first appear. The linear model will not predict any plastic behavior, but the transmission of energy from the compactor

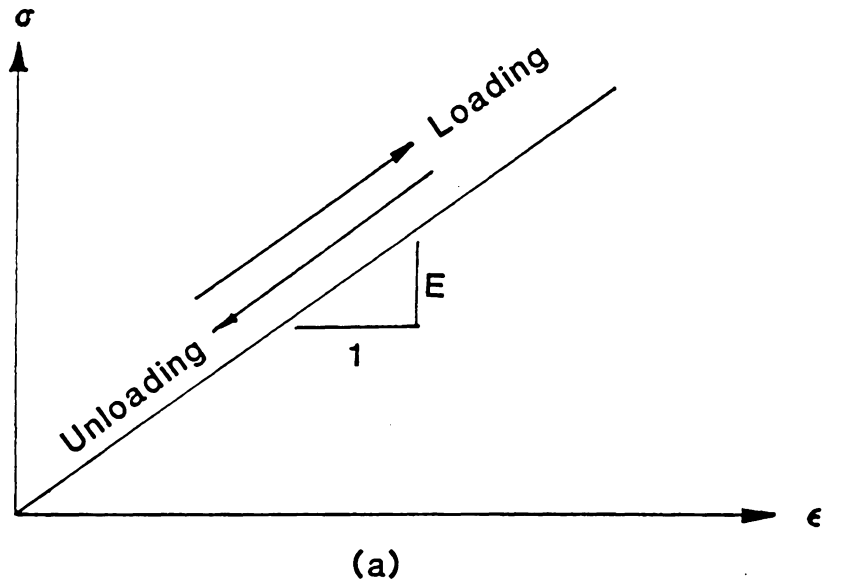

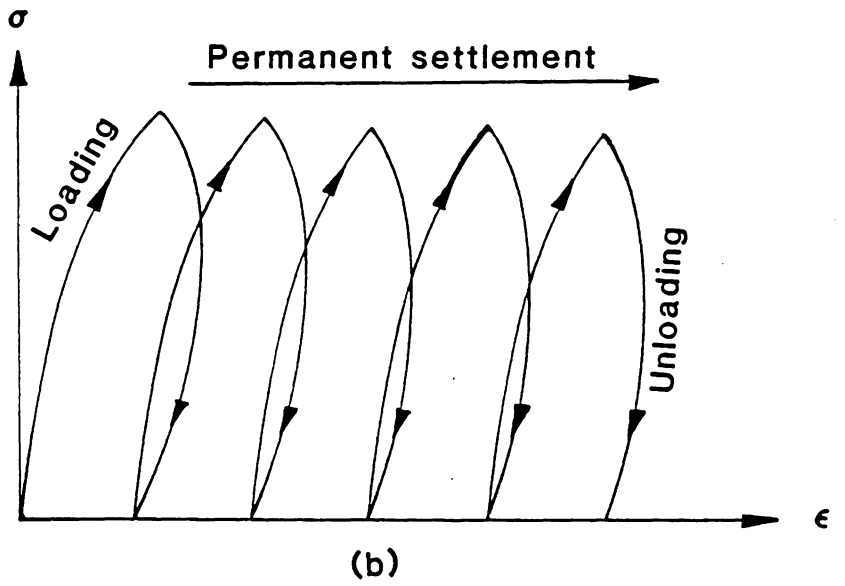

Fig. 4-2. Cyclic loading of (a) linearly elastic material, (b) material with hysteresis damping.

to the soil is intimately connected with stresses and deformations that are largely elastic. It is this transmission of energy, according to Brumund and Leonards (14), that determines the plastic evolution of the medium. The validity of the linear model, at this stage, rests on the relative importance of the elastic and plastic processes during this energy transfer.

Although the linear model does not incorporate material damping, it does model a second mechanism of energy dissipation known as "geometric damping", which is the radiation of energy away from the vicinity of loading. The description of the loss as "geometric" reflects that it is the infinite dimensions of the medium rather than its material properties that permits the conservative model to predict steady-state vibrations. (In the absence of some dissipation, a steady state would not be attainable.) In foundation engineering, it is recognized (12,39) that geometric damping is the dominant mechanism of energy dissipation in soil undergoing steady-state vibration, to the extent that material damping may be neglected in a first estimate of the frequency-response characteristics. Since ours is a steady-state problem as well, the linear model should adequately predict the amplitudes of forces and displacements.

A caution is in order, however, that the soil beneath foundations is already in a compacted state, so that its behavior is more elastic than that of uncompacted soil. We are concerned, by contrast, with soil that is undergoing transition to this state, and the internal damping

supplied by the soil will probably modify the compaction dynamics considerably from those predicted by the linear model. Two features of our problem are encouraging:

(1) The principal effect of damping is to alter the magnitudes of a system's response at resonance. It only weakly affects the frequency at which resonance occurs. Thus, the underdamping of the linear model may cause us to overestimate somewhat the effectiveness of compaction at resonance, but we should still obtain a usable prediction of the desirable frequency of operation.

(2) Satisfactory compaction is almost never accomplished in a single pass of the roller. Typically 5 to 10 passes are required. The greatest plastic deformations accumulate in the earliest stages (6,14), so that the quantitative accuracy of the linear model should improve after a few passes have been made.

This multi-pass requirement also gives us some confidence in our treatment of the soil as a homogeneous mass with isotropic properties. There is certainly some difference in the properties of the soil at the leading and trailing edges of the contact area, owing to the accumulation of residual stress and settlement during the passage of the compactor. Furthermore, the geometry of the drum-soil interface is asymmetric because of the settlement behind the drum. These effects are not treated by the linear model, which is used to estimate the spatial distribution of strains during a single pass of the compactor. If the asymmetry and inhomogeneity introduced by a single pass is not great, the linear model should provide useful estimates.

The constitutive properties of an isotropic, linearly elastic medium are characterized by various parameters: Young's modulus (E), the shearing modulus (G), Lame's constant (λ), and Poisson's ratio (ν). Any two of these are sufficient to determine the others. In this study we have used Poisson's ratio and the shear modulus. Poisson's ratio for granular soils can vary from 0.25 to 0.35 (12); for cohesive soils, it is somewhat higher and can exceed 0.5 for overconsolidated soils (16). Since the principal applications of vibratory compaction are to non-cohesive or moderately cohesive soils, we have assumed a value of 0.3.

The shear modulus of soils is affected by properties and conditions as diverse as the average confining pressure, the void ratio, the degree of saturation, the soil temperature, and the grain sizes and shapes. The two dominant parameters in a non-cohesive soil are the void ratio (e) and the average confining pressure ($\bar{\sigma}_o$). Richart (12) has provided the following correlations,

for round-grained sands:

$$G = 2630 \frac{(2.17 - e)^2}{1 + e} \bar{\sigma}_o^{1/2};$$

for angular-grained sands:

$$G = 1230 \frac{(2.97 - e)^2}{1 + e} \bar{\sigma}_o^{1/2} \qquad (4.4\text{-}1)$$

where G and $\bar{\sigma}_o$ are in lb/in. (For SI units of kPa, substitute 6905 for 2630 and 3230 for 1230.) The formula for angular-grained sands has been used in this study, since it also affords a reasonable estimate for moderately cohesive soils.

The void ratio of a soil declines considerably as compaction proceeds. This in turn has a powerful effect on the stiffening of the soil. In the author's opinion, the worst failing of the model proposed in this study is that it does not track the changes in the void ratio. This is a settlement effect that neither the linear model nor the nonlinear constitutive relations directly predicts, although in Patten's lumped-parameter model the effect is encompassed in the overall plastic deformation by suitable selection of coefficients. The best treatment that the distributed parameter model can accord is to employ an average value (e = 0.8) in all computations. Some empirical correlations for residual settlement have been offered (14,40) but owing to their lack of generality they have not been introduced here. Conceivably, such correlations could be used to update the model properties following each pass of the compactor.

The dependence on confining pressure is more useful to us, since the nonlinear relations of Section 6 predict the augmentation of the confining pressure by induced stresses. We are therefore able to simulate the stiffening properties of soil during compaction. The initial confining pressure at any point in the soil depends on the weight of the soil column overtop and the additonal pressure introduced by the static

weight of the compactor. The average confining pressure in terms of coordinate stresses is

$$\bar{\sigma}_o = \frac{\sigma_x + \sigma_y + \sigma_z}{3} .$$

The contribution of the soil column is

$$\sigma_z = \rho g z$$

$$\sigma_x = \sigma_y = K_o z$$

$$K_o = \frac{\nu}{1 - \nu}$$

where

ρg is the specific weight of the soil,

z is the depth of interest,

K_o is the "coefficient of earth pressure at-rest" (2).

This gives a contribution to the confining pressure

$$\bar{\sigma}_1 = \frac{1 + \nu}{3(1 - \nu)} \rho g z .$$

The effect of the compactor weight is estimated from the formula for uniform loading of an infinite strip on the half-space surface (41). For the geometry shown in Fig. 4-3,

$$\sigma_z = \frac{q}{\pi} [\alpha + \sin \alpha \cos (\alpha + 2 \beta)]$$

$$\sigma_x = \frac{q}{\pi} [\alpha - \sin \alpha \cos (\alpha + 2 \beta)] \qquad (4.4\text{-}2)$$

$$\sigma_y = \nu (\sigma_x + \sigma_z) .$$

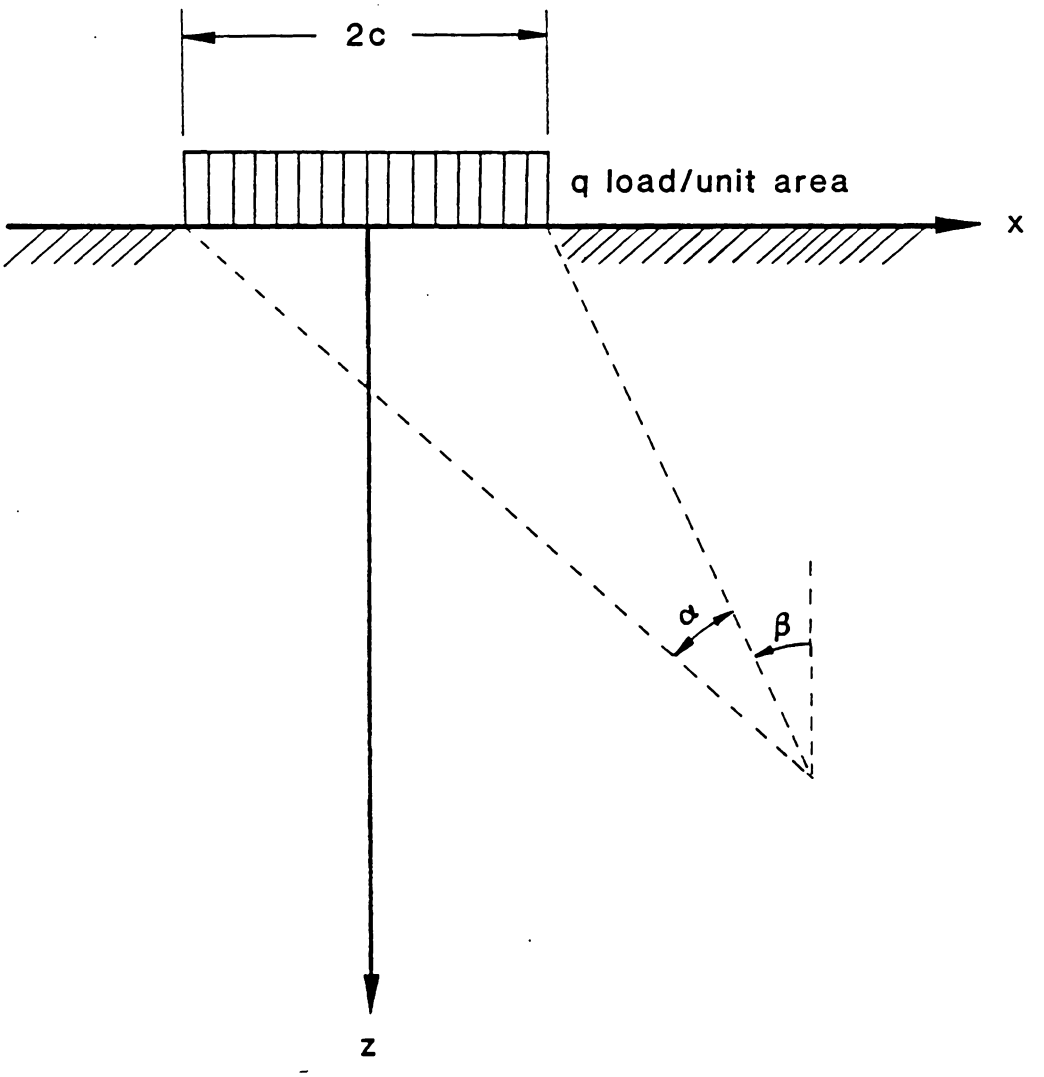

Fig. 4-3. Uniform loading of an infinite strip on the surface of an elastic half-space.

Here, q is the contact stress, assumed uniform; we divide the weight of the compactor at the drum-end by the contact area:

$$q = \frac{W_c}{4\ cd}$$

where

W_c is the static load at the drum,

2c is the contact area width,

2d is the contact area length.

Directly beneath the compactor, Eqs. 4.4-2 reduce to

$$\bar{\sigma}_2 = \frac{4}{3\pi}(1 + \nu)\ q\ \tan^{-1}\frac{c}{z}\ .$$

The initial confining pressure beneath the drum is just the sum of the soil and compactor effects:

$$\bar{\sigma}_o = \bar{\sigma}_1 + \bar{\sigma}_2\ .$$

Figure 4-4 shows the superposition of these effects for both the confining stress and the resulting shear modulus. The depth dependences of the two effects largely cancel and their superposition yields a reasonably uniform distribution for depths greater than 1 ft (0.3m). Based on this results, an average confining pressure of 3 psi (21 kPa) was assumed for uncompacted soil in the linear model. Section 6 discusses the introduction of range and depth dependence in the expressions des-

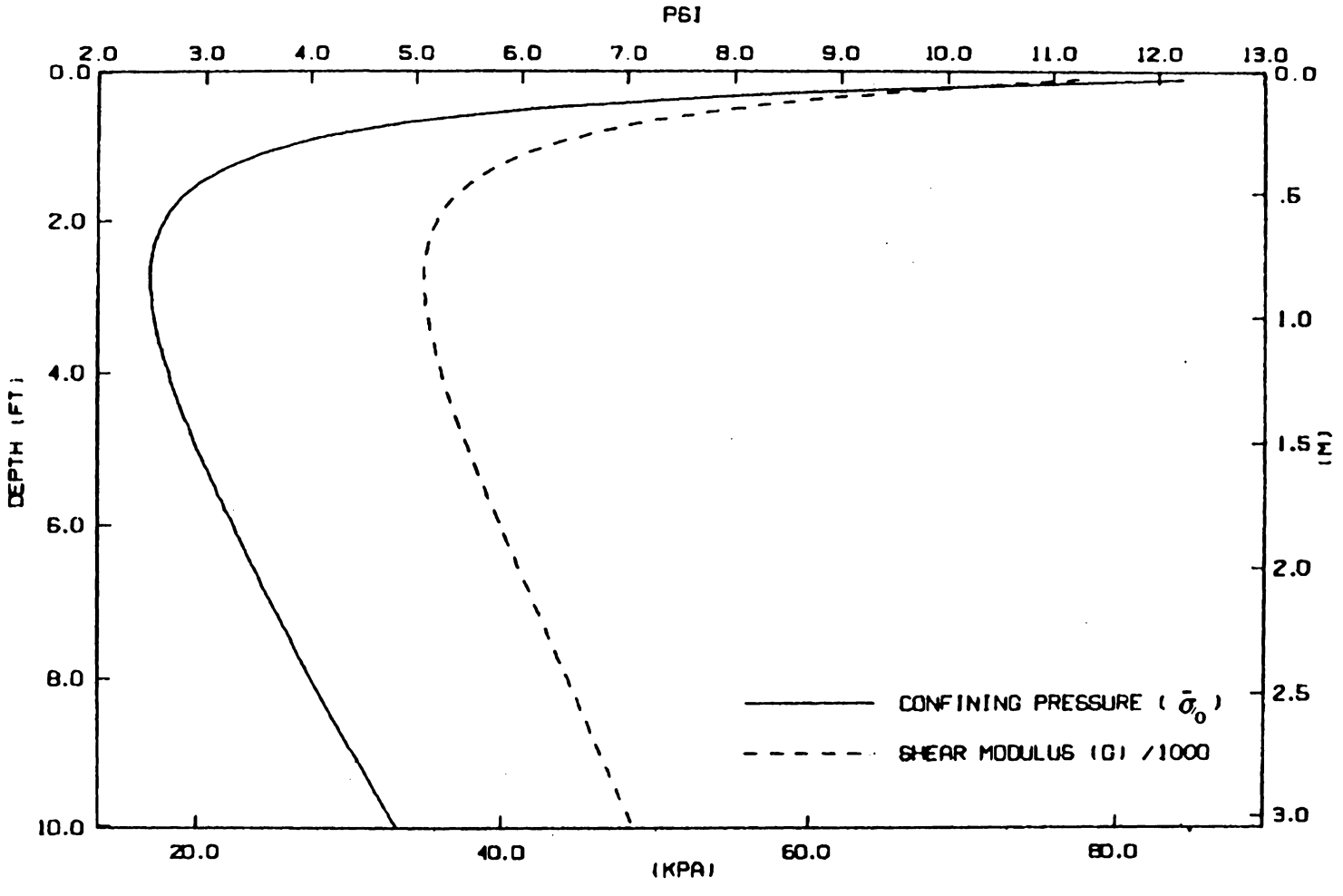

Fig. 4-4. Variation of confining pressure and shear modulus with depth, directly below the compactor.

cribing the growth of residual stress and how the latter is used to update the linear model's simulation of subsequent passes by the compactor.

5. SOLUTION OF THE COUPLED DYNAMICS OF THE COMPACTOR AND THE SOIL

In this section we describe the coupling between the lumped-parameter compactor model and the distributed-parameter linear soil model. We also consider the errors introduced by treating a time-varying contact area as time-invariant.

5.1 Assembly of the Equations

For the compactor model, we have the displacements w_D and w_F of the drum and frame, respectively, in terms of the known applied force F_a and the unknown soil fraction F_s:

$$m_F(j\omega)^2 w_F = (K_1 + jK_2)(w_D - w_F)$$

$$m_D(j\omega)^2 w_D = (K_1 + jK_2)(w_F - w_D) + F_a + F_s \,. \tag{3.0-1}$$

For the soil, we are able to express the surface displacement $w(x,0)$ in terms of the spatial transform of the unknown contact stress distribution $S(x)$:

$$w(x,0) = \frac{1}{\sqrt{2\pi}} \int_{-\infty}^{\infty} \frac{\alpha_1 k^2 \tilde{S}(\beta)}{G\, F(\beta)} e^{j\beta x} d\beta$$

$$\tilde{S}(\beta) = \frac{1}{\sqrt{2\pi}} \int_{-\infty}^{\infty} S(x)\, e^{-j\beta x} dx. \tag{4.2-3}$$

Note the dependence of α_1, k, and $F(\beta)$ on the frequency ω, as given in Section 4.1.

The coupling of the compactor and soil is expressed by requiring

$$w(x,0) = w_D \quad \text{for } |x| < c$$

$$F_s = \int_{-d}^{d} \int_{-c}^{c} S(x)\, dx\, dy = 4cd \int_{o}^{c} S(x)\, dx$$

where c and d are the dimensions of the contact area shown in Fig. 5-1, and where a symmetric distribution of stress about x = 0 has been assumed. Note that the force F_s is taken as positive downwards on the drum and upwards on the soil, which yields a positive (tensile) stress in the soil.

The assumptions here are that the soil and drum remain in contact over one cycle, that the contact area between them is constant, and that the reaction and displacements are all simple harmonic functions at the frequency of the applied force. The first assumption may or may not be true, and the second and third assumptions are certainly false; the gravity of treating an average contact area and ignoring the intermittent separation is discussed at the end of this section.

With the assumptions made, there is still the problem that we do not know the magnitude of the contact force, let along its distribution as contact stresses. We follow the line of attack of Wong and Luco discussed in Section 2 and discretize the contact area by treating N

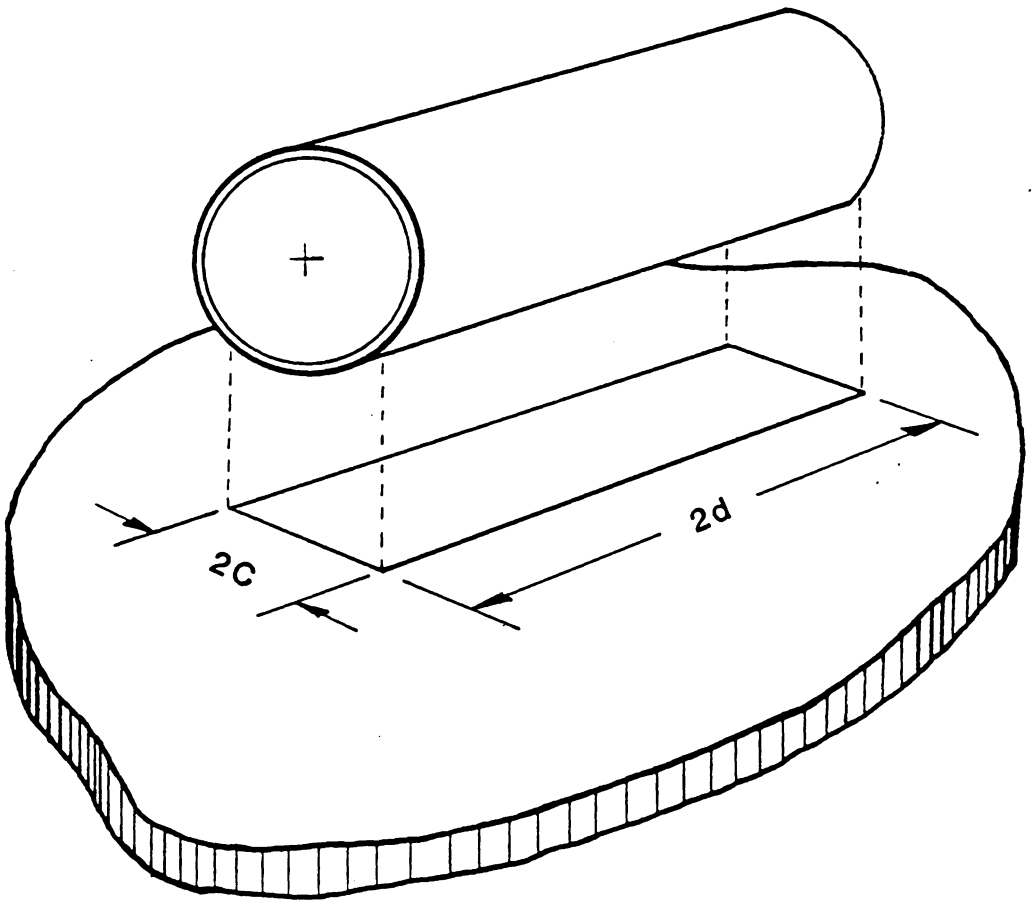

Fig. 5-1. Finite-length contact area.

elemental strips, as shown in Figs. 5-1 and 5-2. The stress across a single strip is assumed uniform, although of unknown magnitude and phase. We first translate the coordinate origin to the center of the j-th element, so that the surface displacement of the i-th point on the surface due to the stress beneath the j-th strip is

$$w_{ij} = \frac{1}{\sqrt{2\pi}} \int_{-\infty}^{\infty} \frac{\alpha_1 k^2 \tilde{S}_j(\beta)}{G\, F(\beta)} e^{j\beta x_{ij}} d\beta$$

$$\tilde{S}_j(\beta) = \frac{1}{\sqrt{2\pi}} \int_{-b}^{b} S_j(x)\, e^{j\beta x} dx$$

$$S_j(x) = \frac{P_j}{2b}$$

where P_j is the contact force per unit length on the j-th strip, 2b is the width of an elemental strip, and x_{ij} is the coordinate of the i-th point relative to the center of the j-th strip. Note that we employ a plane-strain approximation: both the length of a strip and its fraction of the total contact force are actually finite, and the total soil reaction is

$$F_s = \sum_{j=1}^{N} (2d)\, P_j \,.$$

Evaluating the transform of the contact stress for a uniform distribution across the element,

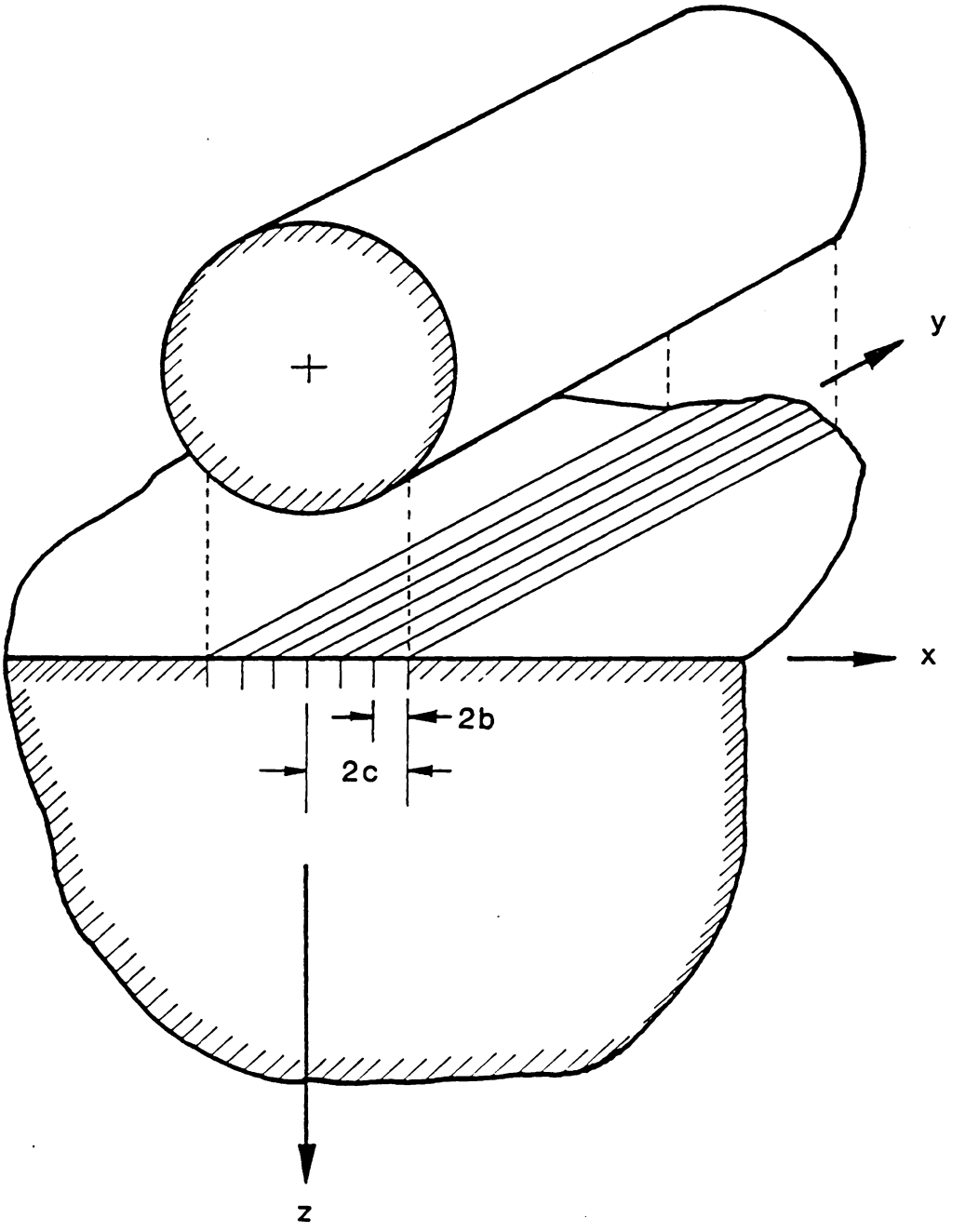

Fig. 5-2. Plane-strain approximation, showing discretization of contact area.

$$\tilde{S}_j(\beta) = \frac{1}{\sqrt{2\pi}} \frac{P_j}{b} \frac{\sin \beta b}{\beta}$$

$$w_{ij} = \frac{P_j}{2\pi b} \int_{-\infty}^{\infty} \frac{\alpha_1 k^2}{G F(\beta)} \frac{\sin \beta b}{\beta} e^{j\beta x_{ij}} d\beta$$

or

$$w_{ij} = H_{ij} P_j \tag{5.1-2}$$

where the compliance H_{ij} is given by

$$H_{ij}(x_{ij}, \omega) = \frac{1}{2\pi b} \int_{-\infty}^{\infty} \frac{\alpha_1 k^2}{G F(B)} \frac{\sin \beta b}{\beta} e^{j\beta x_{ij}} d\beta. \tag{5.1-3}$$

The evaluation of this integral is described in Appendix B.

Equation 5.1-1 thus relates the incremental surface deflection at the i-th point to the contact force per unit length under the j-th strip. The total deflection at the i-th point is

$$w_i = \sum_{j=1}^{N} H_{ij} \cdot P_j.$$

We chose the interpolation points i = 1,...,N to be the centers of the strips j = 1,...,N. Because the drum is rigid, and because the soil at the contact surface is assumed to stay in contact with the drum,

$$w_j = w_D, \qquad i = 1,...,N$$

or

$$\sum_{j=1}^{N} H_{ij} P_j - w_D = 0, \qquad i = 1,\ldots,N. \tag{5.1-4}$$

This gives us N equations in the N unknown forces P_j and the unknown drum displacement. We also have, from Eqs. 3.0-1 and 5.1-1,

$$-\sum_{j=1}^{N} (2d) P_j + [K_1 + jK_2 - m_D \omega^2] w_D$$

$$- [K_1 + jK_2 - m_F \omega^2] w_F = F_a; \tag{5.1-5}$$

$$- [K_1 + jK_2 - m_D \omega^2] w_D$$

$$+ [K_1 + jK_2 - m_F \omega^2] w_F = 0. \tag{5.1-6}$$

We therefore acquire two more equations, with one more unknown (w_F), giving us N + 2 equations in N + 2 unknowns. In fact, the quantities P_j, w_D, w_F, and F_a are all complex, so that there are actually 2(N+2) unknowns; the equations must be separated into expressions for real and imaginary parts.

The solution of these equations yields the discretized distribution of contact stresses. This in turn permits the evaluation of Eq. 4.2-4 by superposition of the elemental effects, which yields the strain field beneath the compactor.

5.2 Effects of a Time-Varying Contact Area

Throughout all of the foregoing the contact area between the soil and drum was assumed constant. In fact, it varies approximately with the square root of the deflection:

$$\frac{A_1}{A_2} = \sqrt{\frac{w_1}{w_2}}$$

where w_1 and w_2 are deflections at the center of the contact area.

The effect of intermittent loss of contact at the edges of the contact area is a clipping of the reactive stress in these regions. This in turn introduces higher harmonics in the stress that the monochromatic model does not consider. Such effects are compounded in a sandy soil when the dynamic force exceeds the static load of the compactor's weight, so that the soil cyclically goes into tension. A noncohesive soil will not support tensile stresses, so that clipping occurs in the subsurface stresses as well. But as noted in Section 3, the compactor inertia possesses a low-pass filter characteristic that makes the drum motion insensitive to the effects of any higher harmonics. We note, moreover, that the Fourier expansion for a clipped sinusoid

$$f(t) = \begin{cases} \sin \omega t, & 0 < \omega t < \pi \\ 0, & \pi < \omega t < 2\pi \\ f(t - \frac{2\omega}{\pi}), & 2\pi < \omega t \end{cases}$$

is

$$f(t) = \frac{1}{\pi} + \frac{1}{2} \sin \omega t - \frac{2}{\pi} \sum_{n=1}^{\infty} \frac{1}{(2n)^2 - 1} \cos (2n)\, \omega t$$

which decays as $1/n^2$. Finally, we note that the linear model is being used to predict subsoil strains and not stresses. Even a noncohesive soil will support tensile strains, in the sense that the soil can dilate under its own inertia. For all these reasons, clipping of the stresses at the edges of the contact surface and beneath it is probably not a major liability to the model's accuracy.

On the other hand, a more serious problem is created if the entire drum rises clear of the soil. Figure 5-3(a) shows measurements made by D'Appolonia et al. (6) of the drum displacement and acceleration of a vibratory compactor that hammers on the soil. Again, the fundamental frequency appears to dominate, and the effect of higher harmonics is not worrisome. But Fu (42) has noted the presence of long-period subharmonics in data published by Cowley (43) which Fu associated with the separation of the drum from the soil. Cowley's data is reproduced in Fig. 5-3(b). It is not clear, however, that the data were taken during steady-state vibration, and they may illustrate a transient associated with too-rapid variation of the driving frequency. In any event, when the compactor is travelling, a soil element can only experience a few pulses associated with a long-period subharmonic.

To summarize, the nonlinear effects introduced by a time-varying geometry generate higher harmonics and possibly subharmonics in the response of even a linear medium. Although a considerable portion of

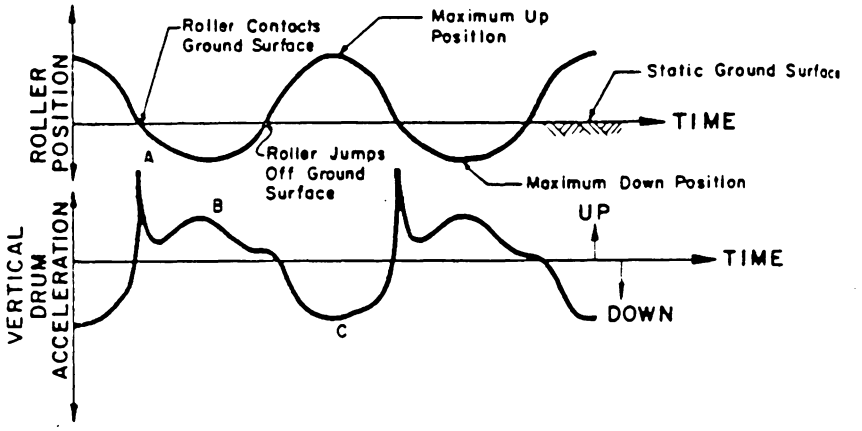

(a)

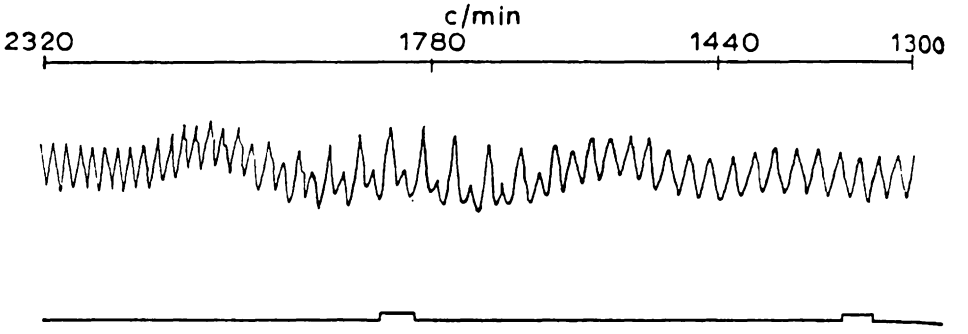

(b)

Fig. 5-3. Effects of separation of compactor drum from the soil.
(a) Drum displacement and acceleration measured by D'Appolonia et al. (6).
(b) Possible subharmonic at 1780 c/min (30 Hz), from Cowley (43).

the stress spectrum is probably associated with frequencies higher than that of the driving force, the implications for the model's predictions of displacements and strains are not severe. The effect of subharmonics, if they exist, is more difficult to gauge, but it seems unlikely that they can promote or hinder the soil compaction in any substantial manner.

6. THE NONLINEAR SOIL MODEL

In this section we introduce the effects of material damping, the growth of residual stresses, and the attendant stiffening of the soil.

Patten (1) has proposed that the stresses in soil be treated as the algebraic sum of an elastic and plastic component:

$$\sigma(\varepsilon,\dot{\varepsilon}) = \sigma_e(\varepsilon,\dot{\varepsilon}) + \sigma_p(\varepsilon,\dot{\varepsilon}) .$$

Both components of the stress are strain-rate dependent, which agrees with experimental results described by Adachi and Okano (44). The proposed functional form for each component is discussed in the next two sections, followed by a description of their implementation in the model. Further treatment of the implementation is given in Appendix B.

6.1 The Elastic Component

The proposed form of the elastic component is

$$\sigma_e(\varepsilon,\dot{\varepsilon}) = \frac{\varepsilon}{\alpha_1 + \alpha_2\varepsilon} e^{\alpha_3\dot{\varepsilon}} . \qquad (6.1\text{-}1)$$

For negligible strain rates (i.e., quasi-static loading), this reduces to

$$\sigma_e(\varepsilon,0) = \frac{\varepsilon}{\alpha_1 + \alpha_2\varepsilon} ,$$

which is the well-known hyperbolic form (45) that models the onset of plastic deformation under static loading. The parameters α_1 and α_2 are the inverses of the initial tangent modulus and the ultimate strength of the soil. Figure 6-1 illustrates the significance of these parameters in a typical stress-strain diagram for sandy soil.

For small stresses well below the ultimate strength, Eq. 6.1-1 can be approximated by

$$\sigma_e = E\ \varepsilon\ e^{\alpha_3 \dot{\varepsilon}}\ , \qquad (6.1\text{-}2)$$

$$E = 1/\alpha_1 = \text{Young's modulus},$$

which is the form employed in this study.

The exponential term in 6.1-1 and 6.1-2 introduces rate-dependence into the constitutive relations, which in turn is associated with energy dissipation through material damping. If either a periodic stress or a periodic strain is prescribed in Eq. 6.1-1, the resulting path on a stress-strain diagram is a closed hysteresis loop (Fig. 6-2). The parameter α_3 determines the area inside the loop, that is, the amount of energy dissipated in one cycle.

Patten (1) has suggested values for α_1, α_2, and α_3 suitable for a lumped-parameter force-displacement model. We require, on the other hand, a constitutive relation for stress and strain at a point, since our model is distributed. The tangent modulus E in Eq. 6.1-2 can be had from the shear modulus and Poisson's ratio, determined in Section 3.4:

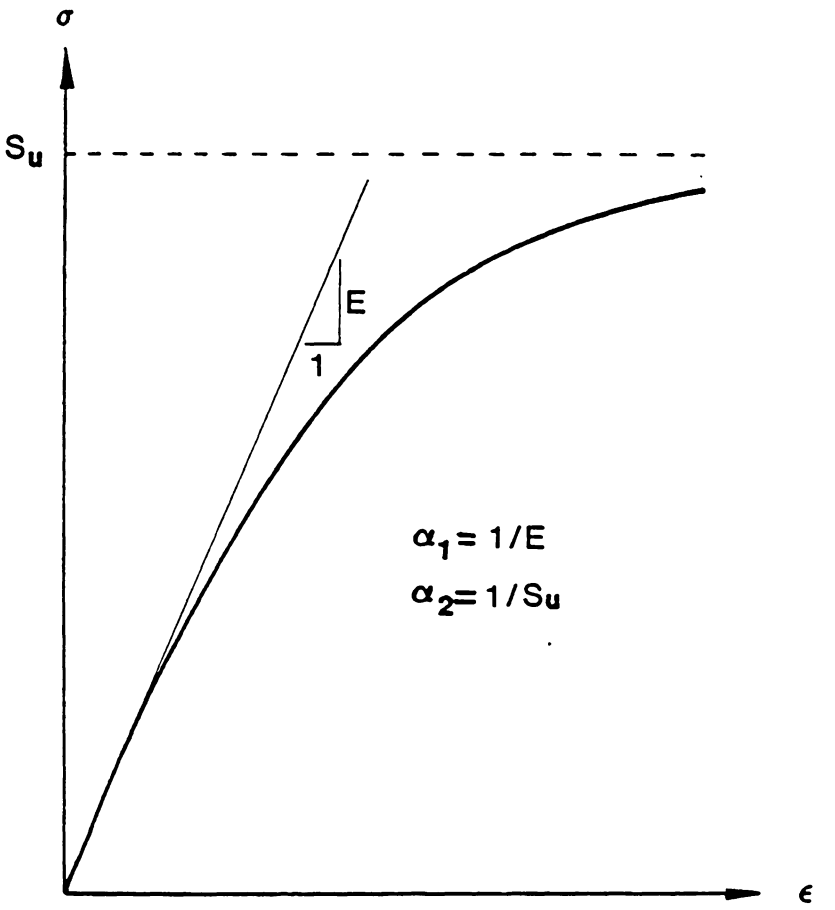

Fig. 6-1. Hyperbolic form of stress-strain relation under static loading.

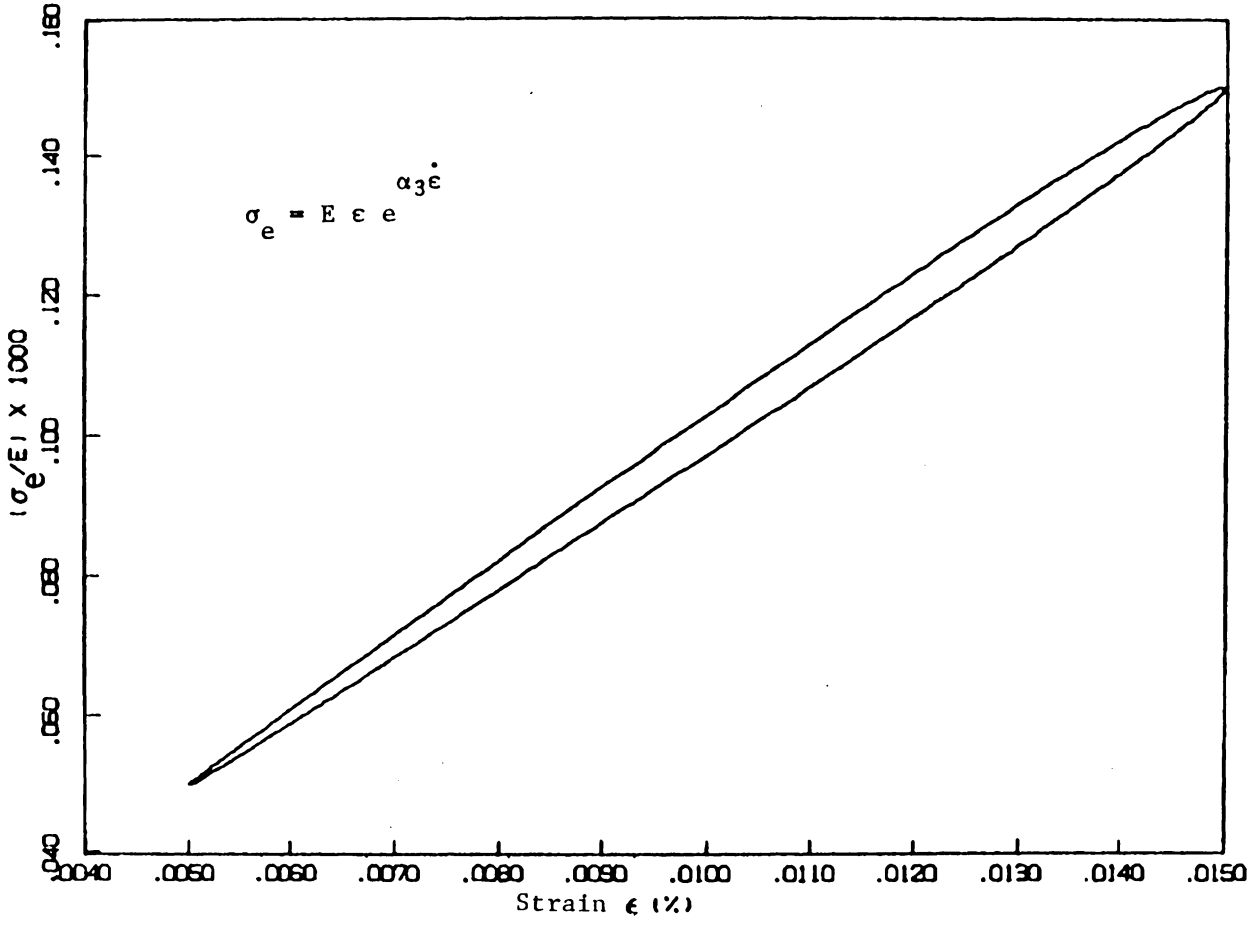

Fig. 6-2. Model prediction of elastic stress component, showing hysteresis loop.

$$E = 2\ (1 + \nu)\ G.$$

The value of α_3 can be estimated from measurements of damping in soils. Two of the more commonly-used descriptors are the logarithmic decrement (δ) and the specific damping capacity (ψ). The logarithmic decrement is obtained from the decaying amplitude of free vibration:

$$\delta = \ln(x_1/x_2),$$

where x_1 and x_2 are successive vibration peaks, as shown in Fig. 6-3(a). The damping capacity is obtained from the steady-state vibration as the ratio

$$\psi = \frac{U_D}{U_P}.$$

U_D is the energy dissipated over one cycle and is given by the area inside the hysteresis loop on a stress-strain diagram (area A_D in Fig. 6-3(b)). The definition of U_P varies from author to author (46,47,48). We follow Hall and Richart (47) and use the area A_P in Fig. 6-3(b). Noting that the width of the loop in this figure is greatly exaggerated by the scaling, we approximate U_P by

$$U_P \approx \frac{1}{2} E\ \varepsilon_a^{\ 2}$$

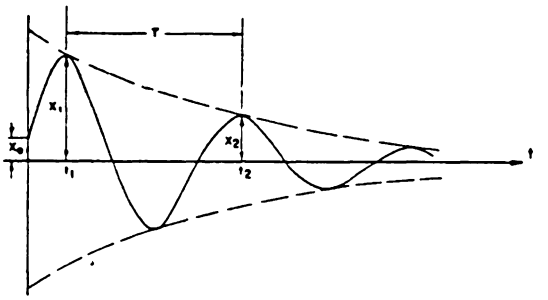

(a)

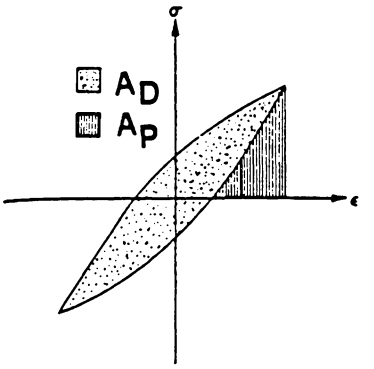

(b)

Fig. 6-3. Description of damping in transient and steady-state vibrations.

(a) Log decrement: $\delta = \ln (x_1/x_2)$.

(b) Damping capacity: $\psi = A_D/A_P$.

From Hall and Richart (47).

where ε_a is the amplitude of the oscillatory component of strain.

The log decrement and the damping capacity are related, according to Hall and Richart, by

$$\psi \approx 1 - e^{-2\delta} .$$

For dry sand in longitudinal oscillation with a confining pressure of 4.3 psi (30 kPa) and an initial strain amplitude on the order of 5×10^5 in./in., Hall and Richart report a log decrement of 0.1, which corresponds to a damping capacity of 18 percent. These conditions most nearly approximate those in the compaction process modelled here.

We determine the damping capacity predicted by Eq. 6.1-2 by prescribing the strain as

$$\varepsilon = \varepsilon_m + \varepsilon_a \sin \omega t.$$

This gives

$$\dot{\varepsilon} = \varepsilon_a \omega \cos \omega t,$$

$$\sigma_e = E(\varepsilon_m + \varepsilon_a \sin \omega t)\, e^{\alpha_3 \varepsilon_a \omega \cos \omega t} .$$

The energy dissipated over one cycle is

$$U_D = \int \sigma_e \, d\varepsilon = \int \sigma_e \, \dot{\varepsilon} \, dt.$$

Letting $\theta = \omega t$, we can substitute from the expressions above to obtain

$$U_C = \int_o^{2\pi} \varepsilon_a (\varepsilon_m + \varepsilon_a \sin \theta) \cos \theta \, e^{\alpha_3 \varepsilon_a \omega \cos \theta} \, d\theta,$$

$$U_P = \frac{1}{2} E \varepsilon_a^2,$$

$$\psi = 2 \int_o^{2\pi} \left[\frac{\varepsilon_m}{\varepsilon_a} + \sin \theta\right] \cos \theta \, e^{\alpha_3 \varepsilon_a \omega \cos \theta} \, d\theta,$$

$$\psi = 2 \int_o^{2\pi} \left[\beta_1 + \sin \theta\right] \cos \theta \, e^{\beta_2 \cos \theta} \, d\theta,$$

$$\beta_1 = \varepsilon_m / \varepsilon_a,$$

$$\beta_2 = \alpha_3 \omega \varepsilon_a.$$

Taking $\beta_1 = 1$ and numerically integrating, we find by trial and error than an 18 percent damping capacity is given by

$$\beta_2 = 0.03.$$

For a frequency of 30 Hz and a strain amplitude of 5×10^{-5}, we arrive at

$$\alpha_3 = 3 \text{ sec } (3 \text{ s})$$

6.2 The Plastic Component

The proposed form for the plastic component of stress is

$$\sigma_p(\varepsilon, \dot{\varepsilon}) = \alpha_4 \{W(\varepsilon, \dot{\varepsilon}) - E_R(\varepsilon, \dot{\varepsilon})\}. \tag{6.2-1}$$

$W(\varepsilon, \dot{\varepsilon})$ is a functional that describes the work history of a soil element:

$$W(\varepsilon, \dot{\varepsilon}) = \int_{\varepsilon_o}^{\varepsilon} \sigma_a d\varepsilon = \int_{o}^{t} \sigma_a(t)\dot{\varepsilon} dt \tag{6.2-2}$$

where σ_a is the applied stress. E_R is a bounding energy configuration related to the recoverable energy at a given stress state:

$$E_R = \alpha_5(T + V) \tag{6.2-3}$$

where T and V are the kinetic and recoverable strain energies, on a volumetric basis:

$$T = \frac{1}{2} \rho \dot{w}^2$$

$$V = \frac{1}{2} E \varepsilon^2 \quad .$$

A principal feature of these expressions is that they relate the growth of residual stresses to the stress history of the soil, a dependence noted by Feda (13). Moreover, the expressions agree with the observations of Brumund and Leonards about the proportionality between the energy transmitted to a soil element and its plastic deformation.

The applied stress in Eq. 6.2-2 is transmitted from element to element by non-conservative elastic forces, but some of the work it performs appears as kinetic energy rather than as strain energy or as energy dissipated by material damping. To see this, we consider a force balance on the element shown in Fig. 6-4. The applied stress is taken as the elastic stress acting on one side of the element while an incrementally smaller elastic stress acts on the other side. A force balance yields

$$\rho(\Delta x\ \Delta y\ \Delta z)\ \ddot{w} = (\Delta x\ \Delta y)(\sigma_a - \sigma_e)$$

or

$$\sigma_a = \sigma_e + \rho\ \ddot{w}\ \Delta z.$$

Integrating for the volumetric energies

$$\int \sigma_a\ d\varepsilon = \int \sigma_e\ d\varepsilon + \int \rho\ \ddot{w}\ \Delta z\ d\varepsilon.$$

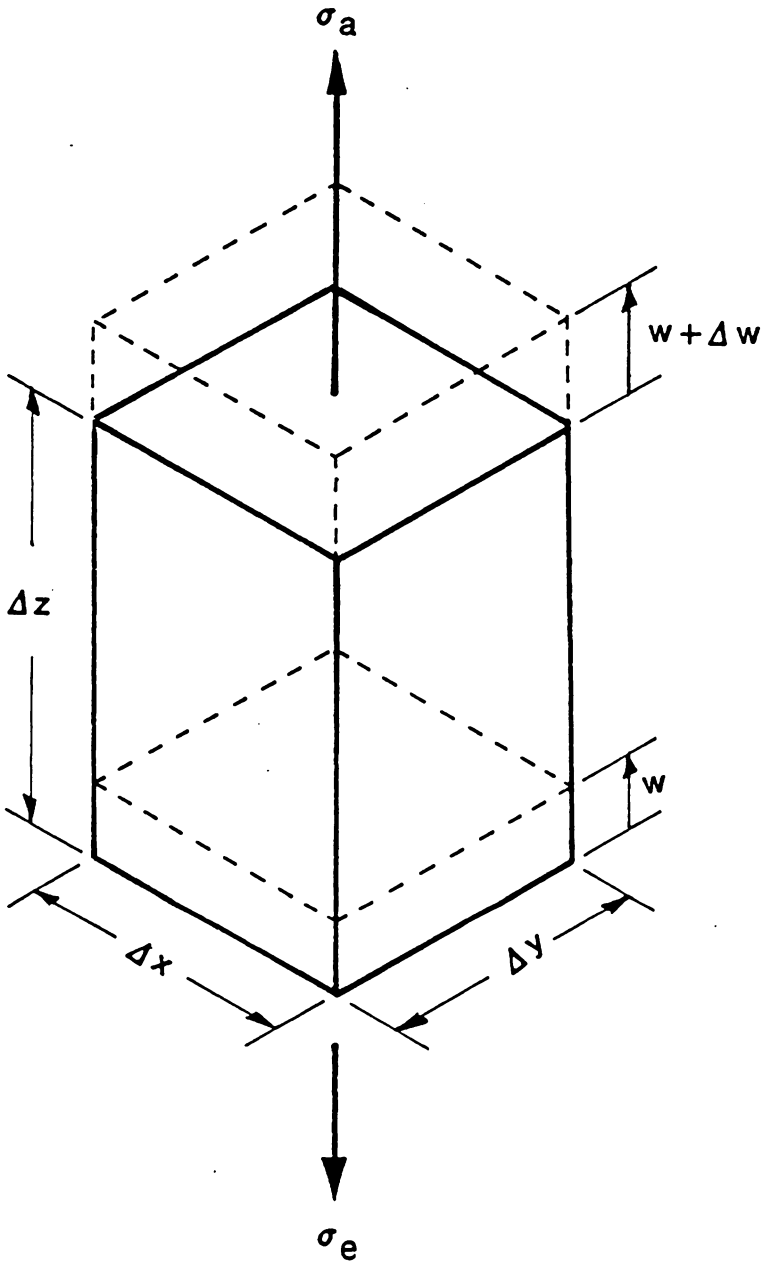

Fig. 6-4. Force balance on a soil element.

We note that

$$(\Delta z)\, d\varepsilon = d(\varepsilon\, \Delta z) - \varepsilon\, d(\Delta z) = dw - \varepsilon\, d(\Delta z).$$

In the limit as $\Delta z \to 0$, the second term vanishes as a second-order differential. Then

$$\lim_{\Delta z \to 0} \int \rho\, w\, \Delta z\, d\varepsilon = \int \rho\, \ddot{w}\, du$$
$$= \frac{1}{2}\, \rho\, \dot{w}^2$$
$$= T \quad .$$

Thus,

$$\int \sigma_a\, d\varepsilon = \int \sigma_e\, d\varepsilon + T,$$

and, for $\alpha_5 = 1$, we can rewrite Eq. 6.2-1 as

$$\sigma_p(\varepsilon, \dot{\varepsilon}) = \alpha_4 \left\{ \int_0^t \sigma_e\, \dot{\varepsilon}\, dt - \frac{1}{2} E\, \varepsilon^2 \right\}. \qquad (6.2\text{-}4)$$

The coefficient α_4 in 6.2-4 governs the rate of growth of the plastic stress. A value of α_4 was estimated from measurements made by D'Appolonia (6) of the residual stresses induced by a vibratory roller similar to the one modelled here. D'Appolonia's measurements are shown in Fig. 6-5. Iterations with the model indicated that a suitable value would be

$$\alpha_4 = 1 \text{ (dimensionless)} .$$

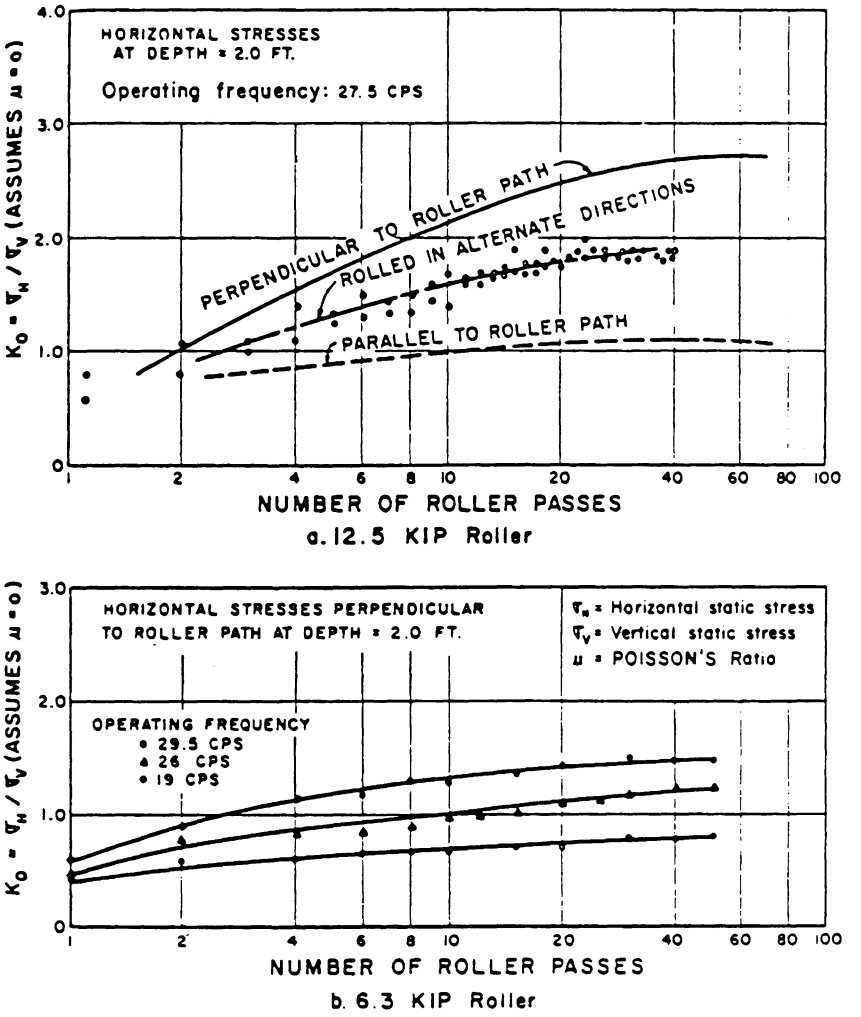

Fig. 6-5. In-situ stresses measured by D'Appolonia et al. (6) following the passage of a vibratory compactor.

6.3 Implementation of the Nonlinear Relations

Figure 6-6 depicts a compactor rolling over a fill with a speed v_o to the left. We consider a soil element initially at a distance x_o to the left of the compactor. If we take the origin of the x axis as being fixed to the base of the drum so that it translates to the left with speed v_o, then we may characterize the position of the soil element relative to the drum as

$$x(t) = v_o t - x_o. \tag{6.3-1}$$

By the assumptions of the linear soil model, the strain field in the soil can be described by

$$\varepsilon(x,z,t) = \varepsilon_S(x,z) + \varepsilon_D(x,z,t), \tag{6.3-2}$$

$$\varepsilon_D(x,z,t) = \hat{\varepsilon}(x,z)\, e^{j\omega t}, \tag{6.3-3}$$

where $\varepsilon_S(x,z)$ is the static strain introduced by the compactor's deadweight and $\varepsilon_D(x,z,t)$ is the assumedly sinusoidal dynamic strain.

If we take $x(0) = x_o$ sufficiently large, then we may consider the strains at earlier instant ($t < 0$) as negligible. Then we can fully characterize the strain history of an element at a given depth, z:

$$\varepsilon(t;\, z) = \varepsilon_S(x(t),z) + \varepsilon_D(x(t),z,t). \tag{6.3-4}$$

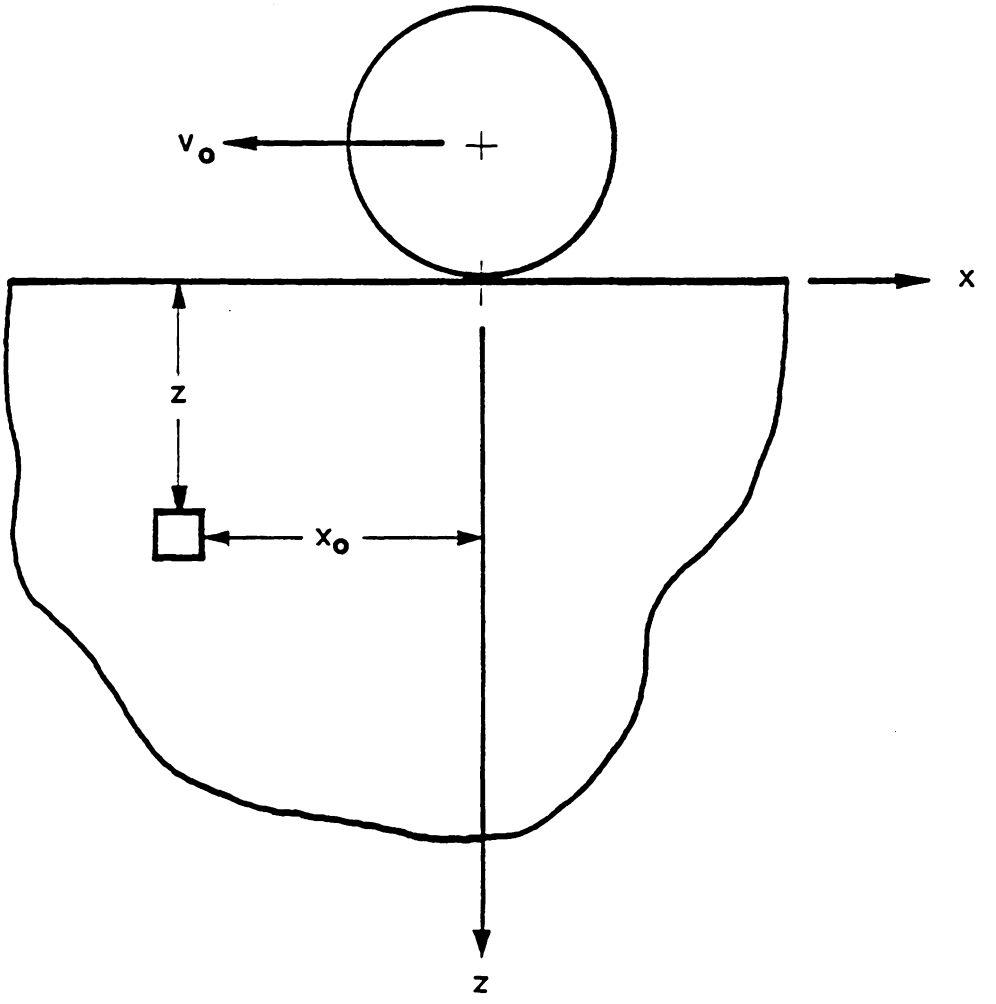

Fig. 6-6. Relative motion of compactor drum and a soil element.

Use of Eq. 6.3-4 with Eq. 6.1-2 permits us to describe the elastic stress as a function of time alone for a given depth; Eq. 6.2-4 then provides us with the growth of the residual stress. Finally, the residual stress can be taken to augment the subsurface confining pressure, which, through Eq. 4.4-1, describes the progressive stiffening of the soil. The effects of previous compaction are thus introduced into the simulation of subsequent passes by the compactor.

In Section 4.4 a formula (Eq. 4.4-2) was introduced for determining the subsurface stresses associated with the uniform static loading of an infinite strip on the surface of an elastic half-space. This permits computation of the strains by Hooke's Law, e.g.,

$$\varepsilon_z = \frac{1}{E} [\sigma_z - \nu(\sigma_x + \sigma_y)] .$$

The static component of strain ε_s in Eq. 6.3-4 can be computed using this formula. A somewhat better approximation is to be had, however, by relaxing the requirement that the static contact stress be uniform. Figure 6-7(a) illustrates the distribution of normal stress beneath a rigid wheel. The deformation of the soil immediately beneath the wheel is plastic, but the distribution can be taken to be approximately that predicted by the Hertz theory of contact stress (17), which provides the semi-ellipsoidal distribution of Fig. 6-7(b):

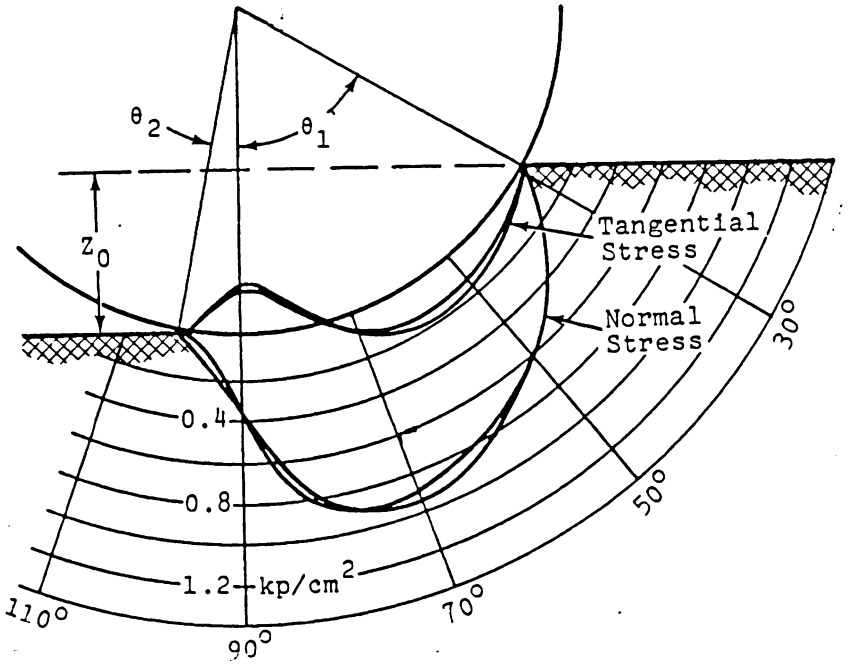

(a)

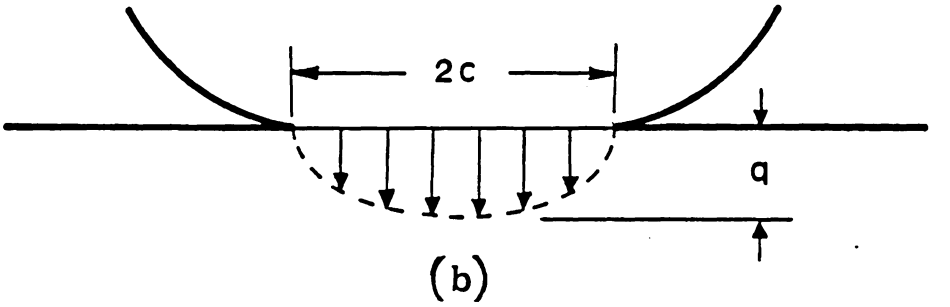

(b)

Fig. 6-7. Distribution of contact stress
(a) under a rigid wheel (from Karafiath (16));
(b) according to Hertz theory of contact stress (Timoshenko and Goodier (17)).

$$\sigma_c(x) = q\sqrt{1 - (x/c)^2}\ , \qquad (6.3\text{-}5)$$

$$q = \frac{W_c}{\pi c d}$$

where, as before, W_c is the compactor deadweight and 2c and 2d are, respectively, the width and length of the contact area.

The subsurface strain fields generated by such a distribution may be obtained by a difficult integration. A somewhat simpler approach is to treat the static contact stress distribution as we did the dynamic contact stresses. We again discretize the contact area into elemental strips whose individual loads are assumed uniform. We then determine the magnitudes of the elemental loads by applying Eq. 6.3-5 at the center of each strip. The strains generated by each elemental load are then to be had from Eq. 4.4-2 and from Hooke's Law, and by superposition we finally obtain the static component of strain at any subsurface point of interest.

The evaluation of the integral in Eq. 4.2-4 yields the complex representation of the dynamic component of strain in terms of the contact stress. Again, the contact stress distribution is discretized (its computation is outlined in Section 5) and superposition is applied to obtain the dynamic strain ε_D at a point. The phasor representation of the strain in Eq. 6.3-3 derives from treating the applied force as

$$F_a(t) = m\, e\, \omega^2\, e^{j\omega t}$$

$$= m\, e\, \omega^2\, (\cos \omega t + j \sin \omega t).$$

If instead we write

$$F_a(t) = m\, e\, \omega^2 \cos \omega t$$

then the dynamic strain may be characterized as

$$\begin{aligned} \varepsilon_D(t;z) &= \mathrm{Re}\ \{\hat{\varepsilon}(x(t),z)\ e^{j\omega t}\} \\ &= (\mathrm{Re}\ \hat{\varepsilon}) \cos \omega t - (\mathrm{Im}\ \hat{\varepsilon}) \sin \omega t. \end{aligned} \tag{6.3-6}$$

In numerically integrating the expression for residual stress over time, it is necessary to employ the static and dynamic strains at numerous instants (at least several times per vibration cycle). It is not computationally feasible to evaluate the static and dynamic components of strain on the correspondingly dense spatial mesh (because some thousands of integral evaluations would be required). However, the strain fields are sufficiently smooth that a somewhat coarser mesh will suffice as a basis for linear interpolation at intermediate points. Figure 6-8 illustrates the discretization that was employed in the computation of the contact stresses and subsurface strains, for both static and dynamic loading. We note in passing that, although Eq. 6.3-6 can be represented as a single sinusoid with a phase lag, the bi-harmonic representation is more suitable for interpolation, since some ambiguity may arise in the selection of the appropriate value of the phase angle. The results described in this study were obtained by separate interpolations in the real and imaginary parts of the dynamic strain.

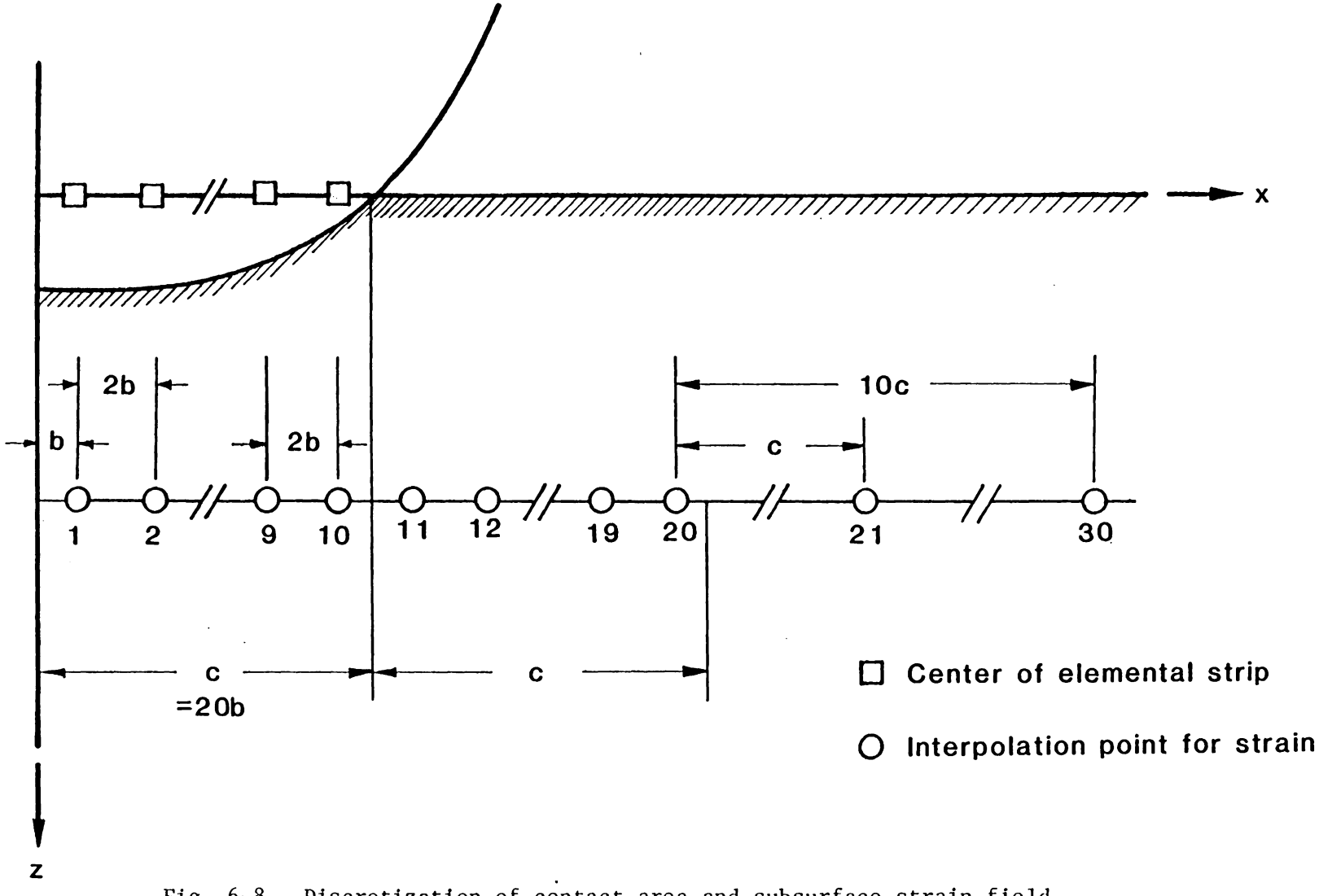

Fig. 6-8. Discretization of contact area and subsurface strain field.

Having the strain field so characterized, the elastic stress may be evaluated immediately using Eq. 6.1-2. The value of Young's modulus E has been permitted to vary with depth and range from the compactor in the computation of the elastic stress, since the spatial variation in confining pressure is directly calculable from the expressions in Section 4.4.

Finally, the residual stress may be obtained by numerically integrating Eq. 6.2-4. Although direct numerical integration is feasible, the author has chosen to rewrite the expression as a differential equation:

$$\dot{\sigma}_p = \alpha_4 \dot{\varepsilon} \{\sigma_e - E\ \varepsilon\}$$

and has used a variable-step Runge-Kutta integration. The Runge-Kutta algorithm affords an estimate of the relative error at each step and adjusts the step size accordingly (49). Moreover, the Runge-Kutta method is easily adapted to a vector representation, so that the residual stresses at several depths may be obtained simultaneously.

The integration is initialized at a large distance (16 ft = 5 m) ahead of the compactor and is continued until the drum has advanced a similar distance beyond the elements. At the end of the pass, the residual stress is averaged over the depth mesh. The averaged residual stress is considered to augment the horizontal components σ_x and σ_y of the average confining pressure,

$$\bar{\sigma}_o = \frac{\sigma_x + \sigma_y + \sigma_z}{3}$$

so that the average pressure is augmented by one third of the computed change in the average residual stress. That is, if we consider the confining pressure at the beginning of a pass (t_1) and at the end of a pass (t_2),

$$\bar{\sigma}_o(t_1) = \frac{[\sigma_x + \sigma_y + \sigma_p(t_1)] + \sigma_z}{3}$$

$$\bar{\sigma}_o(t_2) = \frac{[\sigma_x + \sigma_y + \sigma_p(t_2)] + \sigma_z}{3}$$

$$= \bar{\sigma}_o(t_1) \frac{1}{3} [\sigma_p(t_2) - \sigma_p(t_1),$$

where σ_x, σ_y, and σ_z are taken as identical at t_1 and t_2 because the initial and final points are equidistant from the compactor. The new value of the confining pressure is then used to update the estimates of the overall elastic moduli, for use in the simulation of the next pass.

7. RESULTS AND DISCUSSION

In this chapter we investigate the possibilities of improving compactor performance through several strategies:

(1) redistributing the weight of the frame towards or away from the drum (Section 7.2);

(2) varying the forward speed of the compactor (Section 7.3);

(3) implementing a controller that will track the change in the system resonant frequency from one pass to another (Section 7.4).

The results presented in this chapter estimate the effects of various parameters on the compaction process. The approach taken in the investigation was to vary one parameter at a time while holding all others constant. It was therefore necessary to select certain "default" values. These are tabulated in Appendix A, Table 2. We emphasize that, unless stated otherwise in the discussion below, the value of every parameter is that given by Table A-2.

The predictions made by the linear compactor-soil model using the default values are shown in Figs. 7-1 and 7-2. The soil model employed is that of previously uncompacted earth; that is, the elastic moduli are those predicted by the model on the first pass, without adding in the effects of induced stress. We note several characteristics of these frequency-response functions that seem to hold true in all the cases examined in this investigation:

(1) Two resonance peaks are observed in the response functions for drum displacement, frame displacement, and force transmitted to the

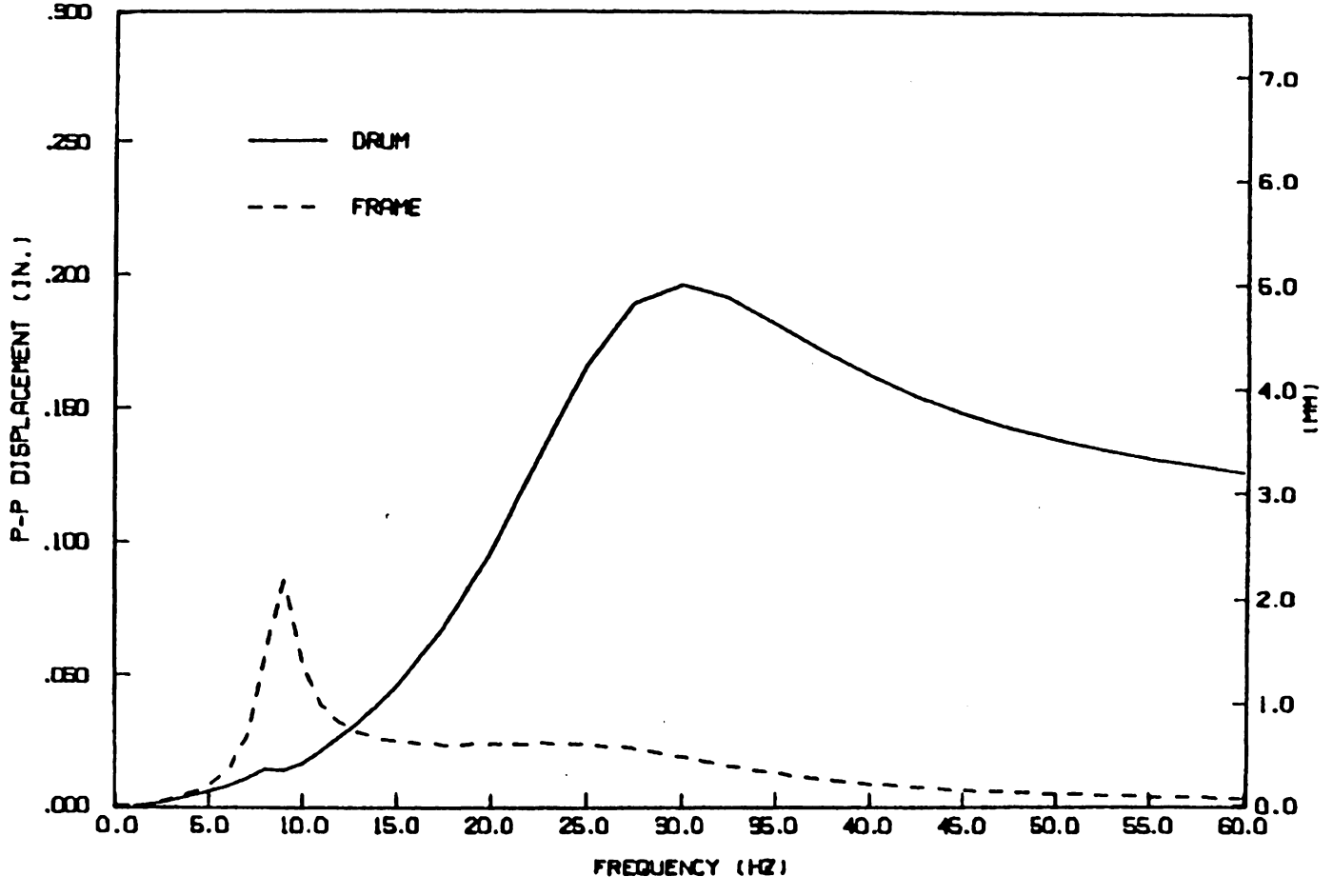

Fig. 7-1. Drum and frame displacement amplitudes for default parameter values.

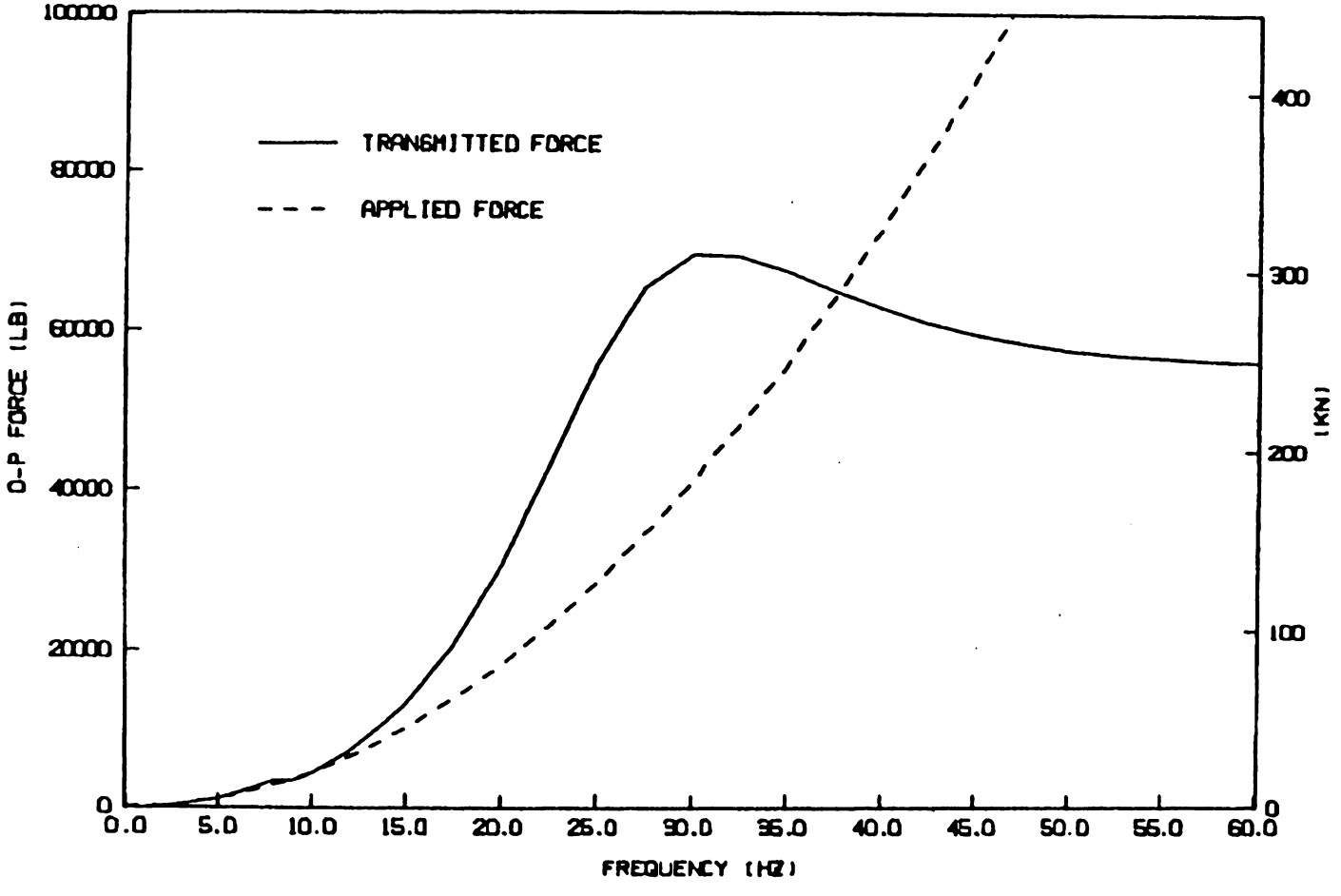

Fig. 7-2. Applied force and force transmitted to soil for default parameter values.

soil. The lower resonant frequency occurs in the range of 5 to 10 Hz and its effects are most pronounced for the frame motion; its presence is barely discernible in the plots of the drum motion and the transmitted force. By contrast, the resonance peak in the range of 25 to 30 Hz seems merely to weaken the high-frequency roll-off in the frame motion, but it magnifies considerably the amplitudes of the drum motion and transmitted force. The implications for design and operation of a compactor are fortunate, since one would like to maximize the transmitted force while minimizing frame vibrations (in the interest of increased operator comfort and reduced maintenance). Most vibratory roller compactors of the size treated here are designed to operate in the range of 20 to 30 Hz, so that, for single-pass compaction at least, they are likely to be operating near the optimum frequency.

(2) The transmitted force is maximized at the same frquency (or slightly higher, by 2 or 3 Hz) as the drum motion. Thus, if the interest is in maximizing the transmitted force, it should prove sufficient to measure the drum motion to determine whether operation is at resonance. (A double integration of an accelerometer output would yield the drum displacement.) We note that, although increasing the operating frequency causes the generated force to grow without bound, the transmitted force slackens and appears to reach a constant value. The implication is that the effectiveness of a compactor cannot be improved simply by driving the eccentric at higher speeds to generate a large force.

(3) The frequency dependence of the magnitudes of both the drum motion and the transmitted force are markedly lopsided. Operation below the resonant frequency incurs a severe penalty in the force transmitted, while operation above resonance is only slightly suboptimal. For operation at a constant frequency, or in the absence of good estimates of soil properties, one should select as high a frequency as possible. As the soil stiffens with repeated coverage, the resonance peak will shift to the right on the frequency-response diagram, but if the initial operating frequency is sufficiently high, the compactor will remain on the "plateau" to the right of the peak. (This is a conclusion at which Converse (11) arrived through experimentation.)

Figure 7-3 illustrates the growth of residual stress with each pass of the compactor for the various default conditions. It also illustrates a deficiency of the model, in its failure to treat plastic failure at the soil's surface (16). The contact stresses immediately beneath a heavy, rigid drum typically exceed the ultimate strength of the soil, so that a small zone of plastic failure occurs. But since the upper foot or two of the sandy soils modeled here do not usually benefit from compaction anyway (11), the failure to treat this region accurately is of lesser concern.

All of these characteristics exhibited by the model were observed in the cases discussed below and are not influenced by the selection of the default parameters: the frame and drum weights and inertias, the suspension stiffness and damping, the contact area dimensions, the

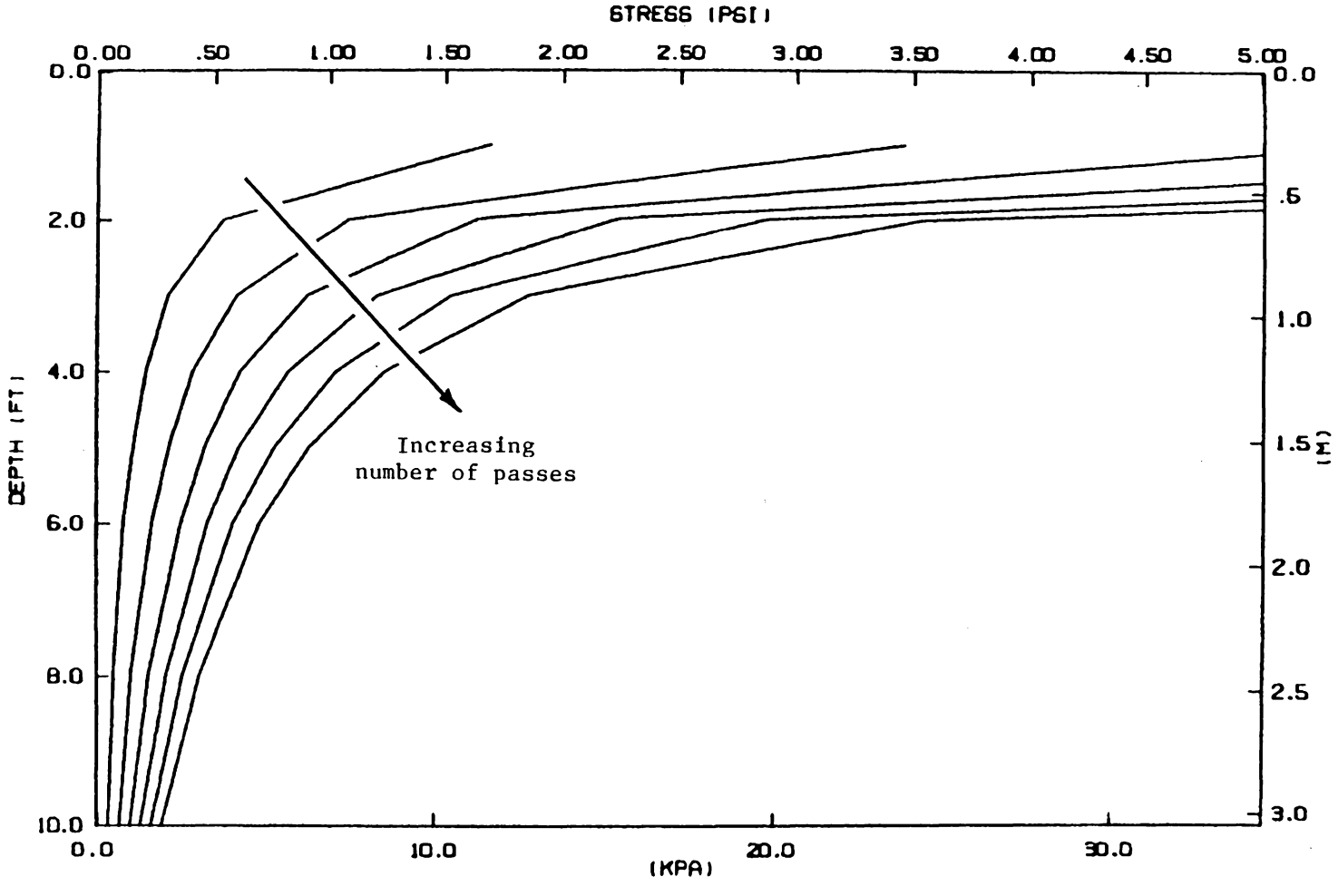

Fig. 7-3. Residual stress profiles for default parameter values. (30 Hz operating frequency)

elastic moduli of the soil, and the parameters appearing in the nonlinear constitutive equations. The compactor weights and suspension stiffnesses were obtained from manufacturors' data, and the computation of the lumped inertias was discussed in Section 3. The elastic moduli of the soil were shown in Section 4.4 to depend on the confining pressure and void ratio. The method of estimating the material constants α_3 and α_4 was described in Section 6. Thus, the only parameters requiring estimation are the contact area width, the average confining pressure, and the void ratio.

The sensitivity of the model to these three parameters is therefore discussed in the following paragraphs as a preface to the discussion of the results of the optimization studies.

7.1 Model Sensitivity to Input Parameters

A value of 9 inches (230 mm) was assumed for the average width (2c) of the contact area during vibration. The static sinkage corresponding to such a dimension is 0.36 in. (9 mm). Referring to Fig. 7-1, the maximum amplitude of the drum vibration (at resonance) is 0.1 in. (3 mm) zero-peak, so that the drum and the soil at the center of contact should remain in contact over one cycle, with a variation in the contact area of -15 percent and +13 percent at the extremes of motion. For the compactor modelled here, our failure to consider variation of the contact area over time would not appear to warrant concern.

The effects of assuming other values for the contact area are shown

in Figs. 7-4, 7-5, and 7-6. Model predictions for six-inch, nine-inch, and twelve-inch widths are shown. The resonant frequency for the widest area is about 7 Hz higher than that for the narrowest area, for the amplitudes of both the drum displacement and the transmitted force. But while the value assumed for the contact area width has a strong effect on the estimated magnitude of drum displacement at resonance, it exerts hardly any effect on the prediction of the maximum force transmitted. Moreover, the high-frequency roll-off in the transmitted force is rather gentle, so that the uncertainty in the model's prediction of the peak frequency is less damaging.

In Section 4.4 it was noted that variations in the void ratio during compaction were not accounted for by the model and probably represent its most serious failure. Unfortunately, the evidence of Figs. 7-7, 7-8, and 7-9 substantiates this conjecture. These figures compare model predictions for void ratios of 0.6, 0.8, and 1.0. As with the effects of uncertainty in the contact area, the conceivable variations in the void ratio introduce a band of uncertainty of about ±5 Hz in the value of the peak frequency. This time, however, it is the magnitude of the transmitted force at resonance and higher frequencies that shows sensitivity to the assumed value of the parameters, whereas the peak response of the drum motion is nearly unaffected. The model simply fails to account for a great deal of stiffening that occurs in compaction through the reduction in void ratio, and therefore it will consistently underestimate the rate of increase in the peak frequency.

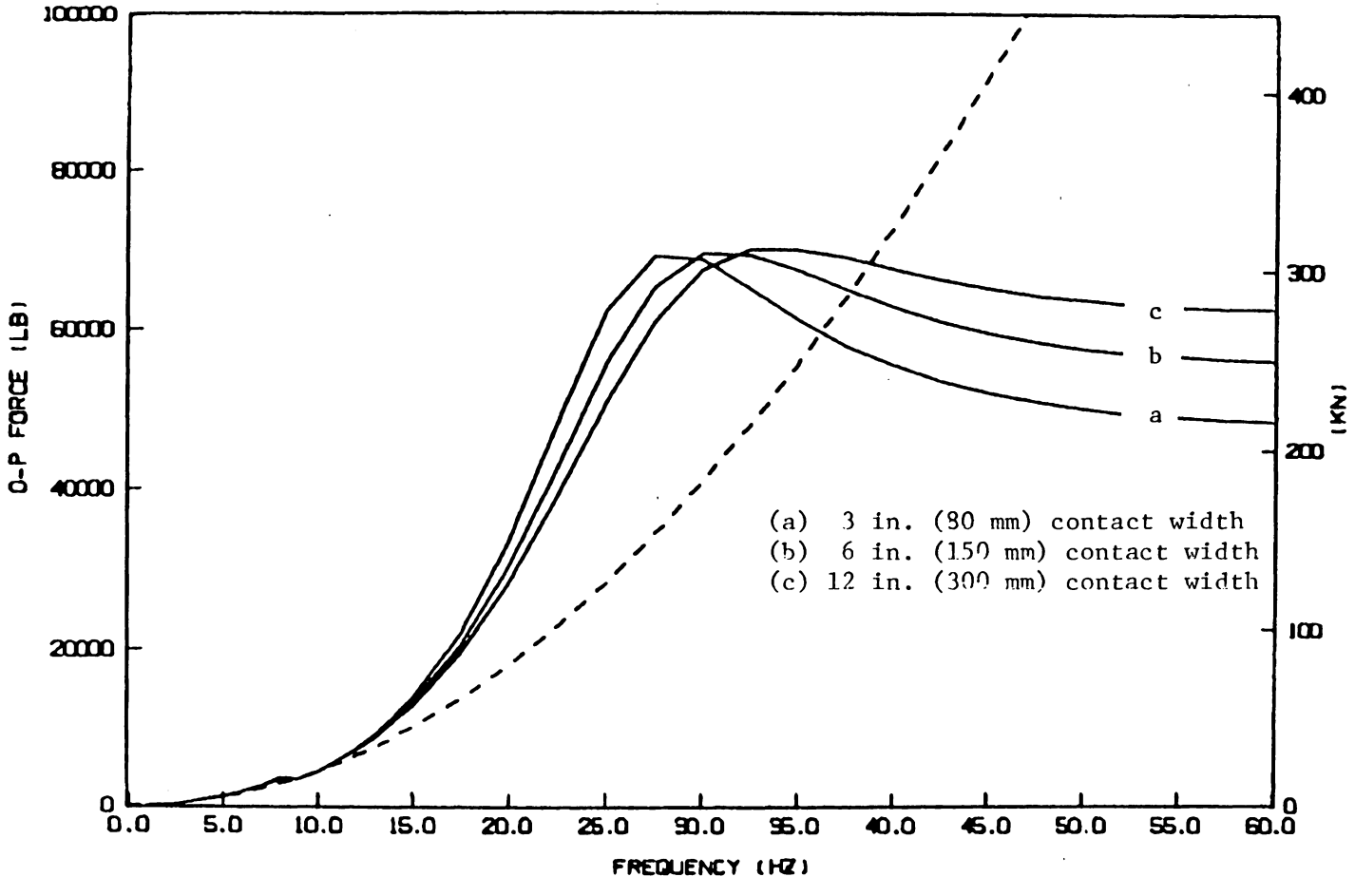

Fig. 7-4. Effect of assumed contact width on prediction of transmitted force.

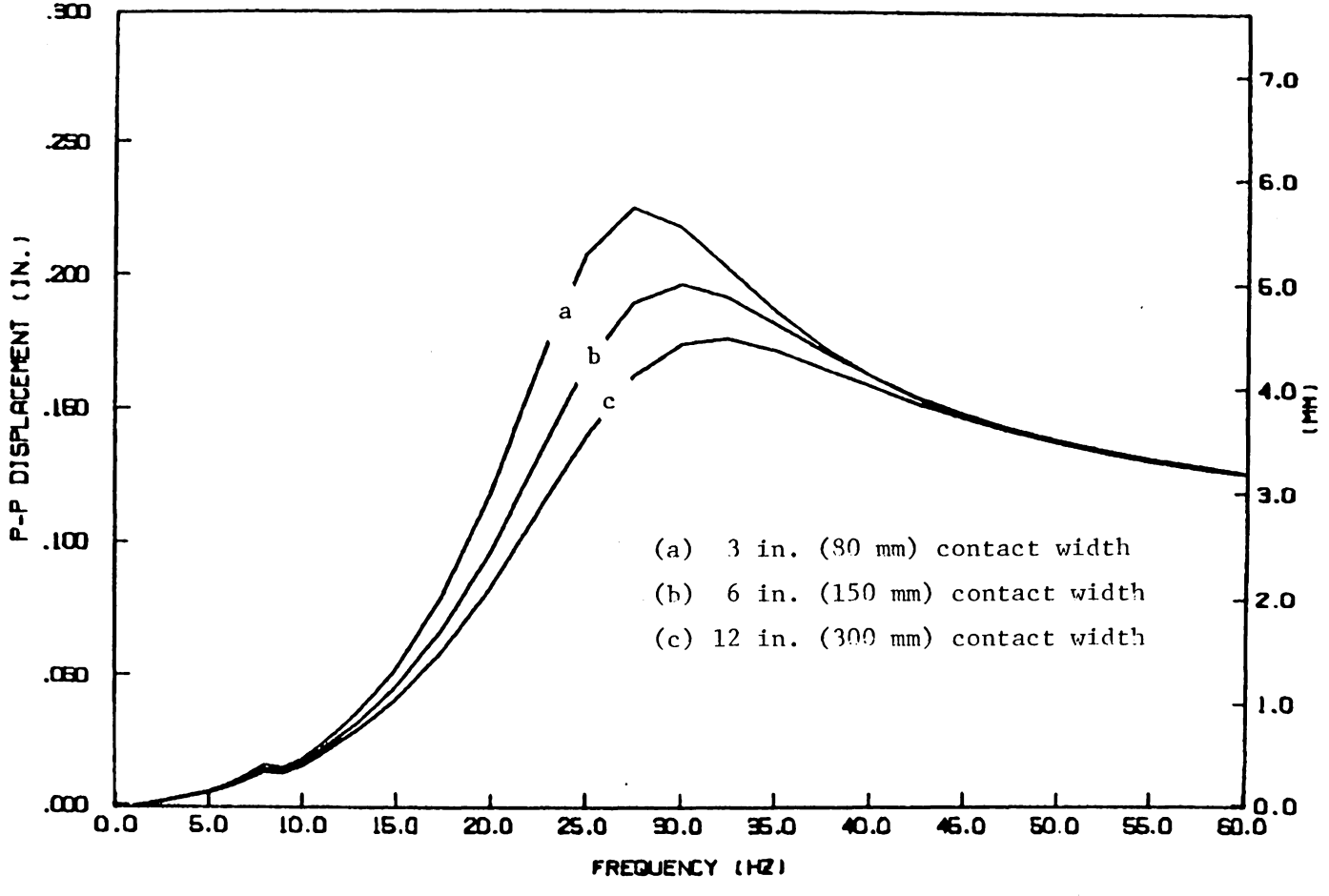

Fig. 7-5. Effect of assumed contact width on prediction of drum displacement amplitude.

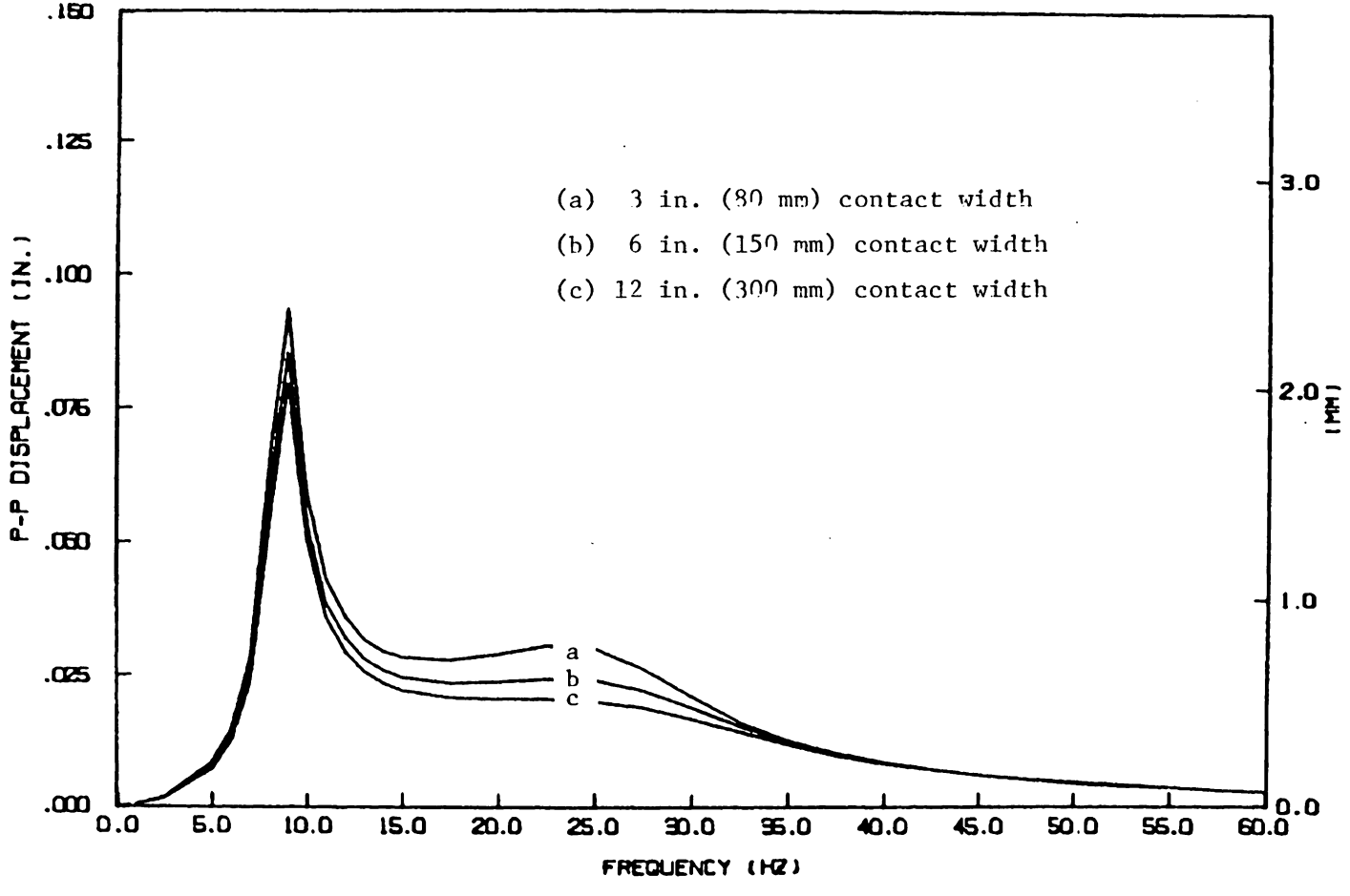

Fig. 7-6. Effect of assumed contact width on prediction of frame displacement amplitude.

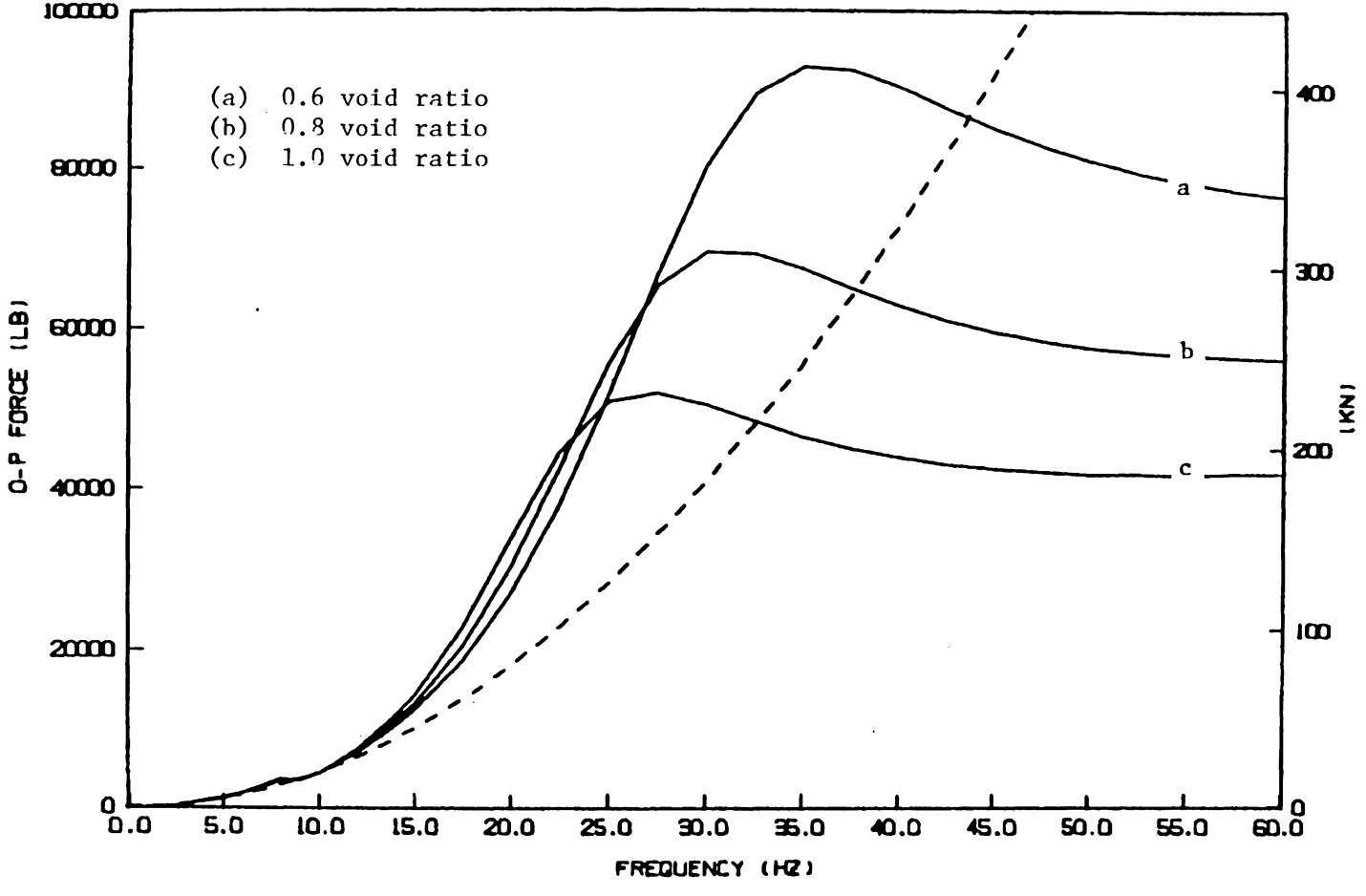

Fig. 7-7. Effect of assumed void ratio on prediction of transmitted force.

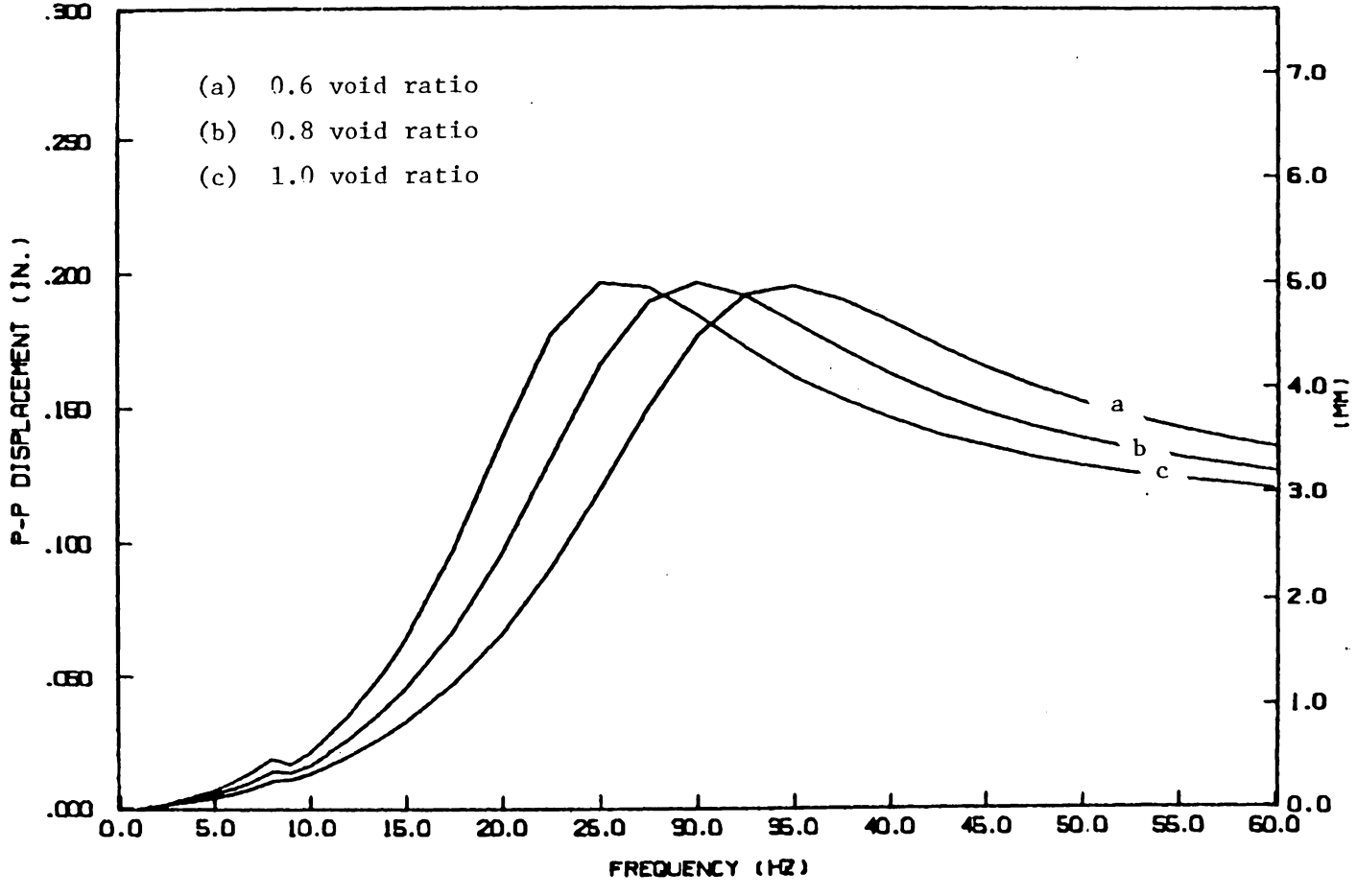

Fig. 7-8. Effect of assumed void ratio on prediction of drum displacement amplitude.

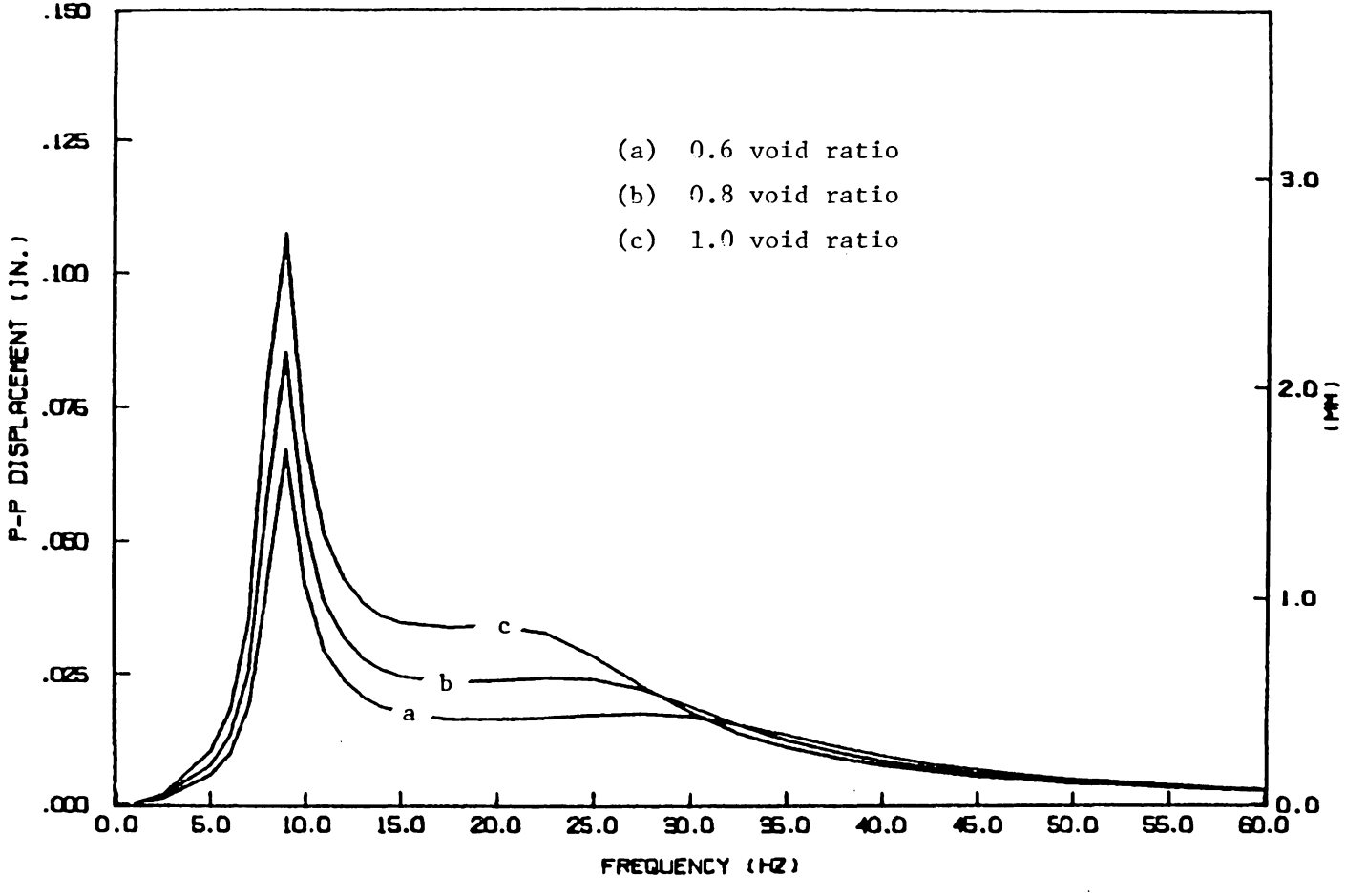

Fig. 7-9. Effect of assumed void ratio on prediction of frame displacement amplitude.

Although damaging to the model's credibility, the failing is less severe than it initially appears. Figures 7-10, 7-11, and 7-12 show the effects of assuming different values for the average confining pressure: pressures of 2, 3, and 5 psi (14, 21, and 34 kPa) are compared. The effects are almost identically those of varying the void ratio. The model of the compaction process employed in this study does treat the variation in confining pressure as compaction proceeds, through its computation of the induced stress. The trends in the two quantities with increasing compaction--toward lower void ratios and higher pressures--cause the same sorts of shifts in the frequency-response characteristics, since both processes increase the soil stiffness. It was noted in Section 6.2 that the parameter α_4 controls the rate of growth of residual stress predicted by the nonlinear relations. It would appear that an adjustment to α_4 which would cause it to overestimate the residual stress would successfully mimic the effects of void ratio reduction. This is not surprising since, first, the void ratio and residual stress (which contributes to the confining pressure) enter into the compactor dynamics in the same fashion--by increasing the elastic moduli. Second, Brumund and Leonards (10) argue that the densification provided by compaction is related to the work transmitted to the soil, and our model of the growth of residual stress is couched in precisely such terms.

Therefore, an empirical correlation between the two processes of void reduction and stress inducement might do much for the accuracy of

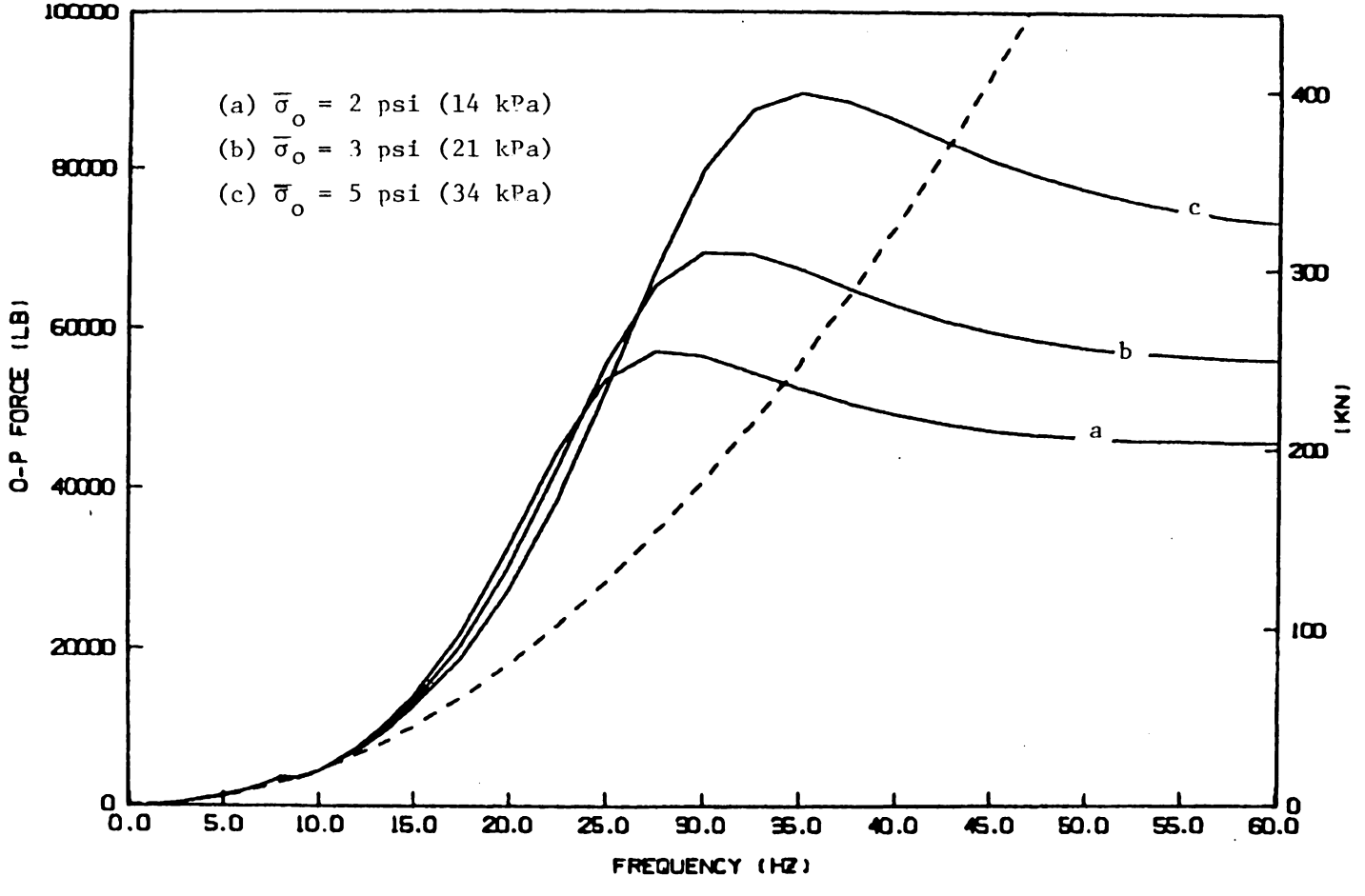

Fig. 7-10. Effect of assumed confining pressure on prediction of transmitted force.

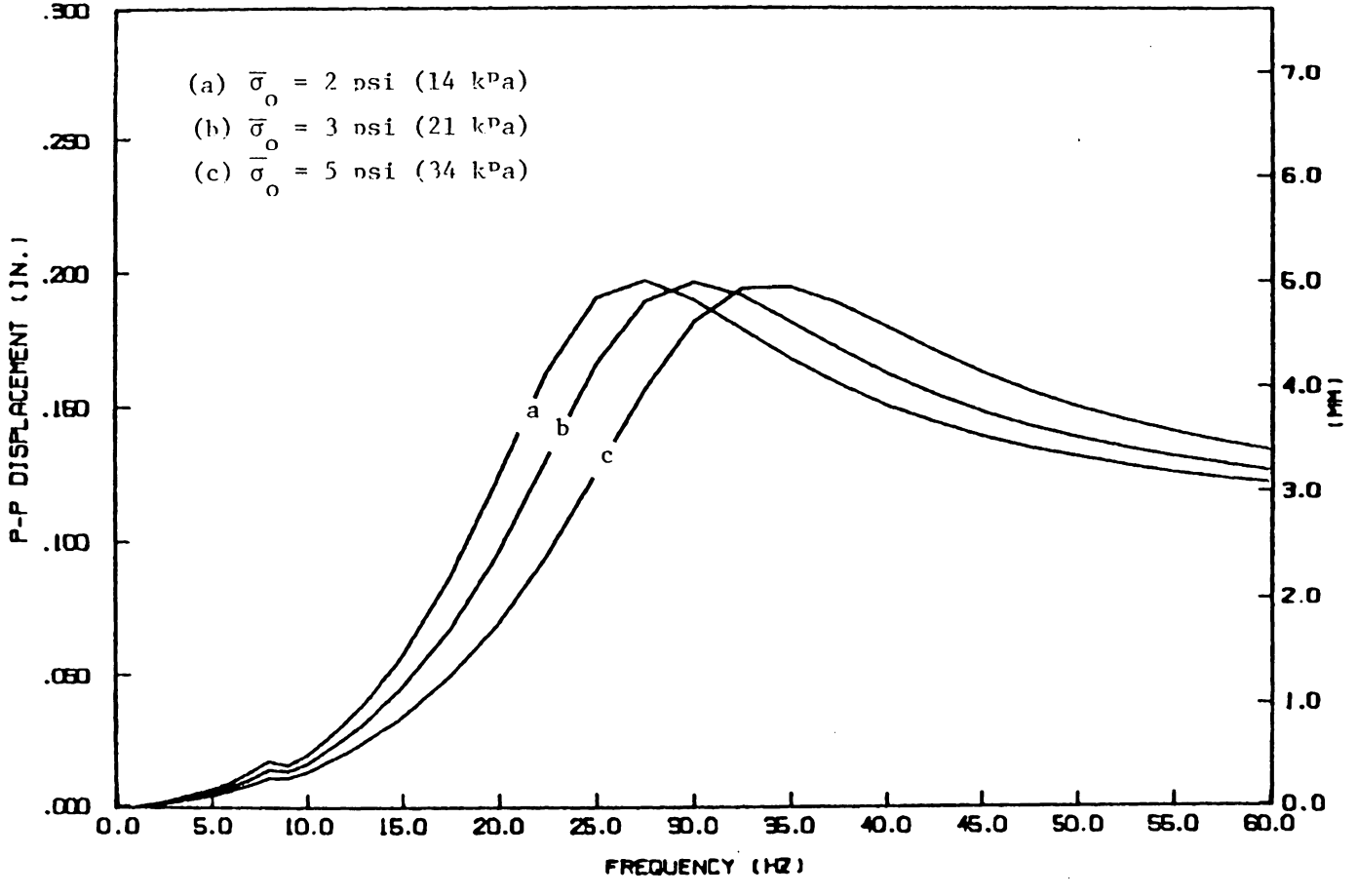

Fig. 7-11. Effect of assumed confining pressure on prediction of drum displacement amplitude.

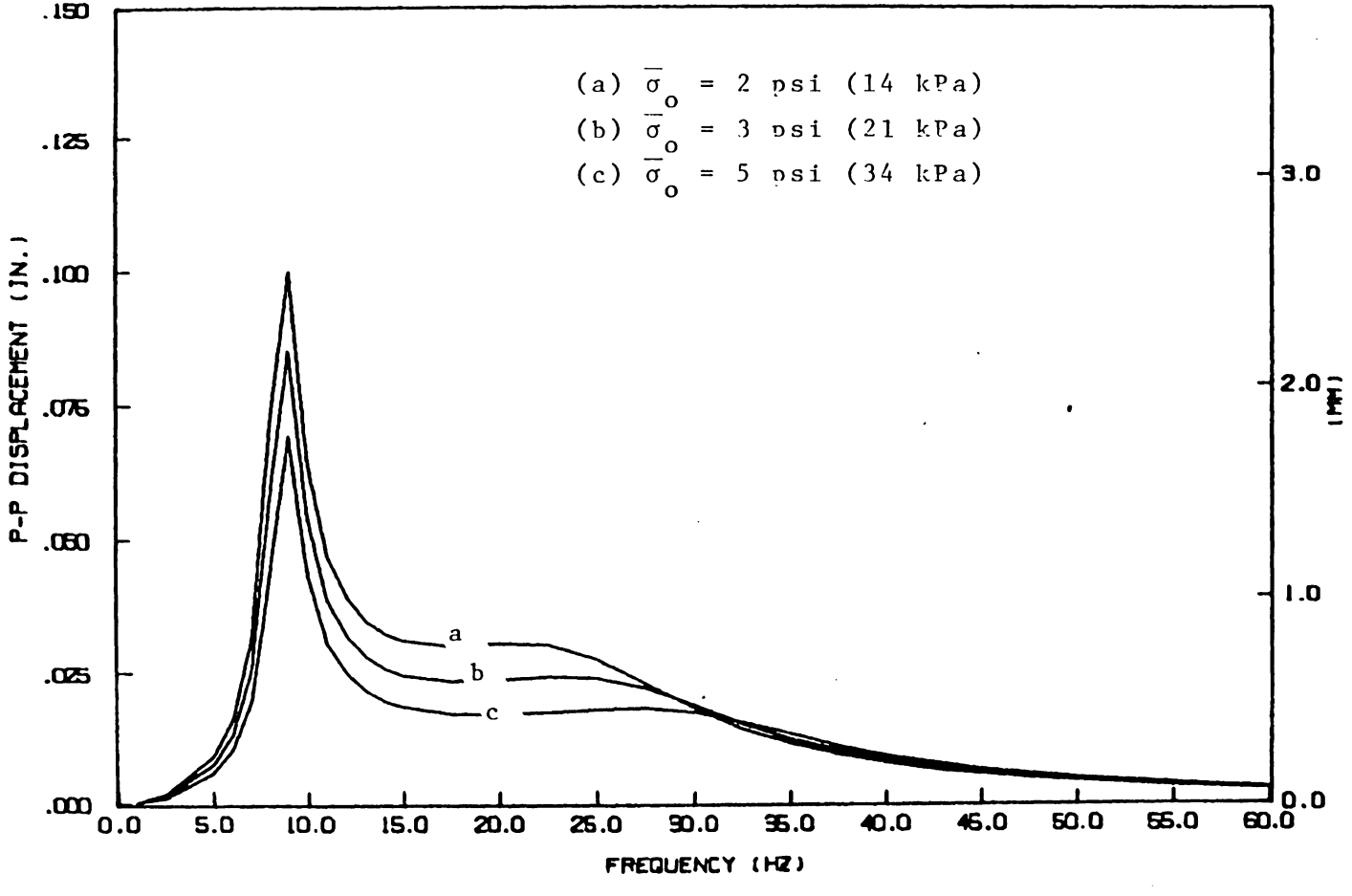

Fig. 7-12. Effect of assumed confining pressure on prediction of frame displacement amplitude.

the model's prediction of the soil and compactor dynamics. Although such a correlation has not been implemented here, we note that any trends suggested by the predicted growth of residual stress are merely reinforced by the process of void reduction, so that some generalizations from the model predictions are still in order.

7.2 Effects of Redistributing Frame Weight

A redistribution of the weight of the frame towards the drum will have several effects:

(1) The static sinkage at the drum will be greater, producing a larger contact area.

(2) The static component of stress in the soil will be increased, but not in direct proportion to the change in weight, since the contact force is spread over a large area.

(3) The average confining pressure in the soil directly beneath the drum will be greater, providing a temporary stiffening in the soil mass that will increase the frequency of resonance.

(4) The effective inertia of the frame will be raised.

The first and third effects both yield an increase in the frequency of resonance. The effect of increasing the contact area is to decrease the amplitude of drum motion at resonance and higher frequencies, while increasing the transmitted force at higher frequencies but leaving the magnitude at resonance unaffected (Figs. 7-4 and 7-5). The effect of increased confining pressure is also to increase the transmitted force,

both at resonance and above. The amplitude of drum motion at higher frequencies is somewhat reduced, however, tending to cancel the effects of increasing the contact area. We note that the work performed on the soil (energy transmitted) depends on both the amplitudes of the contact force and the displacement of the soil surface under the drum, so that the overall effect on the compaction of all these processes is not to be had by inspection of their separate effects.

The interaction of these four effects was gauged in the following fashion. We consider cases where the mass distribution of the frame components is varied in such a way that the effective frame mass changes by -40, -20, 20 and 40 percent, while the total weight remains constant. The assumption is made that the mass is transferred from a point directly over the rubber tires to a point over the drum. Assuming that the effective frame inertia is 25 percent of the total frame mass to begin with, we in effect transfer -10, -5, +5, and +10 percent of the total frame mass to achieve the results stated above. The mass increment previously contributed nothing to the weight of the compactor at the drum, and after its transfer it contributes nothing to the weight at the tires. Therefore, a 40 percent change in the effective mass will produce a 10 percent change in the effective weight, and so forth.

The contact area is estimated to increase in proportion to the square root of the sum of the drum and effective frame weights. This result is predicted by the Hertz theory of contact stresses (17) (which in its entirety is not applicable here, since it assumes elastic

behavior at the contact surface, whereas the soil immediately surrounding the drum undergoes plastic deformation). The assumed proportionality is based on the soil's acting as a linear spring under static loading. The contact area is proportional to the square root of the static deflection. If the deflection is directly proportional to the static load, then we can treat the contact area width as also proportional to the square root of the load:

$$\frac{A_2}{A_1} = \frac{c_2}{c_1} = \sqrt{\frac{\delta_2}{\delta_1}} = \sqrt{\frac{W_2}{W_1}}$$

where the symbols A, c, δ, and W are, respectively, the contact area, contact width, vertical deflection, and total effective weight of the drum and frame.

Figures 7-13, 7-14, 7-15, and 7-16 show the combined effects of the variations in contact area and deadweight on the confining pressure directly beneath the drum. The differences are negligible for depths greater than a few inches, certainly far smaller than the variation of the confining pressure with depth, so that the nominal value of 3 psi (21 kPa) was retained. The weakness of the effect is probably explained by the stress relief associated with the increased contact area.

Thus, the contact areas and effective frame weights and masses were varied to simulate the cases outlined above. The results of the simulation are shown in Figs. 7-17 through 7-19. We note that increasing the frame mass reduces the amplitude of drum motion at

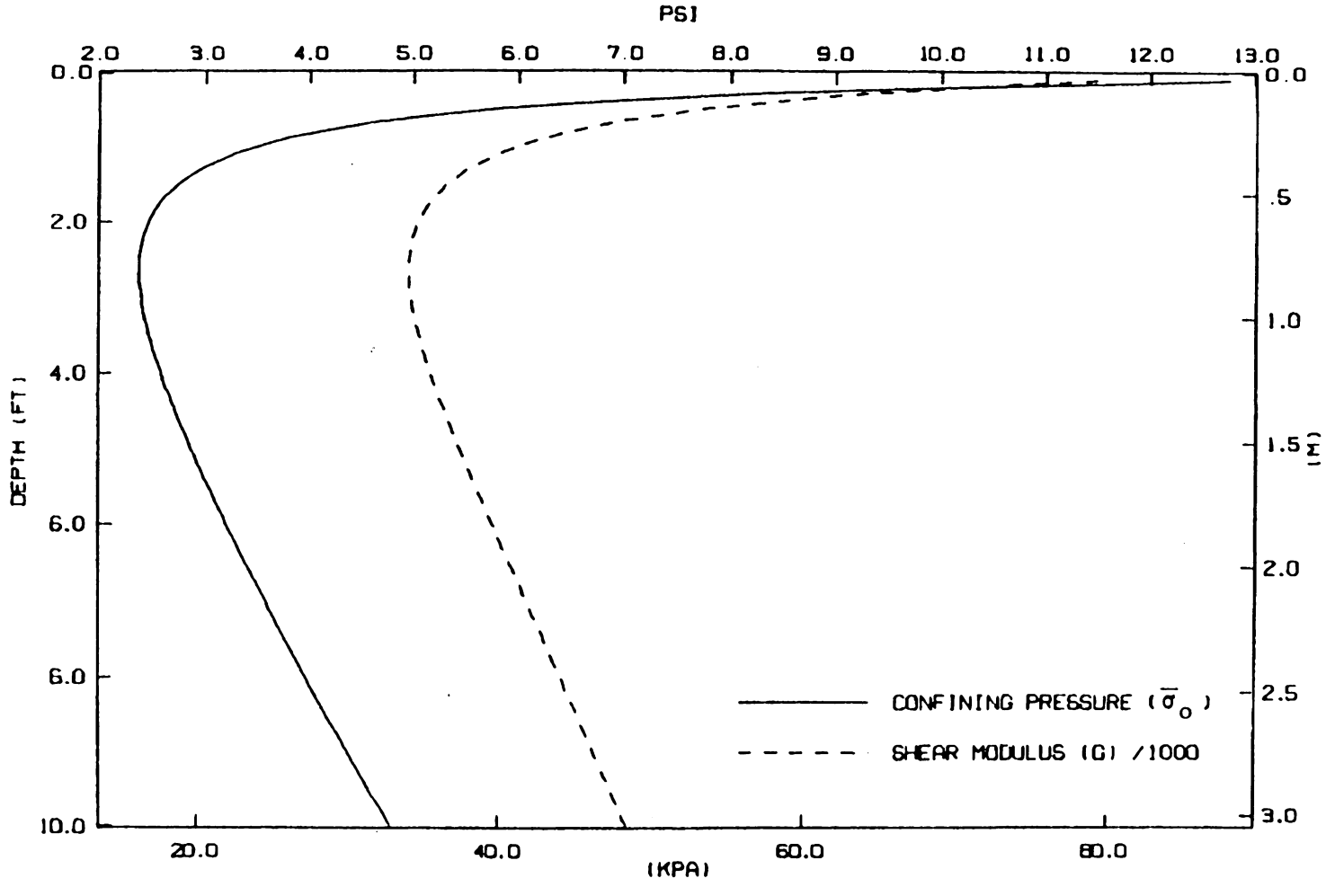

Fig. 7-13. Confining pressure beneath drum for 40% reduction in effective frame mass.

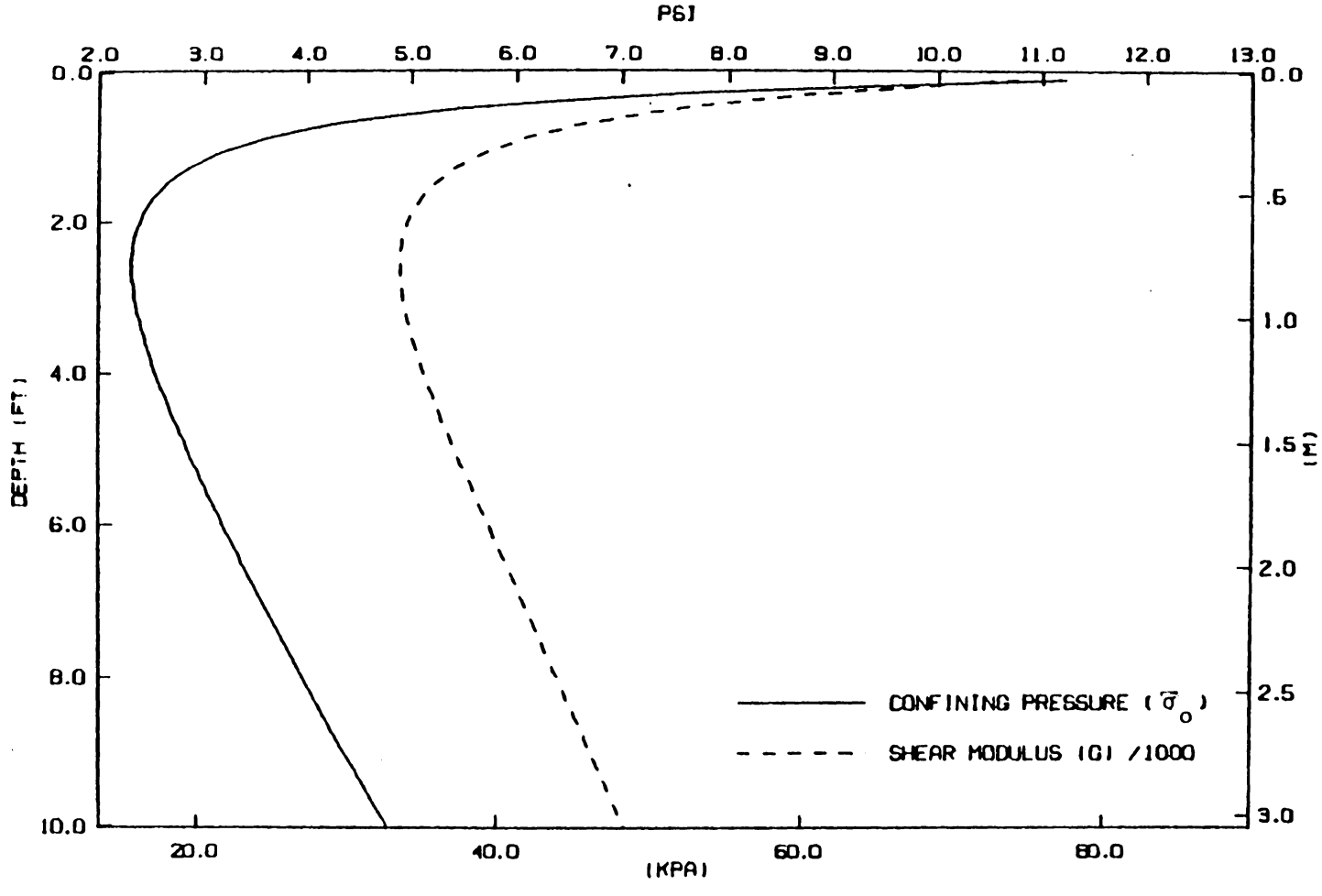

Fig. 7-14. Confining pressure beneath drum for 20% reduction in effective frame mass.

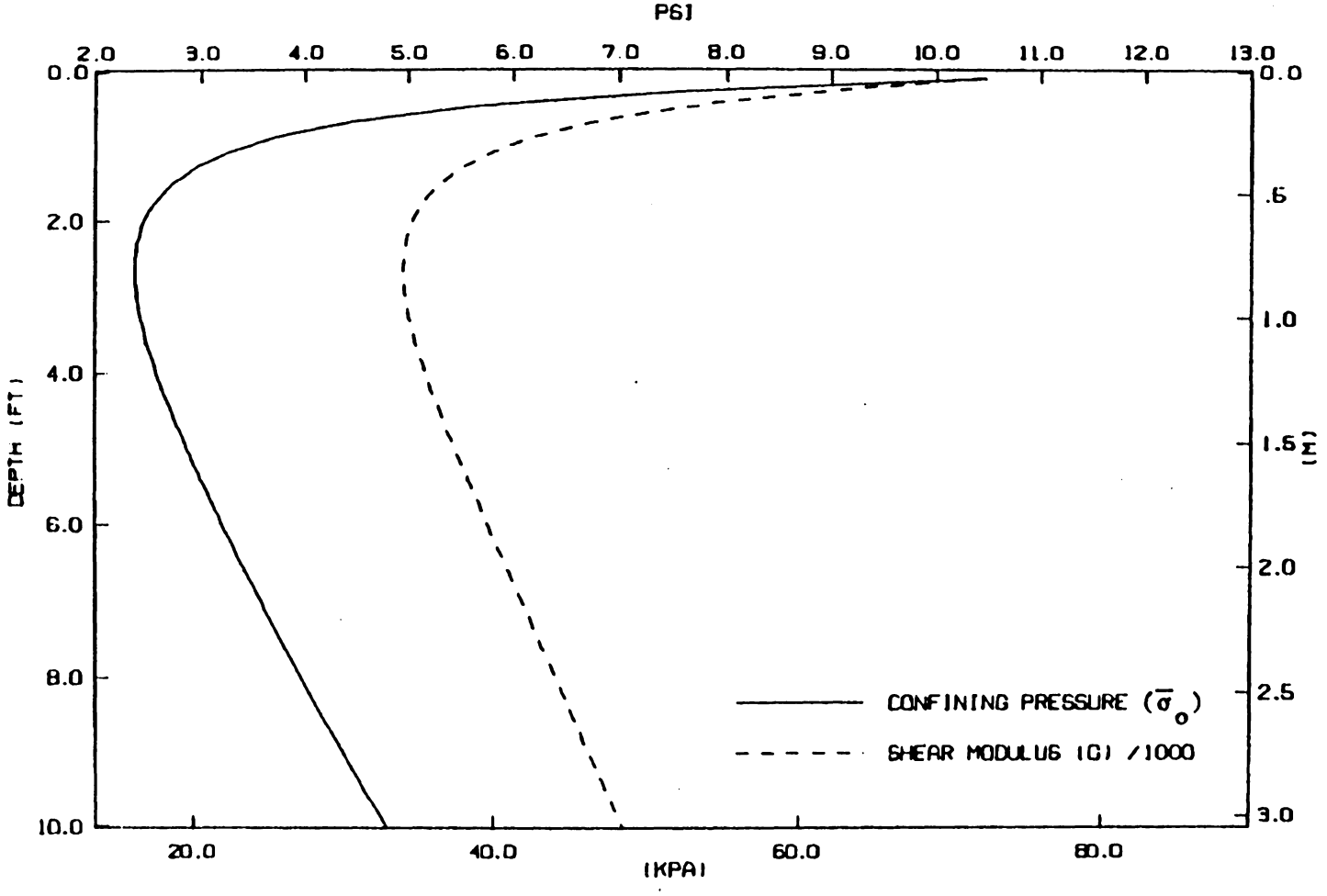

Fig. 7-15. Confining pressure beneath drum for 20% increase in effective frame mass.

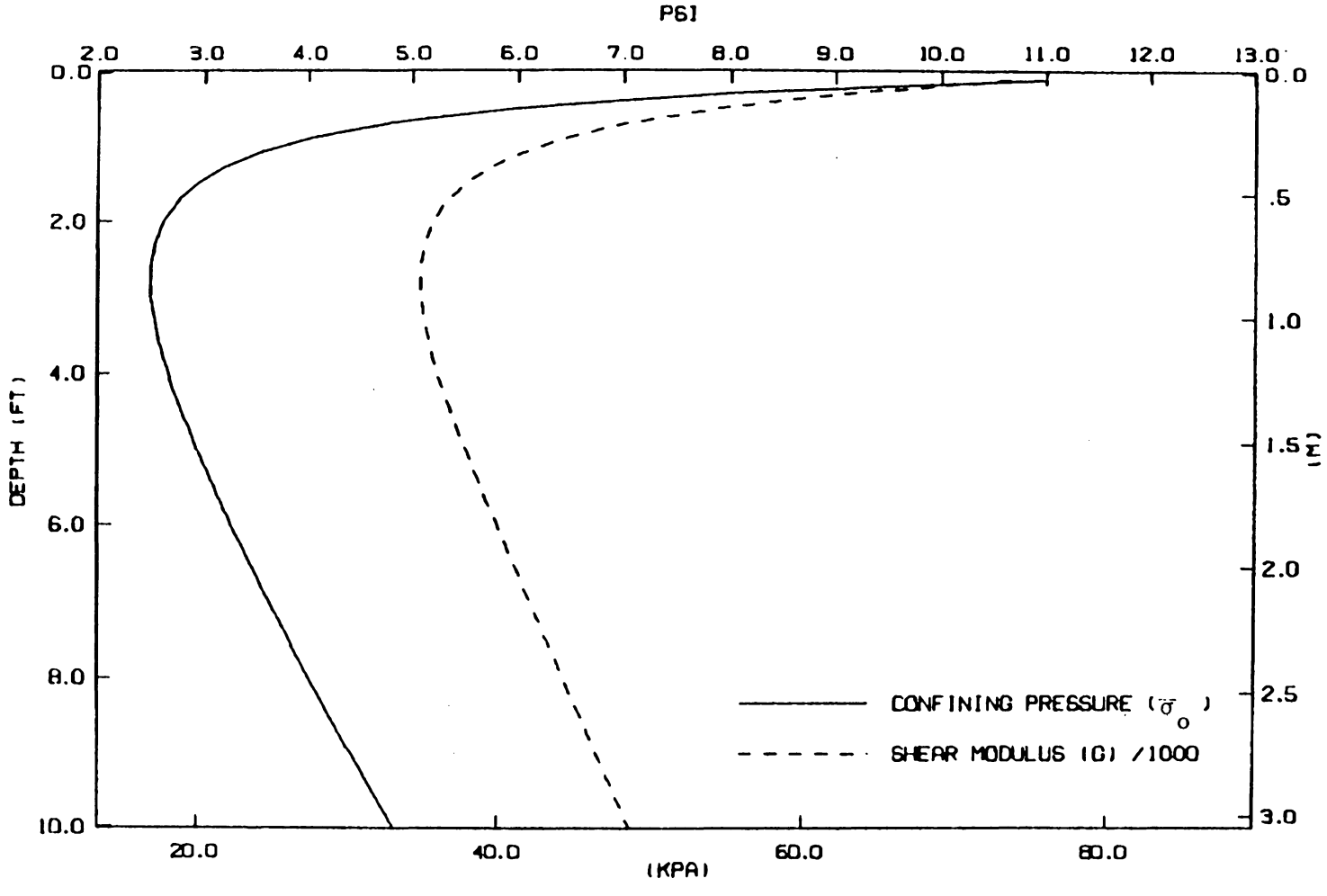

Fig. 7-16. Confining pressure beneath drum for 40% increase in effective frame mass.

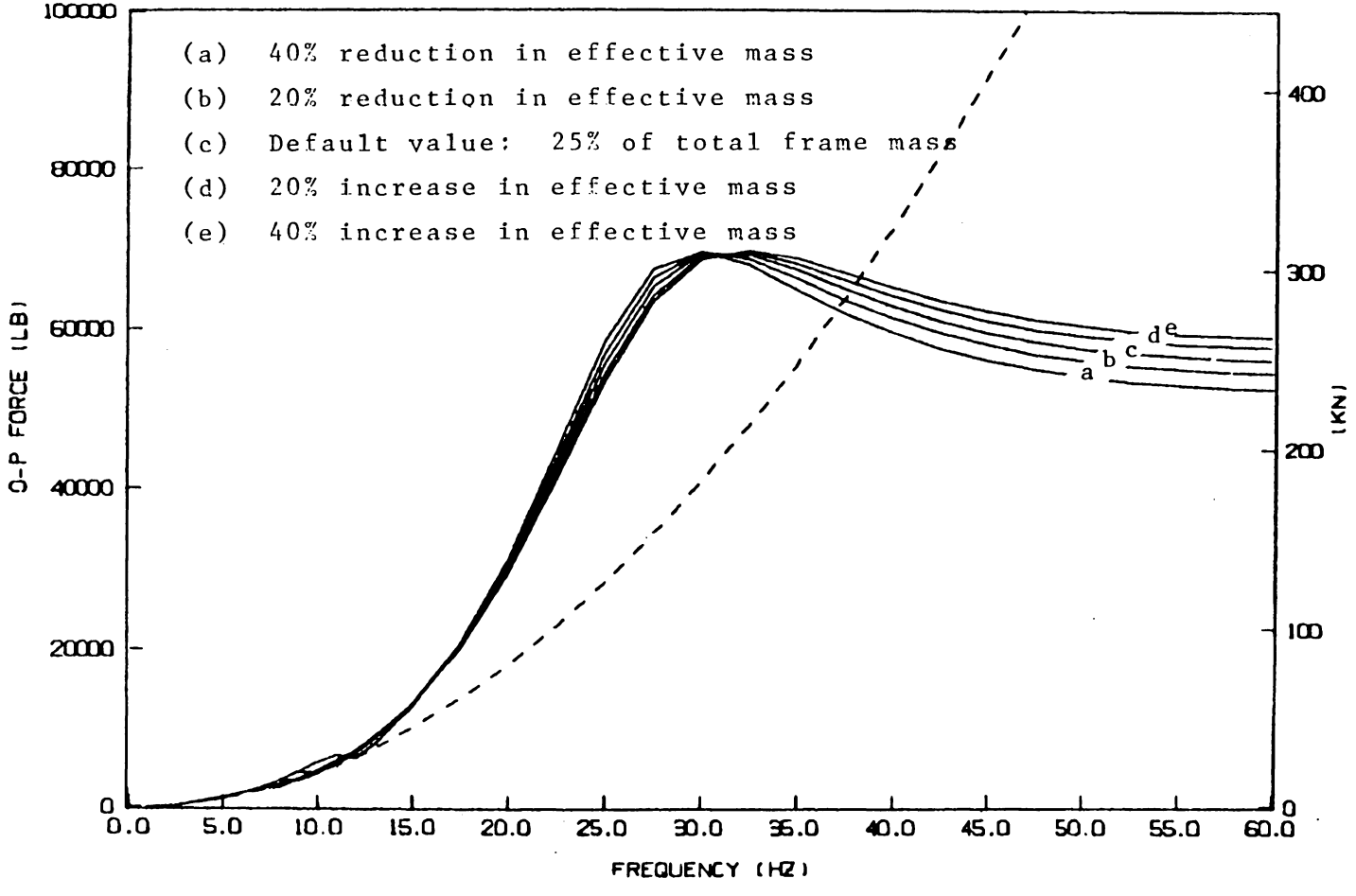

Fig. 7-17. Effect of frame weight redistribution on transmitted force.

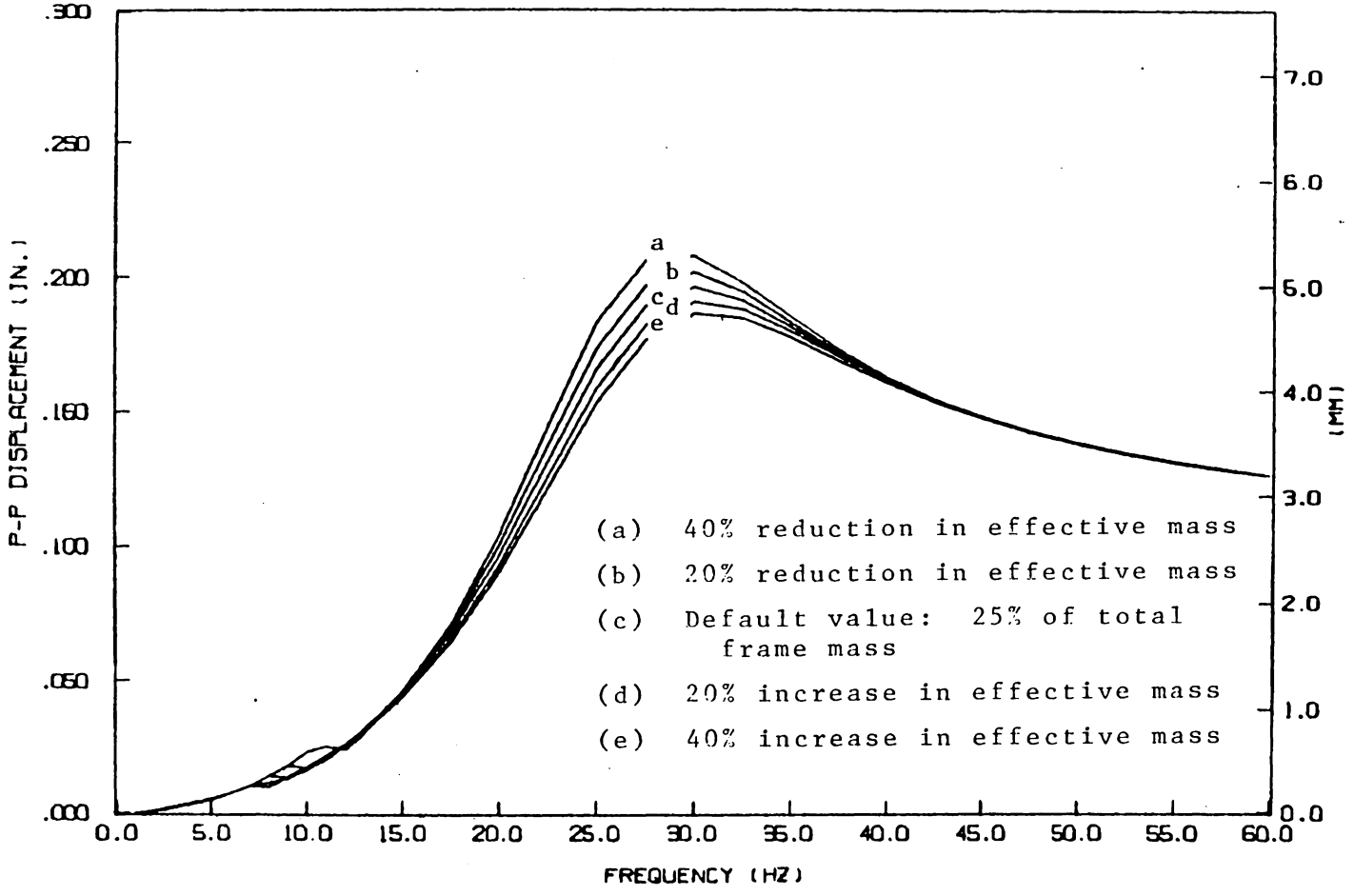

Fig. 7-18. Effect of frame weight redistribution on drum displacement amplitude.

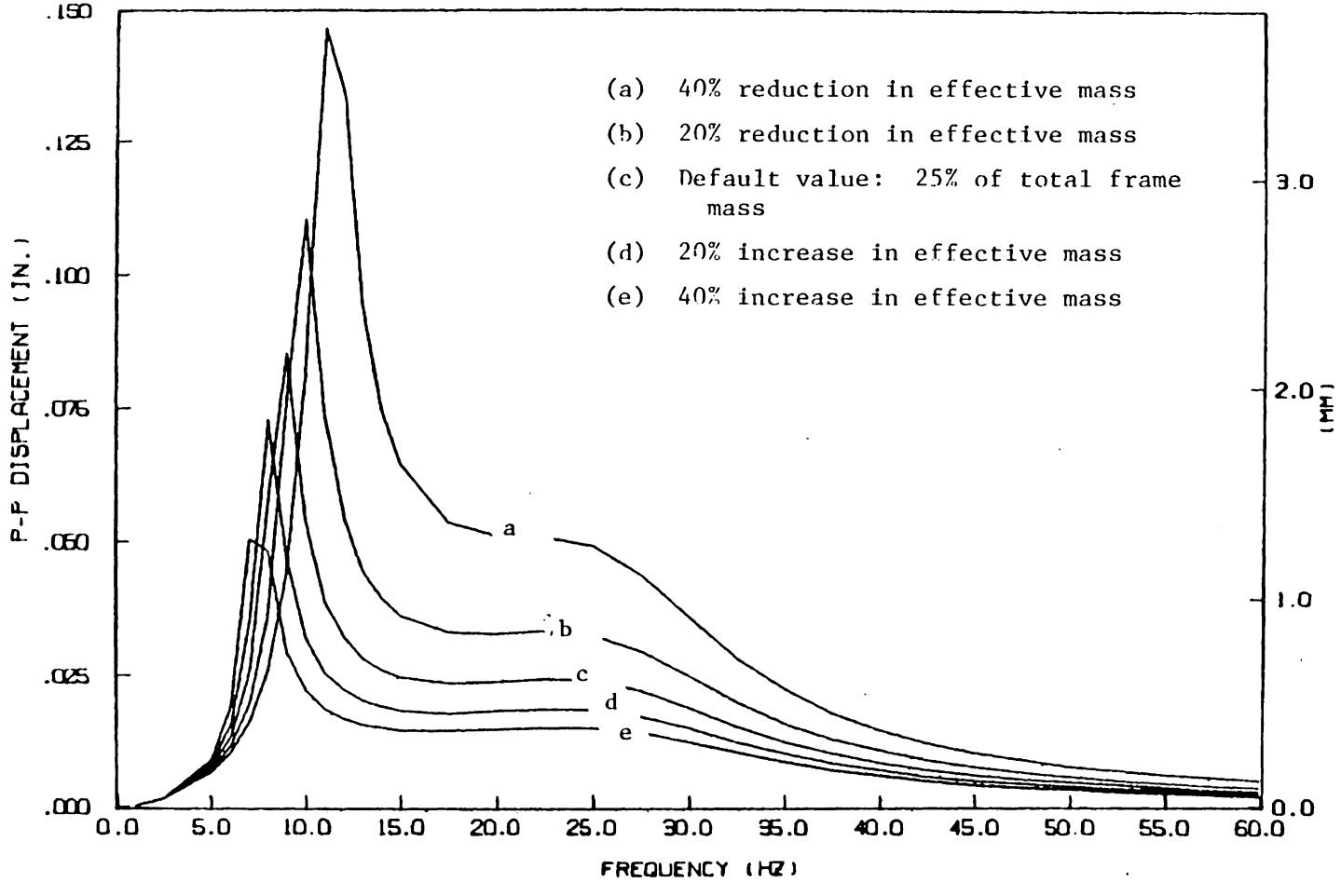

Fig. 7-19. Effect of frame weight distribution on frame displacement amplitude.

resonance but affects it very little at higher frequencies. The force transmitted to the soil at resonance, on the other hand, is hardly affected by reallocation of the weight but is magnified at higher frequencies by shifting the weight towards the drum.

These effects seem to owe more to the increased contact area than to any dynamic effect of the frame inertias. Figures 7-20, 7-21, and 7-22 show variations in the response function occasioned by changes in the effective frame mass of -40, -20, 20, and 40 percent, other parameters such as contact area and static weight being held constant. Practically no effect is exerted on the drum displacement or transmitted force. The frame's amplitude of vibration is magnified considerably by the reduction of its inertia, but this undesirable effect could be cancelled by increasing the suspension stiffness. The frame motion was noted previously to be not much affected by variations in contact area and confining pressure. The implication for design is that the frame mass may be distributed in such a way as to optimize compaction with no attendant increase in frame vibration if the suspension is suitably redesigned.

However, the nature of this optimal distribution is still somewhat ambiguous and seems to depend on the operating frequency. At resonance, the contact force is nearly independent of frame mass; the larger drum motion provided by the reduced frame weights should therefore maximize the energy transmitted to the soil. On the other hand, for operation above resonance the reverse situation occurs, with the contact force

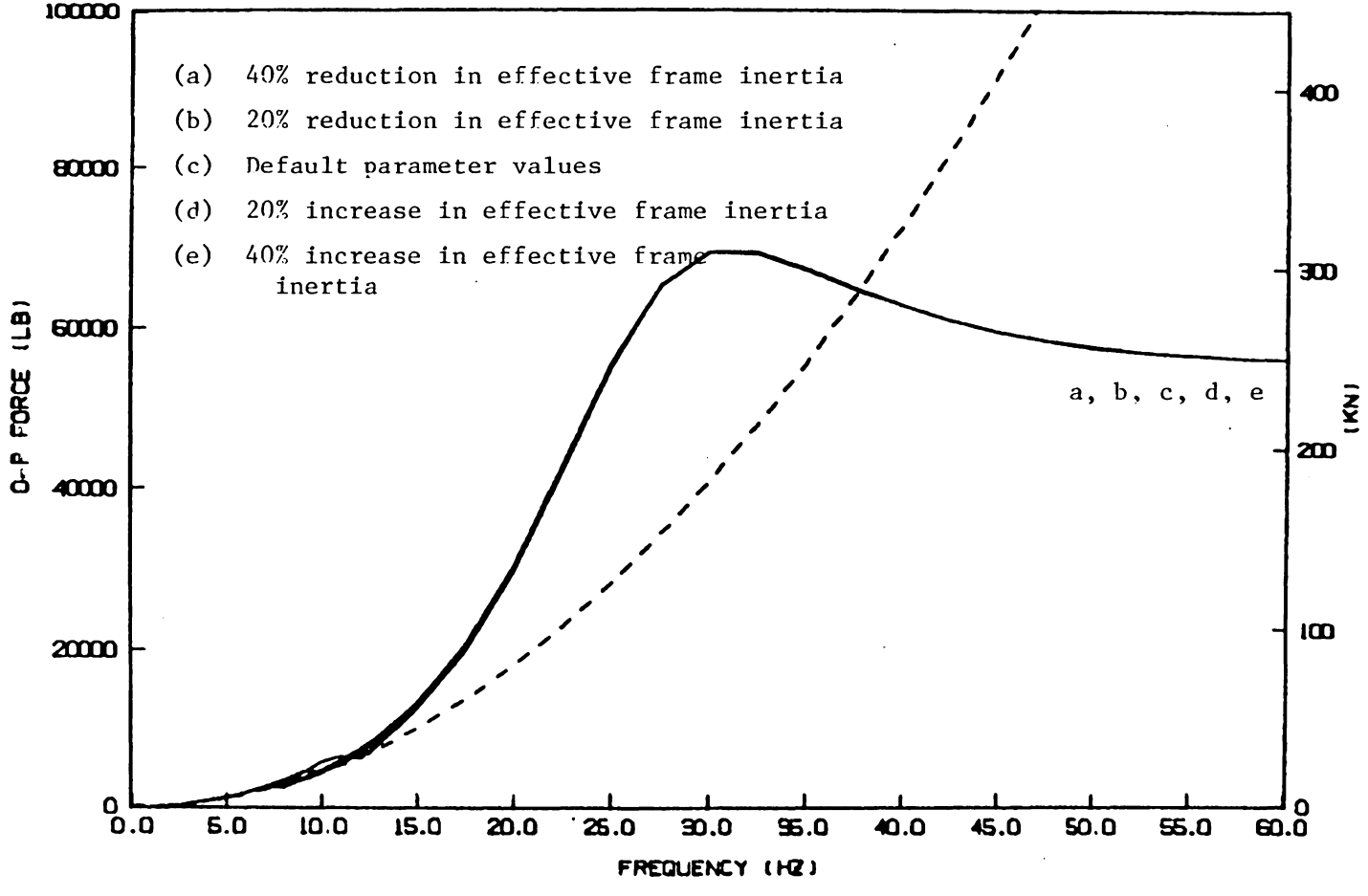

Fig. 7-20. Effect of change in effective frame inertia only on transmitted force.

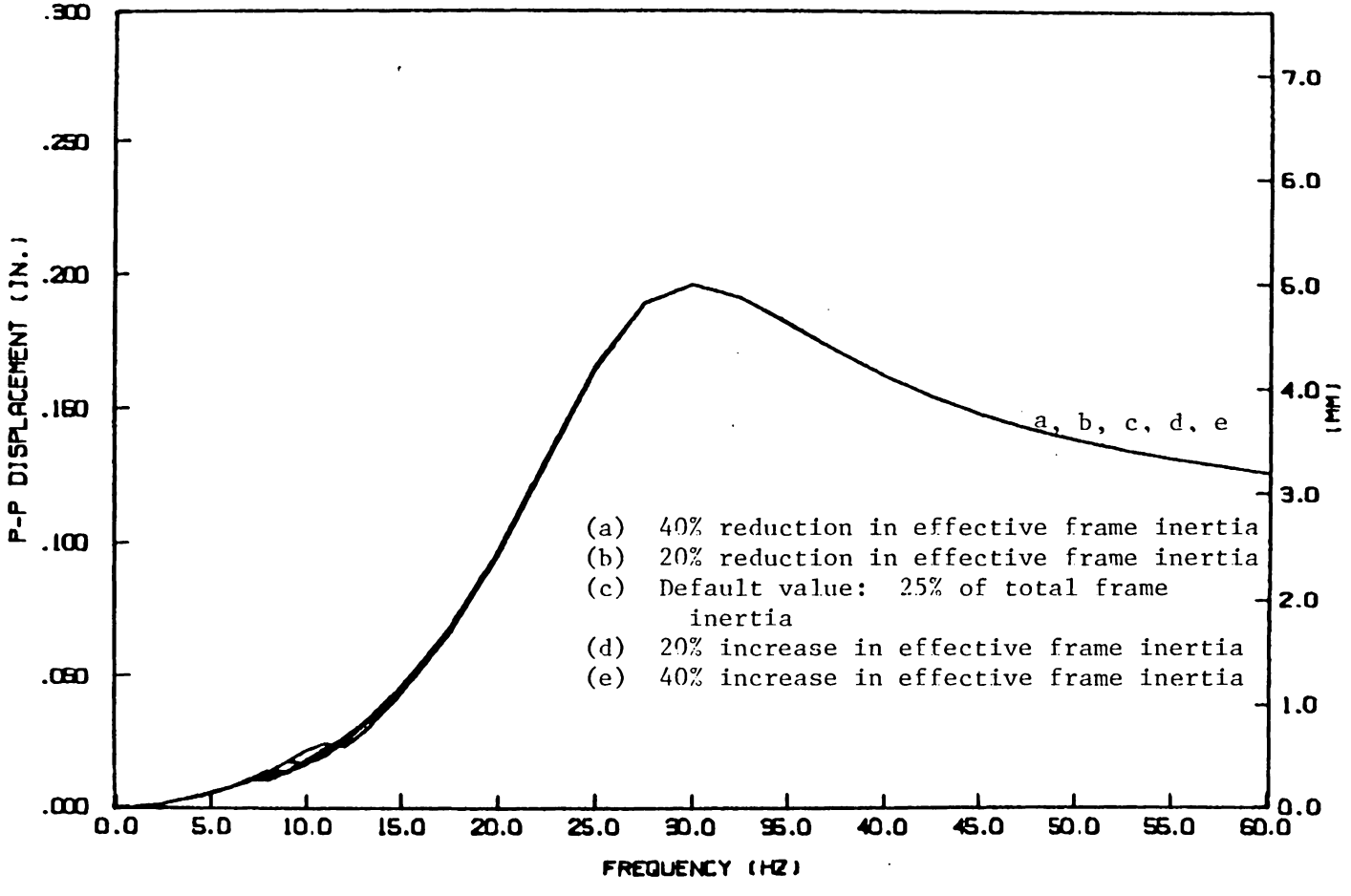

Fig. 7-21. Effect of change in effective frame inertia only on drum displacement amplitude.

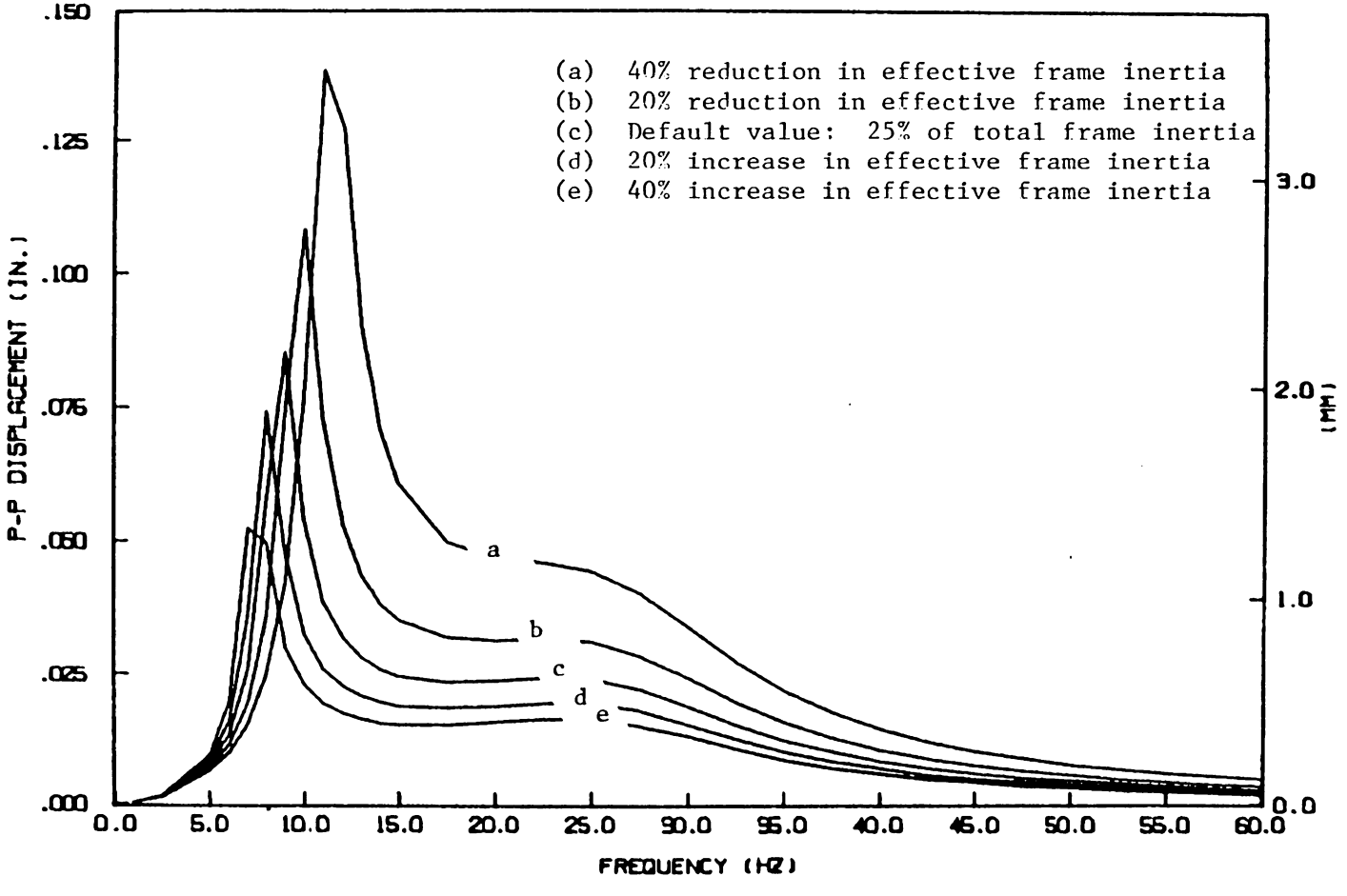

Fig. 7-22. Effect of change in effective frame inertia only on frame displacement amplitude.

being maximized by an increased frame mass.

The predictions for the growth of residual stress indicate the same trends. The evolution of the soil's stress profile with additional compactor passes is shown in Figs. 7-23 through 7-28, for the following cases:

Figs. 7-23 through 7-25: compaction at 30 Hz for variations in effective frame mass of -40, 0, +40 percent;

Figs. 7-26 through 7-28: compaction at 35 Hz for similar variations in the frame mass.

There is apparently some small benefit associated with increased frame mass at the higher frequency, but hardly any difference among the results for the three frame configurations at the lower frequency. Therefore, reallocating the frame mass seems of little utility, since the consequences appear to be frequency-dependent and, in any event, not very significant.

7.3 Effects of Compactor Speed

In all of the foregoing, the forward speed of the compactor was assumed to be 2 mph (3 ft/sec = 0.9 m/s). Figures 7-29 and 7-30 show, respectively, the effects of halving and doubling the compactor speed. As one might expect, the slower-moving compactor generates larger stresses per pass, since the underlying soil experiences more vibration cycles (7). On the other hand, the faster-moving compactor can supply more coverages in a given amount of time. If one compares the results

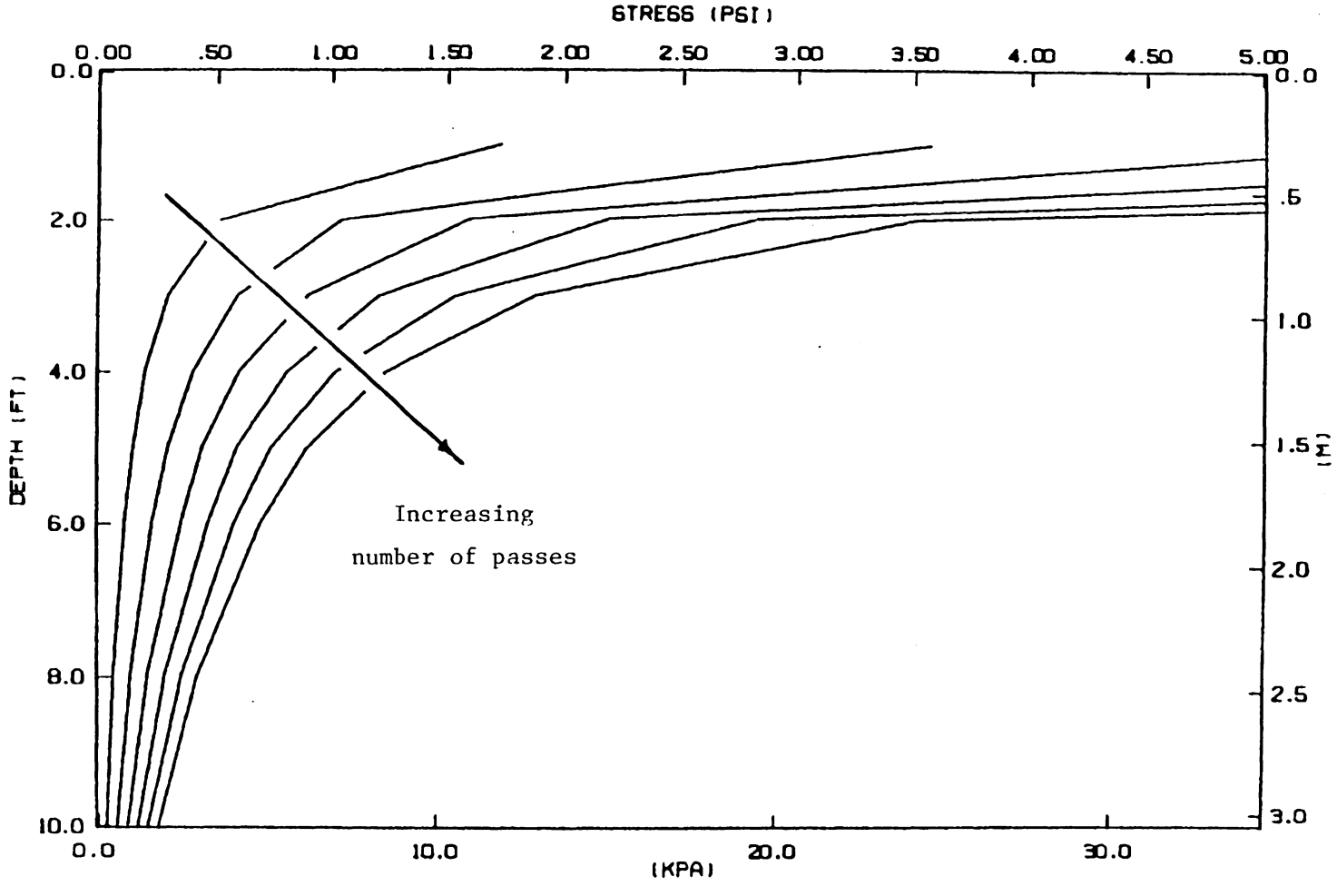

Fig. 7-23. Residual stress: 30 Hz operating frequency, 40% reduction in effective frame mass.

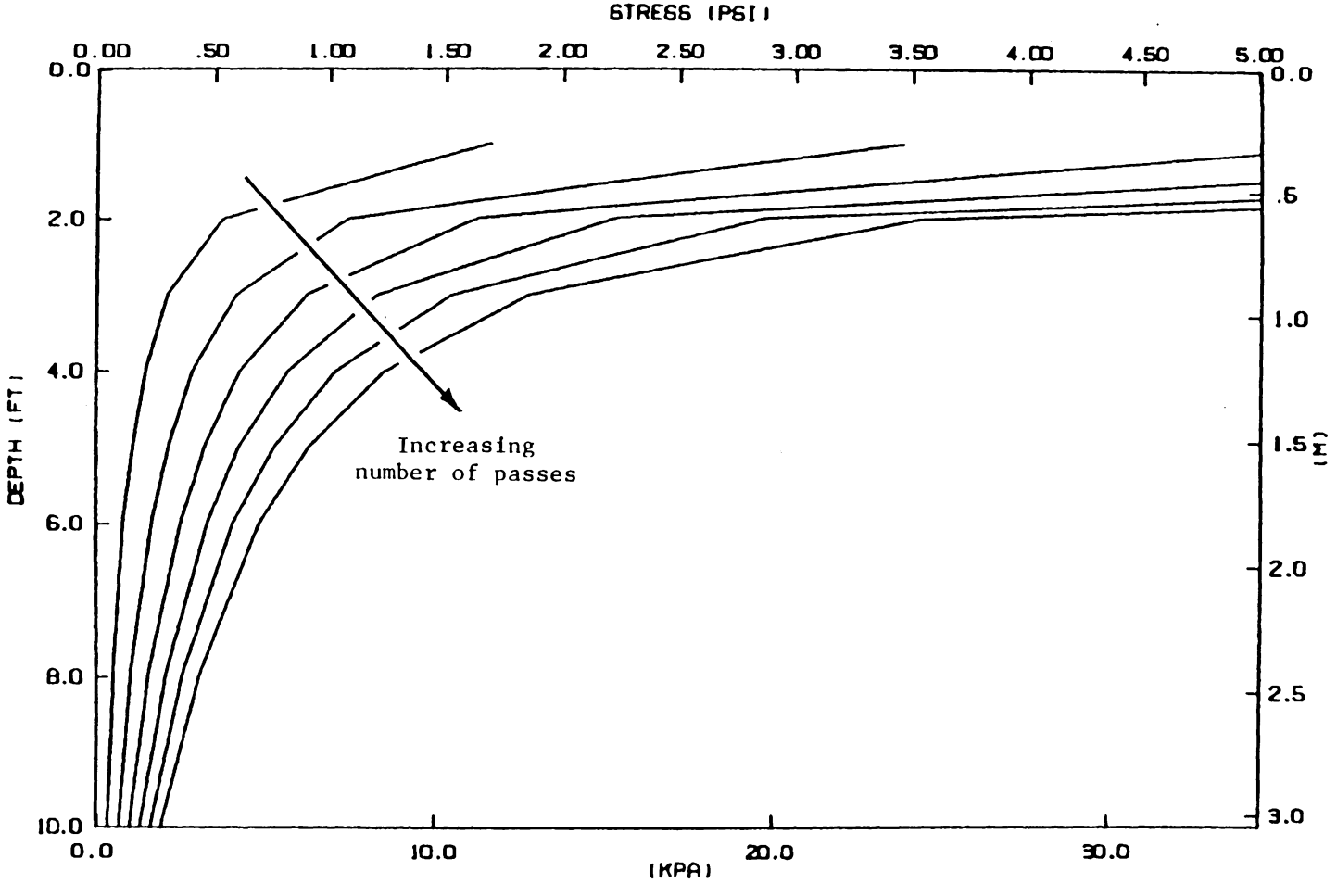

Fig. 7-24. Residual stress: 30 Hz operating frequency, default effective frame mass.

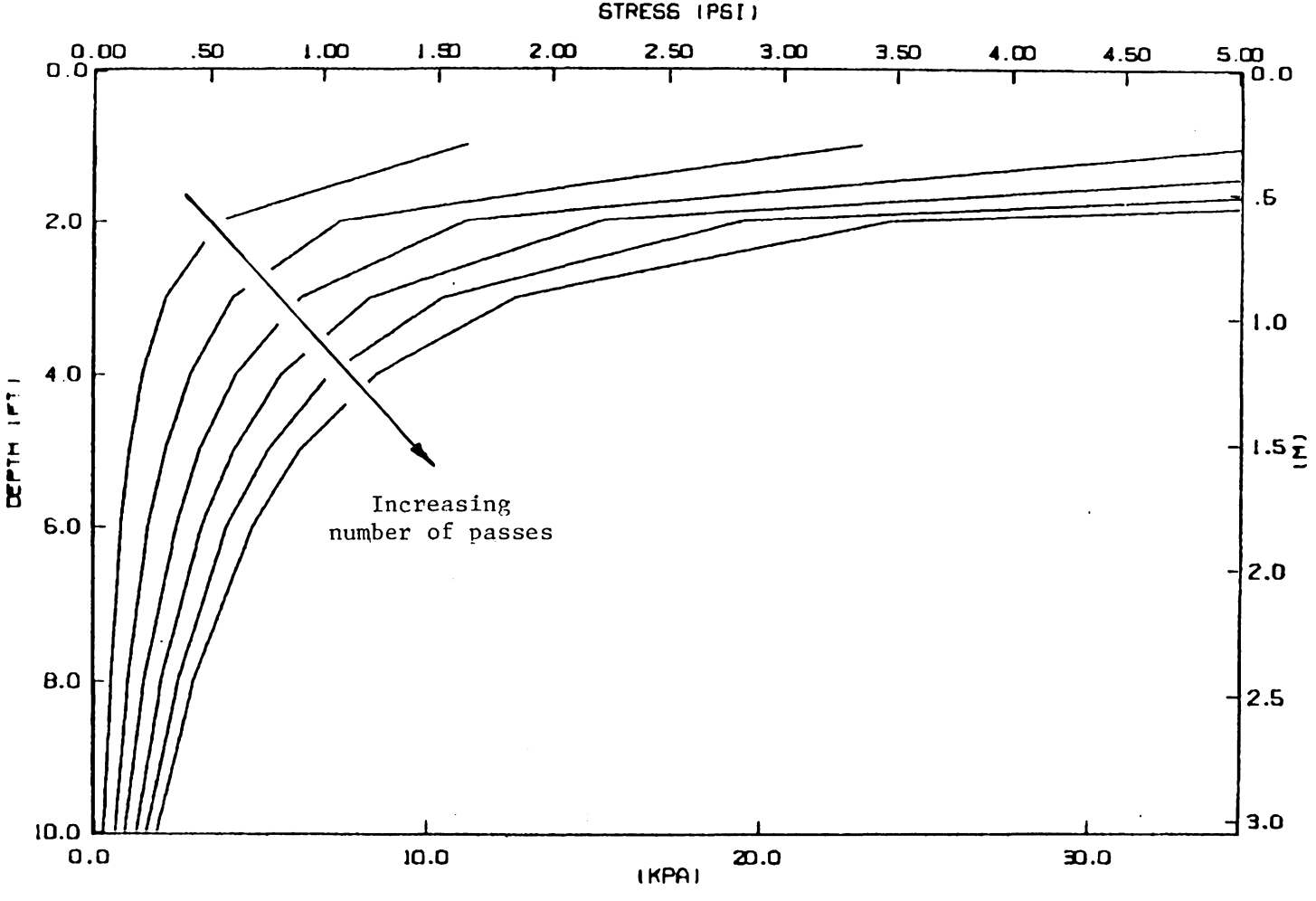

Fig. 7-25. Residual stress: 30 Hz operating frequency, 40% increase in effective frame mass.

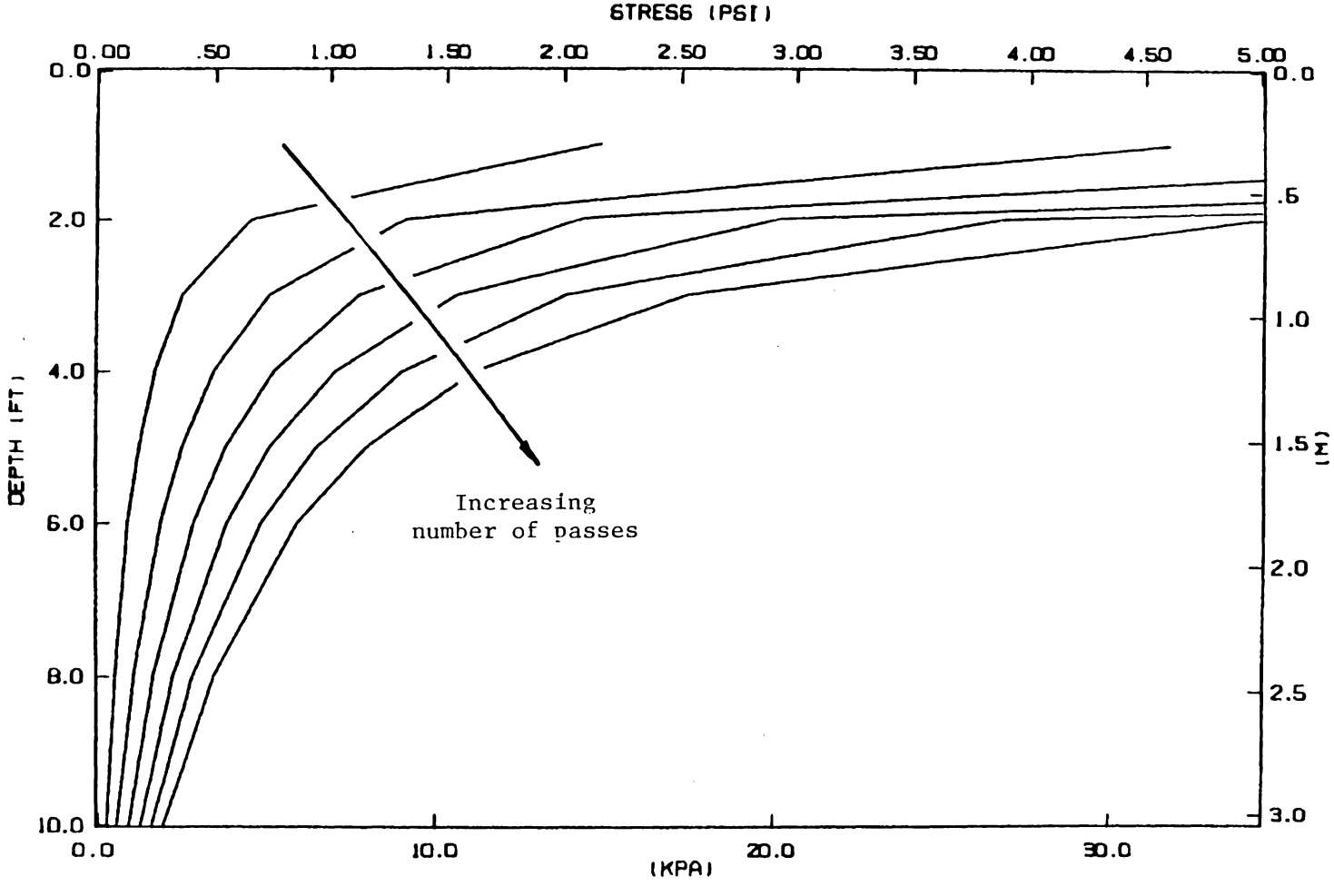

Fig. 7-26. Residual stress: 35 Hz operating frequency, 40% reduction in effective frame mass.

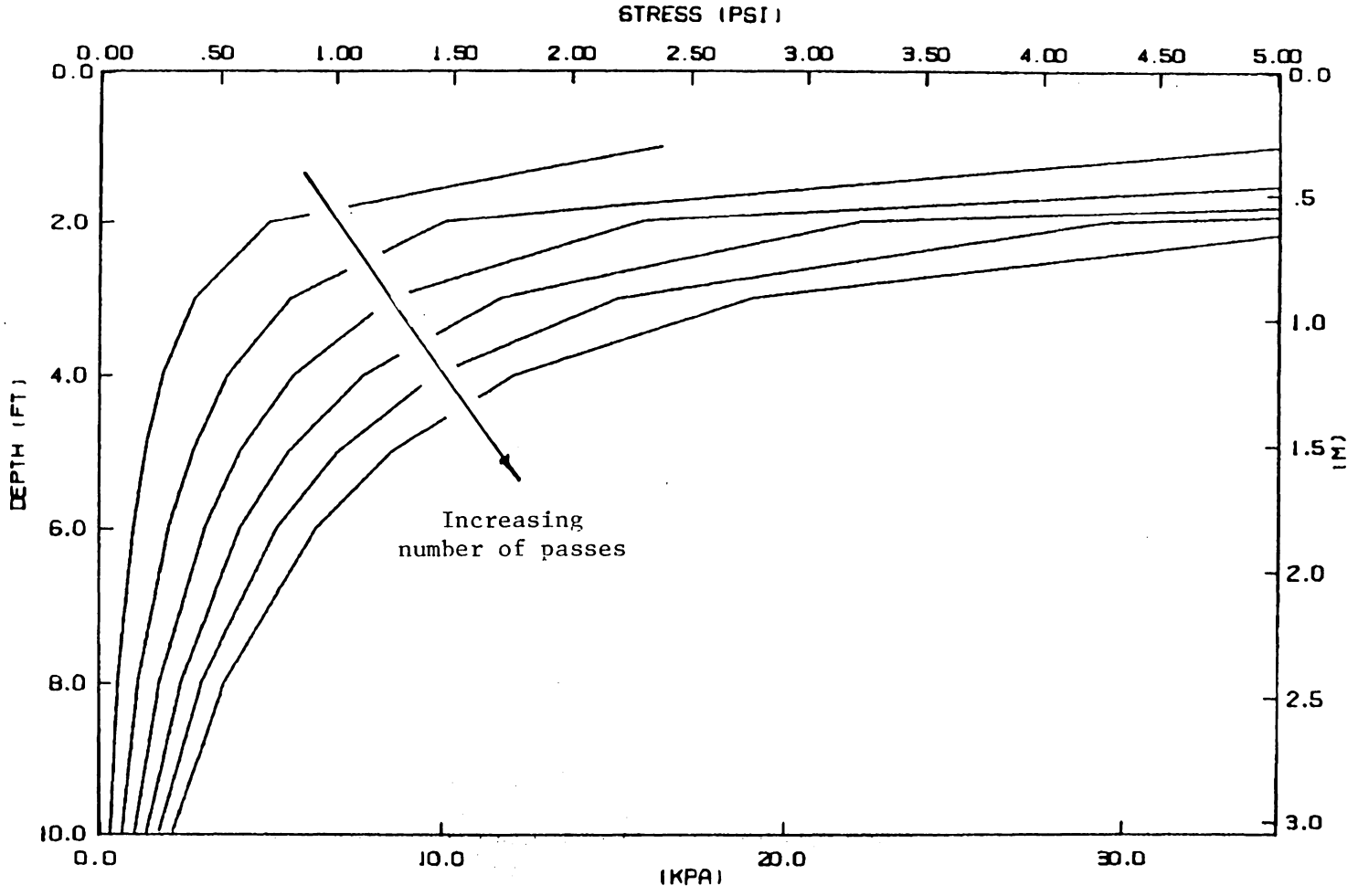

Fig. 7-27. Residual stress: 35 Hz operating frequency, default effective frame mass.

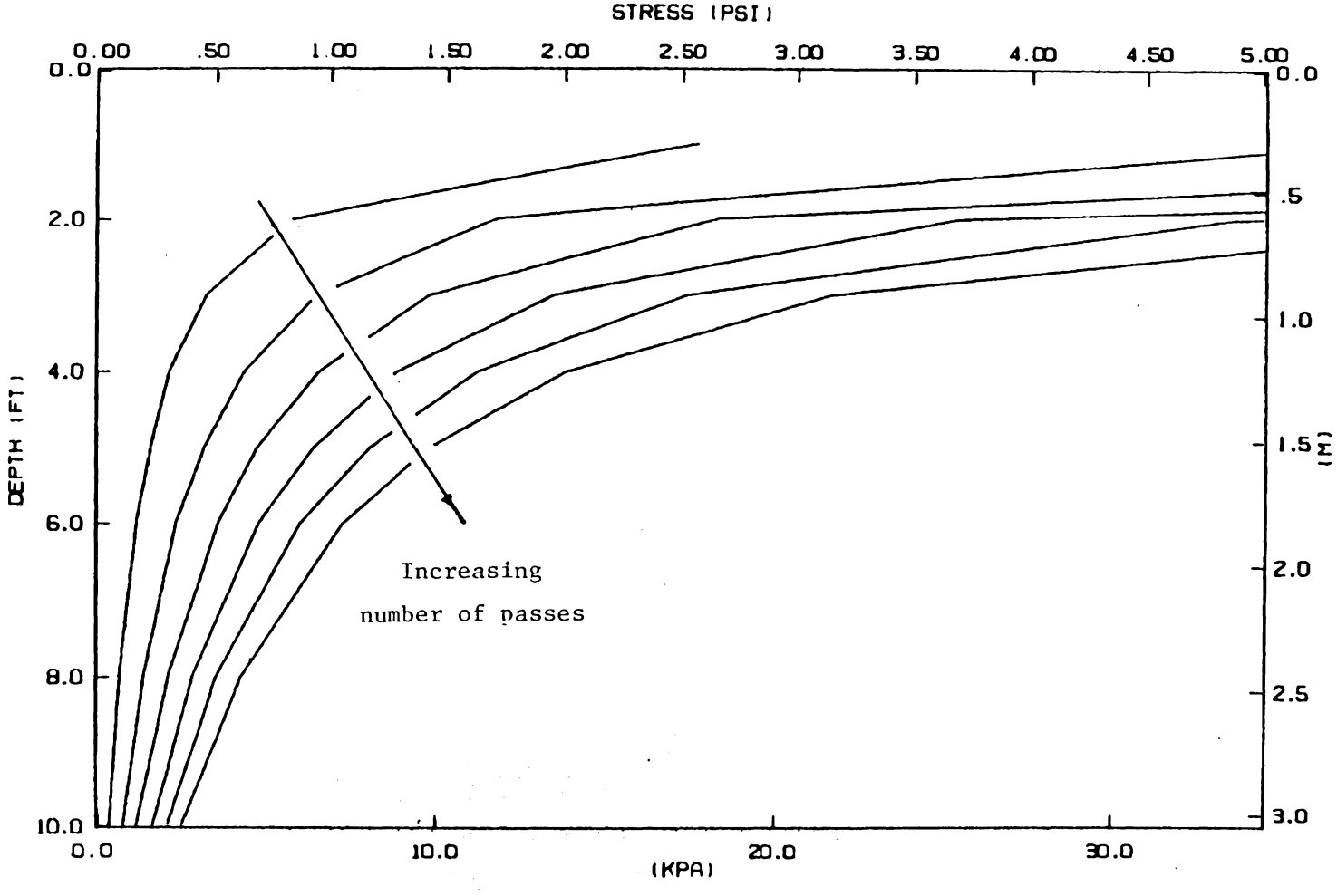

Fig. 7-28. Residual stress: 35 Hz operating frequency, 40% increase in effective frame mass.

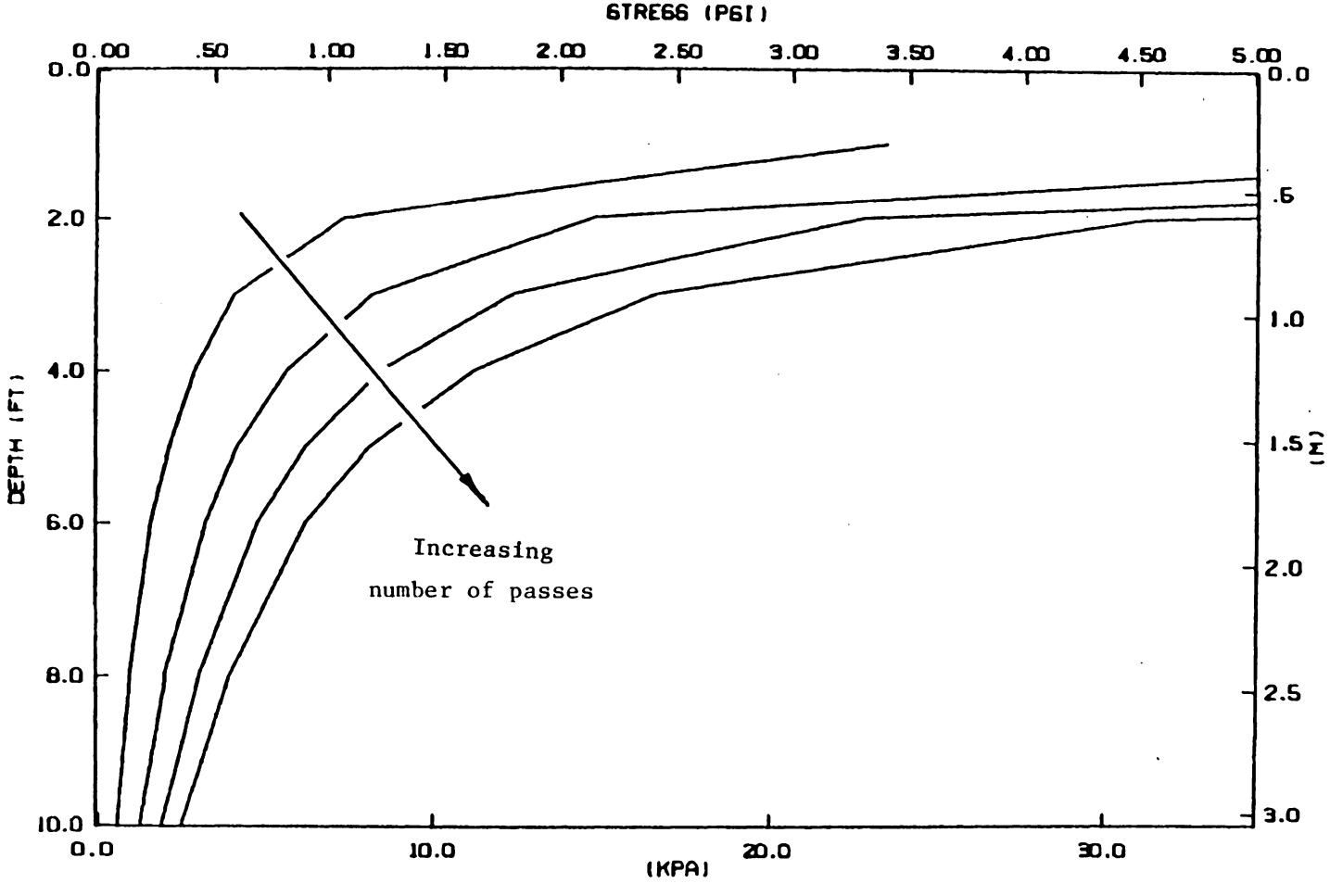

Fig. 7-29. Residual stress: 30 Hz operating frequency, 1 mph (0.4 m/s) forward speed.

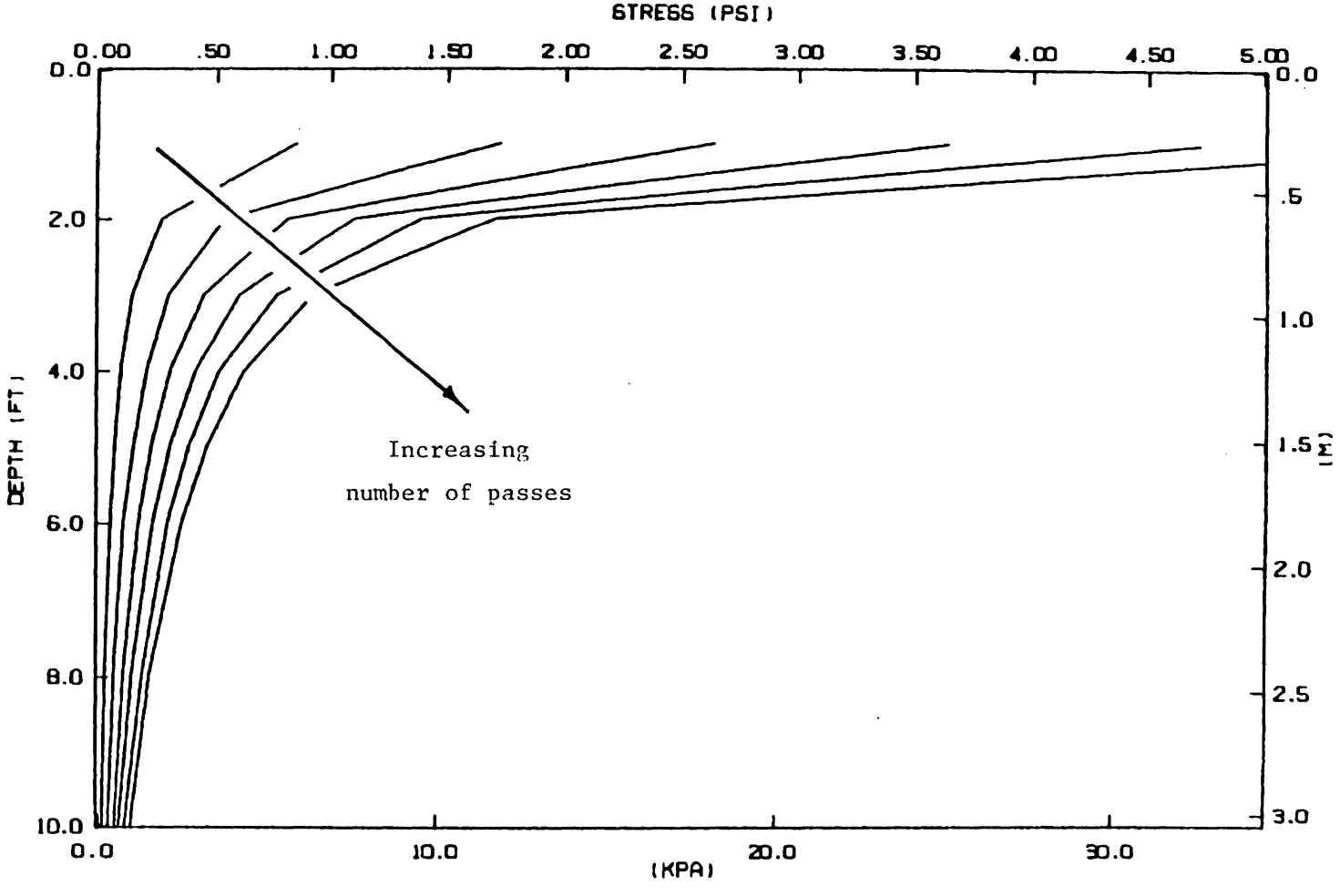

Fig. 7-30. Residual stress: 30 Hz operating frequency, 4 mph (2 m/s) forward speed.

of, say, the first pass by the slowest compactor (Fig. 7-29) with those of the second pass by the medium-speed compactor (Fig. 7-3) or of the fourth pass by the fastest compactor (Fig. 7-30), the differences are barely distinguishable. Therefore, if the goal is to achieve a given state of compaction in minimum time, the forward speed makes little difference. Faster operation merely requires the compactor to supply extra coverages.

7.4 Effects of Tracking Changes in the Resonant Frequency

As the soil stiffens under successive passes by the compactor, the resonant frequency of the soil-compactor system increases. There is the possibility that a compactor operating slightly above resonance will find itself, during subsequent passes, operating at a sub-resonant frequency, where the force transmitted to the soil is greatly reduced. A controller that would track the change in the resonant frequency might therefore provide more efficient compaction than could be obtained by operating at a constant frequency.

Such a scheme was simulated using the various default values of Table A-2. After six simulated passes, the system resonant frequency had risen by only 1 Hz (from 30 Hz to 31 Hz). The results of the simulation, shown in Fig. 7-31, are barely different from those of operating at a constant 30 Hz (Fig. 7-3). It should be pointed out, however, that this simulation is probably not a fair test of the possible benefits of a feedback controller. The actual stiffening of

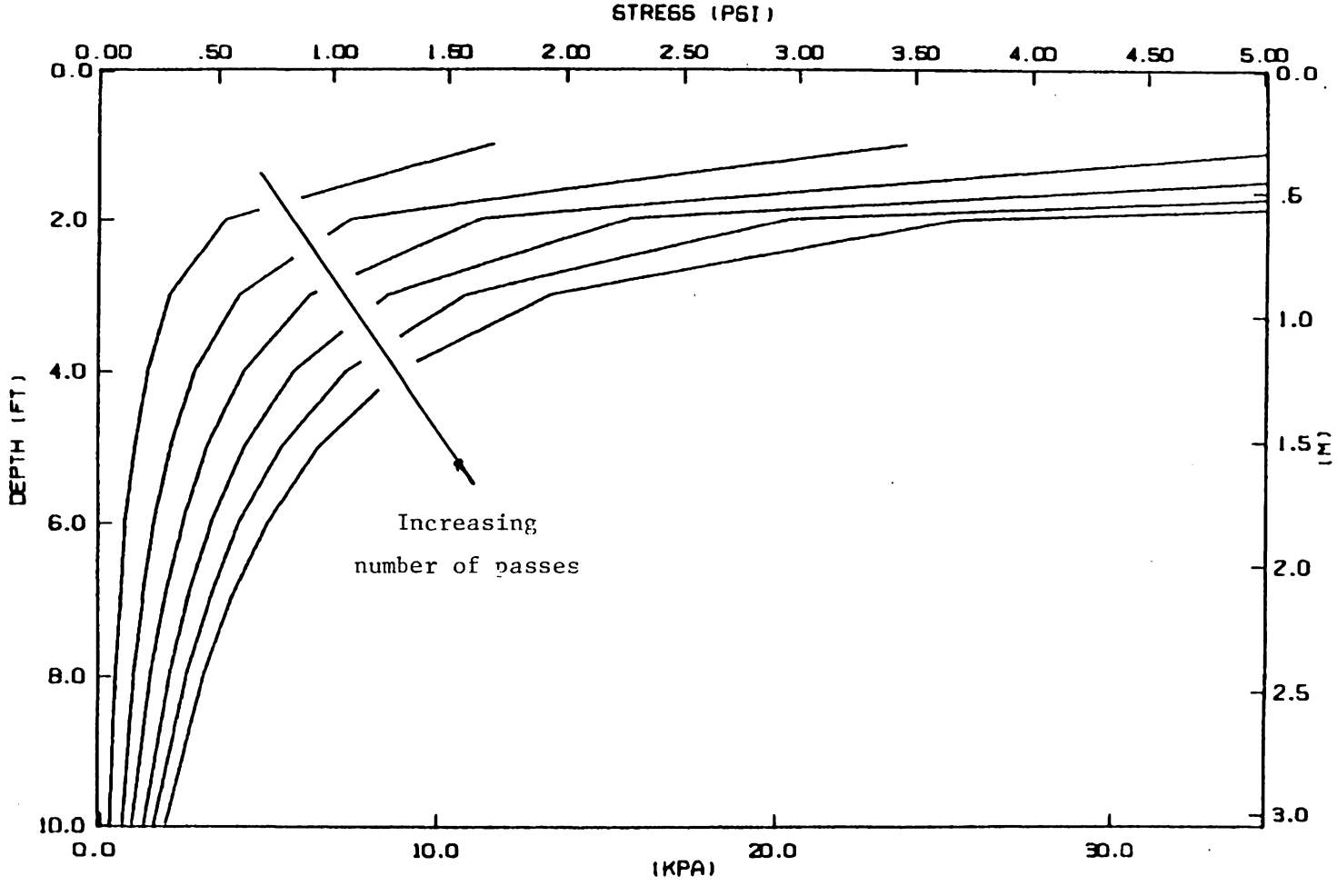

Fig. 7-31. Residual stress: continuous operation at resonance simulating use of hill-climbing controller.

the soil may be far greater than that predicted by the model developed here, which fails to treat the stiffening effects of void reduction.

8. CONCLUSIONS AND RECOMMENDATIONS

In this section we summarize the model predictions concerning the effects of frame weight distribution and operating speed and the usefulness of varying the operating frequency to track the shift in system resonance occasioned by stiffening of the soil during compaction. We also present a critique of the theoretical model of the compaction process upon which the findings are based. Recommendations are made for the improvement of the model.

8.1 Concerning Design and Operation of Vibratory Roller Compactors

In regard to the various optimization strategies examined:

(1) The frequencies at which vibratory compactors currently operate are already close to the resonant frequencies (25 - 35 Hz) of the sandy soils modelled herein. The resonant frequency is the frequency of peak response for both the drum motion and the force transmitted to the soil. Operation at lower frequencies substantially reduces the transmitted force, whereas operation at higher frequencies incurs a smaller penalty. On the one hand, there is no benefit to be had in redesigning the eccentric drive of a compactor for much higher frequencies because, even though the generated force increases without bound at frequencies above resonance, the force transmitted to the soil approaches a steady value. On the other hand, compaction at a frequency slightly above resonance carries only a small penalty and provides an operating margin to accomodate changes in the peak frequency caused by

stiffening of the soil.

(2) Redistributing the weight of the frame, either towards the drum or away from it, seems to have little effect on the force transmitted to the soil or in the generation of residual stress in the soil, for operation at resonance. For operating frequencies above resonance, there is a slight improvement to be had from a heavier frame.

(3) A slowly-moving compactor generates greater residual stresses in its path than does a fast-moving compactor. However, the faster compactor is capable of supplying more coverages in the same time span. For a minimum-time criterion, there seems to be no marked advantage in operating at any of the speeds examined here.

(4) A feedback controller that would monitor the drum motion for changes in the resonance condition would be of little practical value. For the conditions modelled here, the resonant frequency increased by only 1 Hz during 6 simulated passes of the compactor, so that compaction at a constant frequency yielded results almost identical to those obtained by modelling a feedback controller. On the other hand, there is reason to believe that the model underestimates the actual stiffening that occurs in the soil because of its failure to treat void reduction. Therefore the effectiveness of a feedback controller warrants further examination.

In summary, the current designs and procedures employed in vibratory compaction appear to be already very close to optimum, and none of the predictions of the model of the compaction process developed

in this study holds out much promise of improvement over existing designs and methods.

8.2 Concerning the Validity of the Model and Improvement of its Estimates

The following strengths and weaknesses of the model of the compaction process developed in this work should be pointed out:

(1) The model does not consider the effects of settlement and void reduction in the path of the compactor. The asymmetric geometry introduced by settlement was not reckoned to be a serious problem but the failure to treat void reduction causes the model to underestimate the stiffening of the soil considerably.

(2) The model does treat the cumulative effects of induced stresses, which contribute to the confining pressure in the soil and thereby increase its stiffness.

(3) The effects of void reduction and stress inducement are quite similar in that they both enter into the system dynamics through enhancement of the soil stiffness. Therefore, the trends indicated by the model's treatment of the evolution of residual stresses would only appear more strongly in the results of a model that adequately treated the effects of void reduction. For this reason, the implications for compactor design and operation given in the preceding section are considered by the author to be valid.

(4) The effects of other untreated nonlinearities and inhomogeneities--variations in the contact area over a vibration cycle

and spatial variations in material properties--seem to pose less serious threats to the model's validity.

In summary, the model can be most improved by the additional treatment of void reduction. This might be accomplished by an empirical correlation of densification with energy transmitted to the soil, as suggested by Brumund and Leonards. In other respects, the model should yield a useful characterization of the dynamics of the compaction process and the resulting enhancement of the mechanical properties of soil.

REFERENCES

1. Patten, W. N., "A Time Continuous Model of Soil Compaction," Manuscript, August 1984.

2. Sowers, G. F., Introductory Soil Mechanics and Foundations: Geotechnical Engineering, 4th ed., Macmillian Publishing Company, Inc., New York, 1979.

3. Piggott, Stuart, Ancient Europe from the beginning of Agriculture to Classical Antiquity, Aldine Publishing Company, Chicago, 1965.

4. Reischauer, E. O., and Fairbanks, J. K., East Asia, The Great Tradition, Houghton Mifflin Company, Boston, 1960.

5. Shatlova, I. G., Gorbunov, N. S., and Likhtman, V. I., "Physiochemical Principals of Vibratory Compacting," Vibratory Compacting, Principles and Methods, ed. H. H. Hausner, Plenum Press, New York, 1967.

6. D'Appolonia, D. J., Whitman, R. V., and D'Appolonia, E., "Sand Compaction with Vibratory Rollers," Journal of the Soil Mechanics and Foundations Division, American Society of Civil Engineering, Vol. 95, No. SM1, January 1969, pp. 263-284.

7. Selig, E. T., and Yoo, T.-S., "Fundamentals of Vibratory Roller Behavior," Proceedings, Ninth Internatinal Conference on Soil Mechanics and Foundation Engineering, Tokyo, Vol. 2, 1977, pp. 375-380.

8. Lewis, W. A., "Recent Research into the Compaction of Soil by Vibratory Compaction Equipment," Proceedings, Fifth International Conference on Soil Mechanics and Foundation Engineering, Paris, 1961, Vol. 2, pp. 261-263.

9. Selig, E. T., "Compaction Procedures, Specifications, and Control Considerations," Transportation Research Record 897: Earthwork Compaction, Transportation Research Board, National Research Council, Washington, D.C., 1982, pp. 1-8.

10. Brumund, W. F., and Leonards, B. A., "Subsidence of Sand Due to Surface Vibration," Journal of the Soil Mechanics and Foundations Division, ASCE, Vol. 98, No. SM1, January 1972, pp. 27-42.

11. Converse, F. J., "Compaction of Cohesive Soil by Low Frequency Vibration," Papers on Soils, ASTM Special Technical Publication No. 206, 19.

12. Richart, F. E., Jr., Woods, R. D., and Hall, J. R., Jr., Vibrations of Soils and Foundations, Prentice-Hall, Inc., Englewood Cliffs, New Jersey, 1970.

13. Feda, Jaroslav, Stress in Subsoil and Methods of Final Settlement Calculations, Elsevier Scientific Publishing Company, New York, 1978.

14. Yoo, T.-S., and Selig, E. T., "Dynamics of Vibratory-Roller Compaction," Journal of the Geotechnical Engineering Division, American Society of Civil Engineers, Vol. 105, No. GT10, October 1979, pp. 1211-1231.

15. Whiffin, A. C., "The Pressures Generated in Soil by Compaction Equipment," Symposium on Dynamic Testing of Soils, ASTM Special Technical Publication No. 156, 1953, pp. 124-137.

16. Karafiath, L. L., and Nowatzki, E. A., Soil Mechanics for Off-Road Vehicle Engineering, Trans. Tech Publications, Clausthal, Germany, 1978.

17. Timoshenko, S. P., and Goodier, J. N., Theory of Elasticity, 3rd ed., McGraw-Hill Book Company, New York, 1970.

18. Lamb, Horace, "On the Propagation of Tremors Over the Surface of an Elastic Solid," Philosophical Transactions of the Royal Society of London, Vol. 203, Series A, 1904, pp. 1-42.

19. Reissner, E., "Stationare, axialsymmetrische durch eine Schuttelnde Masse erregte Schwingungen eines homogenen elastichen Halbraumes," Ingenieur-Archiv, Vol. 7, Part 6, December 1963, pp. 381-396.

20. Sung, T. Y., "Vibrations in Semi-Infinite Solids Due to Periodic Surface Loading," Symposium on Dynamic Testing of Soils, ASTM Special Technical Publication No. 156, 1953, pp. 35-63.

21. Quinlan, P. M., "The Elastic Theory of Soil Dynamics," Symposium on Dynamic Testing of Soils, ASTM Special Technical Publication No. 156, 1953, pp. 124-137.

22. Arnold, R. N., Bycroft, G. N., and Warburton, G. B., "Forced Vibrations on a Body on an Infinite Elastic Solid," Journal of Applied Mechanics, American Society of Mechanical Engineers, Vol. 77, 1955, pp. 391-401.

23. Thomson, W. T., and Kobori, Takuji, "Dynamical Compliance of Rectangular Foundations on an Elastic Half-Space," Journal of Applied Mechanics, American Society of Mechanical Engineers, Vol. 30, Series E, No. 4, December 1963, pp. 579-584.

24. Ewing, W. M., Jardetsky, W. S., and Press, Frank, Elastic Waves in Layered Media, McGraw-Hill Book Company, Inc., New York, 1957.

25. Hildebrand, F. B., Advanced Calculus for Application, 2nd ed., Prentice-Hall, Inc., Englewood Cliffs, New Jersey, 1976.

26. Longman, I. M., "On the Numerical Evaluation of Cauchy Principal Values of Integrals," Mathematical Tables and Other Aids to Computation, Vol. 12, No. 63, July 1958, pp. 205-207.

27. James, M. L., Smith, G. M., and Wolford, J. C., Applied Numerical Methods for Digital Computation, 2nd ed., Harper & Row, Publisher, New York, 1977.

28. Kobori, Takuji, "Dynamical Response of Rectangular Foundations on an Elastic Half-Space," Proceedings, Japan National Symposium on Earthquake Engineering, 1962, pp. 81-86.

29. Awojobi, A. O., and Grootenhuis, P., "Vibration of Rigid Bodies on Semi-Infinite Elastic Media," Proceedings of the Royal Society, London, England, Vol. 287, Series A, 1965, pp. 27-63.

30. Karasudhi, P., Keer, L. M., and Lee, S. L., "Vibratory Motion of a Body on an Elastic Half Plane," Journal of Applied Mechanics, American Society of Mechanical Engineers, Vol. 35, Series E, No. 4, pp. 697-705.

31. Elorduy, J., Nieto, J. A., and Szekely, E. M., "Dynamic Response of Bases of Arbitrary Shape Subjected to Periodic Vertical Loading," Proceedings, International Symposium on Wave Propagation and Dynamic Properties of Earth Materials, Albuquerque, New Mexcio, 1967.

32. Wong, H. L., and Luco, J. E., "Dynamic Response of Rigid Foundations of Arbitrary Shape," Earthquake Engineering and Structural Dynamics, Vol. 4, 1976, pp. 579-587.

33. Kitamura, Y., and Sukurai, S., "Dynamic Stiffness for Rectangular Rigid Foundations on a Semi-Infinite Elastic Medium, "International Journal for Numerical Analytical Methods in Geomechanics, Vol. 3, No. 2, April-June 1979, pp. 159-171.

34. Adeli, H., Hejazi, M. S., Keer, L. M., and Nemat-Nasser, S., "Dynamic Response of Foundations with Arbitrary Geometries," Journal of the Engineering Mechanics Division, American Society of Civil Engineers, Vol. 107, No. EM5, October 1981, pp. 953-967.

35. Whittaker, W. L., and Christiano, Paul, "Dynamic Response of Plate on Elastic Half-Space," Journal of the Engineering Mechanics Division, American Society of Civil Engineers, Vol. 108, No. EM1, February 1982, pp. 133-154.

36. Converse, F. J., "Compaction of Sand at Resonant Frequency," Symposium on Dynamic Testing of Soils, ASTM Special Technical Publication No. 156, 1953, pp. 124-137.

37. Moorhouse, D. C., and Baker, G. L., "Sand Densification by Heavy Vibratory Compactor," Journal of the Soil Mechanics and Foundations Division, American Society of Civil Engineers, Vol. 95, No. SM4, July 1969, pp. 985-994.

38. Personal communication from W. Benoit, Lord Corporation, Industrial Products Division, July 15, 1984.

39. Richart, F. E., Jr., and Whitman, R. V., "Comparison of Footing Vibration Tests with Theory," Journal of the Soil Mechanics and Foundations Division, American Society of Civil Engineers, Vol. 93, No. SM6, November 1967, pp. 143-168.

40. Bergman, E. P., "Compaction," Journal of Terramechanics, Vol. 16, No. 1, 1979, pp. 23-32.

41. Das, B. M., Advanced Soil Mechanics, McGraw-Hill Book Company, New York, 1983.

42. Fu, C. C., "TM-780 Roller Compactor Optimization," memorandum (Ingersoll-Rand).

43. Cowley, H. R., "The Tandem Vibration Roller: Its Design and Development in the Field of Dynamic Compaction," Proceedings of the Institution of Mechanical Engineers, Vol. 181, Pt 23, No. 3, 1966-67, pp. 110-132.

44. Adachi, T., and Okano, M., "A Constitutive Equation for Normally Consolidated Clay," Soils and Foundations, Vol. 14, No. 4, December 1974, pp. 55-73.

45. Duncan, J. M., and Cheng, C. Y., "Non-linear Analysis of Stress and Strain," Journal of the Soil Mechanics and Foundations Division, American Society of Civil Engineers, Vol. 96, No. SM5, September 1970, pp. 1629-1654.

46. Weissmann, G. F., and Hart, R. R., "The Damping Capacity of Some Granular Soils," Symposium on Soil Dynamics, ASTM Special Technical Publication No. 305, 1961, pp. 45-59.

47. Hall, J. R., Jr., and Richart, F. E., Jr., "Dissipation of Elastic Wve Energy in Granular Soils," Journal of the Soil Mechanics and Foundations Division, American Society of Civil Engineers, Vol. 89, No. SM6, November 1963, pp. 27-56.

48. Hardin, B. O., and Drnevich, V. P., "Shear Modulus and Damping in Soils: Measurement and Parameter Effects," Journal of the Soil Mechanics and Foundations Division, American Society of Civil Engineers, Vol. 98, No. SM6, June 1972, pp. 603-624.

49. Johnson, L. W., and Riess, R. D., Numerical Analysis, 2ed., Addison-Wesley Publishing Company, Reading, Massachusetts, 1982.

50. Longman, I. M., "Note on a Method of Computing Infinite Integrals of Oscillatory Functions," Proceedings of the Cambridge Philosophical Society, Vol. 52, part 4, 1956, pp. 764-768.

51. U.S. Department of Commerce, National Bureau of Standards, Handbook of Mathematical Functions with Formulas, Graphs, and Mathematical Tables, ed. Milton Abramowitz and Irene A. Stegun, Applied Mathematics Series, No. 55, 1972.

APPENDIX A

COMPACTOR SPECIFICATIONS AND MODEL INPUTS

The tables in this section give nominal values for the compactor specifications and default values for the model inputs. All data presented in the text were obtained using the values given here, except where other values are explicitly stated to have been used.

Table A-1

Weights and Dimensions for Ingersoll-Rand SP56-DU Compactor

	Symbol	FORTRAN Variable Name	Customary	(SI)
Weights / masses				
Overall				
@ drum	--	--	7980 lbf	(3619 kg)
@ tires	--	--	12720 lbf	(5768 kg)
Total:			20700 lbf	(9387 kg)
Components:				
Drum	--	DWGHT	8777 lbf	(3981 kg)
Frame	--	FWGHT	11923 lbf	(5406 kg)
Total:			20700 lbf	(9387 kg)
Eccentric moment	m e	ECCENT	444 lbm in.	(5.12 kg m)
Lineal dimensions				
Wheelbase	L	WB	127 in.	(3.3 m)
Drum length	2d	DLNGTH	84 in.	(2.1 m)
Drum radius	--	RADIUS	28 in.	(0.7 m)

Table A-2

Model Inputs

	Symbol	FORTRAN Variable Name	Customary	(SI)
I. Compactor				
Effective weights:				
Drum	--	DRUMW	8777 lbf	(39040 N)
Frame	--	FRAMEW	3974 lbf	(17680 N)
Effective inertias:				
Drum	m_D	DRUMM	8777 lbm	(3980 kg)
Frame	m_F	FRAMEM	2981 lbm	(1350 kg)
Contact area:				
Length	2d	DLNGTH	84 in.	(2.1 m)
Width	2c	2.*CWIDTH	9 in.	(0.2 m)
Suspension:				
Stiffness	K_1	STIFF	24054 lbf/in.	(4210 kN/m)
Damping	K_2	DAMP	3849 lbf/in.	(674 kN/m)
Speed	V_o	SPEED	3 ft/sec	(0.9 m/s)
II. Soil				
Average confining Pressure[a]	$\bar{\sigma}_o$	PRESSC	3 psi	(21 kPa)
Void ratio	e^o	VOIDR	0.8	
Density	ρ	DNSITY	0.06 pci	(1660 kg/m)
Linear model:				
Poisson's ratio	ν	PR,POIS	0.3	
Shear modulus[a]	G	GMOD	5570 psi	(38 MPa)
Young's modulus[a]	E	EMOD,EMODZ	14490 psi	(100 MPa)
Nonlinear model:				
--	α_3	ALPHA(3)	3 sec	(3 s)
--	α_4	ALPHA(4)	1	

[a] Uncompacted soil (values updated for multiple passes).

APPENDIX B

Numerical Methods

This appendix describes the numerical procedures used in evaluating the Fourier integrals for the elemental surface displacements and the subsurface strains; the reduction of the overall compliance matrix used to compute contact stresses; the integration of the residual stress equation.

The Fourier integral evaluations and the matrix reductions were performed in double-precision (64-bit) arithmetic on a VAX 11/780. The numerical integration of the residual stress equation was carried out in single-precision (32-bit) arithmetic. A program listing is provided in Appendix C.

B.1 Inversion of Transforms

We are faced with the evaluation of integrals like

$$w(x,0) = \frac{1}{\sqrt{2\pi}} \int_{-\infty}^{\infty} \frac{\alpha_1 k^2 \tilde{S}(\beta)}{G\, F(\beta)} e^{j\beta x} d\beta \qquad (4.2\text{-}3)$$

$$\varepsilon(x,z) = \frac{1}{\sqrt{2\pi}} \int_{-\infty}^{\infty} \frac{\tilde{S}(\beta)}{G\, F(\beta)} \{(2\beta^2 - k^2)\ \alpha_1\ e^{-\alpha_1 z}$$

$$-2\ \alpha_1 \alpha_2 \beta^2\ e^{-\alpha_2 z}\}\ e^{j\beta x} d\beta \qquad (4.2\text{-}4)$$

where

$$\tilde{S}(\beta) = \frac{1}{\sqrt{2\pi}} \int_{-c}^{c} S(x)\, e^{-j\beta x} dx,$$

$$F(\beta) = (2\beta^2 - k^2)^2 - 4\beta^2 \alpha_1 \alpha_2,$$

$$\alpha_1 = (\beta^2 - h^2)^{1/2},$$

$$\alpha_2 = (\beta^2 - k^2)^{1/2}.$$

For each elemental compliance function, the contact stress S(x) is assumed unform, which gives

$$S(x) = \frac{P}{2b}$$

$$\tilde{S}(x) = \frac{1}{\sqrt{2\pi}} \frac{P}{b} \frac{\sin \beta b}{\beta}$$

where P is the force per unit length on the elemental strip and 2b is the strip width. Then

$$w(x,0) = \frac{P}{2\pi b} \int_{-\infty}^{\infty} \frac{\alpha_1 k^2}{G\, F(\beta)} \frac{\sin \beta b}{\beta} e^{j\beta x} db \qquad \text{(B.1-1)}$$

$$\varepsilon(x,z) = \frac{P}{2\pi b} \int_{-\infty}^{\infty} \frac{1}{G\, F(\beta)} \{(2\beta^2 - k^2)\, \alpha_1{}^2 e^{-\alpha_1 z} - 2\alpha_1 \alpha_2 \beta^2 e^{-x_2 z}\}$$

$$\cdot \frac{\sin \beta b}{\beta} e^{j\beta x} d\beta . \qquad \text{(B.1-2)}$$

We first note that the terms multiplying $e^{j\beta x}$ in both integrands are even functions of β, so that we can write

$$w(x,0) = \frac{P}{\pi b} \int_{0}^{\infty} \frac{\alpha_1 k^2}{G\beta F(\beta)} \sin \beta b \cos \beta x\, d\beta, \qquad \text{(B.1-3)}$$

$$\varepsilon(x,z) = \frac{P}{\pi b} \int_{0}^{\infty} \frac{1}{G\beta F(\beta)} \{(2\beta^2 - k^2)\alpha_1{}^2 e^{-\alpha_1 z} - 2\, \alpha_z \alpha_2 \beta^2 e^{-\alpha_2 z}\}$$

$$\cdot \sin \beta b \cos \beta x \, d\beta \, . \qquad \text{(B.1-4)}$$

The expressions may be non-dimensionalized by the following substituions:

$$u = \beta/k$$
$$n = h/k = C_S/C_D = \left(\frac{1 - 2\nu}{2(1 - \nu)}\right)^{1/2}$$
$$a_o = \omega/C_S = kb.$$

This permits us to write

$$w(x,0) = \frac{P}{\pi G a_o} \int_o^\infty \frac{H_o(u)H_1(u)}{u\, F(u)}\, du \qquad \text{(B.1-5)}$$

$$\varepsilon(x,z) = \frac{P}{\pi G b} \int_o^\infty \frac{H_o(u)H_2(u)}{u\, F(u)}\, du \qquad \text{(B.1-6)}$$

where

$$F(u) = (2u^2 - 1)^2 - 4u^2(u^2 - n^2)^{1/2}\,(u^2 - 1)^{1/2}$$
$$H_o(u) = \sin a_o u \cos \frac{x}{b} a_o u$$
$$H_1(u) = (u^2 - n^2)^{1/2}$$

$$H_2(u) = (2u^2 - 1)\,(u^2 - n^2)^{1/2} \exp\left[-\frac{a_o z}{b}(u^2 - n^2)^{1/2}\right]$$
$$- 2u^2\,(u^2 - n^2)^{1/2}\,(u^2 - 1)^{1/2} \exp\left[-\frac{a_o z}{b}(u^2 - 1)^{1/2}\right] .$$

Although the numerator terms $H_1(u)$ and $H_2(u)$ are somewhat different, the denominators are identical. It is the simple pole u_o contributed by

F(u),

$$F(u_o) = 0,$$

that requires us to obtain the principal value of the integral by the methods discused in Section 4.3.

We begin by noting that, although u multiples F(u) in the denominator, both integrands have limits as $u \to 0$:

$$\lim_{u \to o} \left\{ \frac{H_o(u)H_1(u)}{u\ F(u)} \right\} = j\ a_o\ n$$

$$\lim_{u \to o} \left\{ \frac{H_o(u)H_2(u)}{u\ F(u)} \right\} = a_o\ n \exp\ (-\ j\ a_o\ n\ \frac{z}{b}).$$

As $z \to \infty$, both integrands vanish.

We next consider the behavior of the integrand terms on different intervals:

Interval	u	F(u)	$H_1(u)$	$H_2(u)$
1a	$0 < u < n$	Real	Imaginary	Complex
1b	$n < u < 1$	Complex	Real	Complex
2a	$1 < u < u_o$	Positive Real	Real	Real
--	$u = u_o$	0	Real	Real
2b	$u < u < (2u_o - 1)$	Negative Real	Real	Real
3	$(2u_o - 1) < u < u_1$	Negative Real	Real	Real
4	$u_1 < u$	Negative Real	Real	Real

(Here, the interval $(1, 2u_o - 1)$ is symmetric about the pole, as required by the methods of Section 4.3. The value of u_1 depends on the method of integration that we employ on the semi-infinite interval 4, and its selection is discussed below.)

Although the interval (0,1] contains the two branch points (n and 1), we are not concerned because we do not employ a closed-contour integration. A straightforward evaluation by Simpson's rule is employed on intervals 1a and 1b. (We note in passing that the integrands are rather poorly behaved near the branch points, so that a reduced step size was employed in their neighborhoods.)

In integrating around the pole, we employ Longman's method, as discussed in Section 4.3 and in reference (26). We divide the integrands into even and odd components and integrate the even component over interval 2a. To ensure adequate convergence, we progressively halve the step size as we approach the pole, and halt the approach when the product

$$\frac{H_o \, H_{1,2}}{u \, F(u)} \, \Delta u$$

is sufficiently small.

An additional technique introduced by Thomson and Kobori (23) is employed in this region. As $u \to U_o$ and F(u) becomes small, precision is lost in the computation of the integrand. Therefore, we linearize the denominator near the pole, writing

$$F(u) \simeq F'(u_o)\ (u - u_o)\ .$$

The radius of linearization is computed from the second order residual of the Taylor polynomial expansion:

$$F(u) = F'(u_o)\ (u - u_o) + R(a),$$

$$R(a) = F''(a)\ (a - u_o)\ ,$$

$$|a - u_o\ | \leq |u - u_o|.$$

Taking $F''(a) \simeq F''(u_o)$, we can select a to yield an acceptably small error term R.

Although the integrands diminish with increasing u, they do so only slowly. Interval 3 just beyond the pole contributes substantially to the value of the integrand, and care must be taken in the evaluation in this region. An adaptive-integration scheme described by Johnson and Riess (49) is employed here. The algorithm compares the values of 3-ordinate and 5-ordinate Simpson's Rule approximations at each step to estimate the error of the approximation. The step size is varied to control the error.

The adaptive integration is terminated at $u = u_1$, the value of which depends on the approximation employed in the last interval, 4. Different methods have been employed for the strain and displacement integrals, although the first method may be used for both.

The first method, also developed by Longman (50) and introduced to soil-vibration problems by Thomson and Kobori (23), is an adaptation of

a technique for acelerating the convergence of a slowly converging alternating series. The series

$$V_o - V_1 + V_2 - \cdots$$

can be rewritten in terms of forward differences:

$$\sum_{n=o}^{\infty} (-1)^n V_n - \frac{2}{2} V_o - \frac{1}{4} \Delta V_o + \frac{1}{8} \Delta^2 V_o - \cdots \qquad \text{(b.1-7)}$$

where

$$\Delta V_n = V_{n+1} - V_n, \quad \Delta^{r+1} V_n = \Delta^r V_{n+1} - \Delta^r V_n.$$

Two conditions must be satisfied by the original series:

(1) $V_n > 0$ (i.e., the series alternates);

(2) $V_n > V_{n+1}$ (i.e., the terms in the series are uniformly decreasing.)

If these conditions are met, then the convergence of the forward-difference representation is quite rapid.

This technique can be adapted to the evaluation of the integral of an oscillatory function on a semi-infinite interval. We divide the interval into subintervals whose endpoints are the zeroes of the integrand. The terms V_n in the series treated in Eq. B.1-7 are just the

integrals evaluated over each successive subinterval:

$$\int_{u_1}^{\infty} f(u)\,du = \int_{u_1}^{u_2} f(u)\,du + \int_{u_2}^{u_3} f(u)\,du + \ldots$$

$$= \quad V_o \quad + \quad (-V_1) \quad + \ldots \quad .$$

To use this method, we select u_1 to be the first zero of $H_o(u)$ beyond $(2u_o - 1)$. We employ a Simpson's rule evaluation of the successive half-cycle intervals V_n. After each evaluation, we update the forward-difference table and add a new term to the series in Eq. B.1-7 and check for convergence.

Several difficulties do arise in the application of this method. The satisfaction of conditions (1) and (2) above requires that the integrand oscillate about $f(u) = 0$ and that the magnitudes of the half-cycle integrals be decreasing. The term $H_o(u)$ does oscillate but in no simple fashion for $x/b \neq 1$. It is better to write

$$H_o(u) = \sin a_o u \cos \frac{x}{b} a_o u$$

$$= \frac{1}{2}\left[\sin\left(a_o + \frac{x}{b}\right) u + \sin\left(a_o - \frac{x}{b}\right) u\right]$$

and then integrate each term separately by Longman's method. Each function will have a fixed period, and the denominator term $F(u)$, which grows without bound, will provide a diminishing magnitude to successive integrals.

For the surface displacement $w(x,0)$, a simpler method was found to work. For sufficiently large u, we can approximate

$$\frac{H_1(u)}{u\ F(u)} \simeq \frac{1}{2(n^2 - 1)\ u^2} .$$

At $u = 10$, the error of the approximation is 0.7 percent for $\nu = 0.3$ and it diminishes with larger u. We therefore take $u_1 = 10$ and write

$$\int_{u_1}^{\infty} \frac{H_o(u)\ H_1(u)}{u\ f(u)} \simeq \int_{u_1}^{\infty} \frac{1}{2(n^2 - 1)\ u^2} \sin a_o u \cos \frac{x}{b} a_o u \ du.$$

The approximation can be evaluated in terms of the cosine integral:

$$\int_{u_1}^{\infty} \frac{1}{2(n^2 - 1)\ u^2} \sin a_o u \cos \frac{x}{b} a_o u \ du$$

$$= \frac{1}{4(n^2 - 1)} \left\{ \frac{\sin k_1 u_1 + \sin k_2 u_1}{u} \right.$$

$$\left. - k_1 \ Ci(\ | \ k_1 u_1 \ | \ ) - k_2 \ Ci(\ | \ k_2 u_1 \ | \ ) \right\}$$

where

$$k_1 = a_o \ (1 + x/b)$$

$$k_2 = a_o \ (1 - x/b)$$

$$Ci(v) = - \int_{v}^{\infty} \frac{\cos(u)}{u} \ du \ .$$

The series representation used for evaluating Ci(v) is, from reference (51),

$$Ci(v) = \gamma + \ln v + \sum_{n=1}^{\infty} \frac{(-1)^n v^{2n}}{2n\,(2n)!}$$

where γ is Euler's number. For large v ($v > 20$), the asymptotic expansion

$$Ci(v) = f(v) \sin v - g(v) \cos v$$

$$f(v) \simeq \frac{1}{v}\left(1 - \frac{2!}{v^2} + \frac{4!}{v^4} - \frac{6!}{v^6} + \ldots\right)$$

$$g(v) \simeq \frac{1}{v}\left(1 - \frac{3!}{v^2} + \frac{5!}{v^4} - \frac{7!}{v^6} + \ldots\right)$$

is used. We note that if k_1 or k_2 is zero, the product

$$k_i\ Ci\ (\ |\ k_i\ u_2\ |\ ) \to 0,$$

even though Ci(0) does not exist.

The remaining operation in the evaluation is the subtraction of the residue term $j\pi\, Res(u_o)$,

$$Res(u_o) = \frac{H_o(u_o)\, H_i(u_o)}{u_o\, F'(u_o)} \qquad i = 1,2$$

where

$$F'(u) = f\left\{4u^3 - 2u - \frac{4u^5 - 3(n^2+1)\,u^3 + 2n^2 u}{[u^4 - (n+1)\,u^2 + n^2]^{1/2}}\right\}.$$

B.2 Solution of the Coupled Dynamics of the Linear Models

In Section 5, N + 2 equations were derived that permit us to solve for N discrete values of the contact stress, plus the drum and frame displacements (Eqs. 5.1-4,5,6). Some complication is introduced because the coefficients and the unknowns are complex, but each complex equation may be written as two real expressions. That is,

$$\sum_i (a_i + j\, b_i)\,(c_i + j\, d_i) = e + jf$$

may be rewritten as

$$a_i c_i - b_i d_i = e$$

$$a_i d_i + b_i c_i = f$$

and the unknowns c_i and d_i solved for in terms of the coefficients a_i and b_i and the right-hand terms e and f. The solution method used here was Gauss elimination with implicit pivoting (49).

B.3 Numerical Integration of the Nonlinear Relations

A variable-step vector Runge-Kutta algorithm (subroutines RK0 and RK1 in Appendix C) was used to integrate the relation

$$\dot{\sigma}_p(t) = \alpha_4\, \dot{\varepsilon}\, (\sigma_e - E\, \varepsilon)\,. \qquad (6.2\text{-}4)$$

Johnson and Riess (49) provide an extensive discussion of the methods employed for estimating the error at each step and for adjusting the

step size accordingly.

APPENDIX C

Program Listing

The theoretical model developed in this study was implemented in the VAX FORTRAN program listed in the following pages. Three subprograms called in subroutine DYNMCS (FACTOR, SOLVE, and AKAPPA) are not listed here. FACTOR and SOLVE triangularize the compliance matrix by Gauss elimination; AKAPPA estimates the matrix's condition number. These subroutines may be replaced by similar routines from any mathematical library (e.g., IMSL).

```
C     ****************************************************************
C     COMPACTION MODEL WITH HYSTERETIC STRESS GENERATION
C     ****************************************************************
C
      IMPLICIT REAL*8(A-H),REAL*8(O-Z)
C
      COMMON /UNIT/ NPRT,NDBUG,NPLOT,NSTRS,NIN,NOUT,NDBASE
C
      INTEGER TITLE(20)
      CHARACTER DAY*9,THYME*8
C
      PRINT 1000
 1000 FORMAT(' ENTER TITLE')
      READ(NIN,1100) TITLE
 1100 FORMAT(20A4)
      WRITE(NPRT,1200) TITLE
 1200 FORMAT(//,1X,20A4)
      CALL DATE(DAY)
      CALL TIME(THYME)
      WRITE(NPRT,1300) DAY,THYME
 1300 FORMAT(' PROGRAM RUN ON:  ',A9,3X,A8)
      WRITE(NPLOT) TITLE,DAY,THYME
C
C     INITIALIZE SOME PARAMETERS FROM DATA BASE
      CALL INIT
C
C
C     LOOP ON ROLLER PASSES
      NPASS = 0
 10   CONTINUE
      NPASS = NPASS + 1
C
C     LINEAR MODEL TO ESTIMATE STRAIN AMPLITUDES
C
C         DYNAMIC SOLUTION FOR CONTACT STRESS AND COMPACTOR MOTION
          CALL DYNMCS(NPASS)
C
C         GENERATE STRESS AND STRAIN FIELD
          CALL FIELD(NPASS)
C
C     HYSTERETIC STRESS
      CALL STRESS (NPASS)
C
```

```
      PRINT 2000
 2000 FORMAT(' ANOTHER PASS? (Y/N)')
      READ(NIN,2010) IYN
 2010 FORMAT(A1)
      IF(IYN .EQ. 1HY) GO TO 10
C
C
      STOP
      END
```

```
      BLOCKDATA
C
C     ***********************************************************
C     INITIALIZE COMMON
C     NOTE ALL DIMENSIONS IN INCHES, LB F, LB M.
C     (EXCEPT ROLLER SPEED, IN IN FT/SEC)
C     ***********************************************************
C
      IMPLICIT REAL*8 (A-H), REAL*8(O-Z)
C
      COMMON /UNIT/ NPRT,NDBUG,NPLOT,NSTRS,NIN,NOUT,NDBASE
C
      COMMON /SOIL/ EMOD,GMOD,PR,DNSITY,VOIDR,CSFT,PRESSC
C
      REAL*4 ALPHA
      COMMON /HYS/ ALPHA(5)
C
      COMMON /CMPCTR/ DLNGTH,CWIDTH,RADIUS,WBASE,FWGHT,DWGHT,
     1                ECCENT,FREQH,DAMP,STIFF,SPEED
C
C     LINEAL DIMENSIONS
      DATA DLNGTH,CWIDTH,RADIUS,WBASE
     1    /84.D0,4.5,28.D0,127.D0/
C
C     STATIC WEIGHTS AND ECCENTRIC MOMENT.  NOTE THESE ARE OVERALL
C     WEIGHTS, **NOT EQUIVALENT!** (I.E., MUST BE REFLECTED TO
C     DRUM END)
      DATA FWGHT,DWGHT,ECCENT
     1   /11923.D0,8777.D0,444.29D0/
C
C     SUSPENSION AND FORWARD SPEED.  NOTE THAT THE DAMPING COEFFICIENT
C     IS STRUCTURAL ( IN LB/IN.) AND SHOULD BE MULTIPLIED BY THE
C     AMPLITUDE OF DISPLACEMENT, NOT VELOCITY.  THE SPEED IS IN
C     FT/SEC.  2 MPH = 3. FT/SEC
      DATA DAMP,STIFF,SPEED
     1 /3849.D0,24054.D0,3.D0/
C
C     DEFAULT SOIL PARAMETERS
      DATA EMOD,GMOD,PR
     1    /0.D0,  0.D0, 0.3D0/
      DATA DNSITY,VOIDR
     1  /   0.06D0,0.8D0/
      DATA ALPHA / 0., 0., 3., 1., 0.  /
C
C     I/O
      DATA NPRT,NDBUG,NPLOT,NSTRS,NIN,NOUT,NDBASE
```

```
     1  /    1,    2,    3,    4,  5,   6,     7/
C
      END
```

```
      SUBROUTINE INIT
C
C     ****************************************************************
C     OBTAIN SOME PARAMETERS FROM DISK  (TIRESOME TO INPUT FROM
C     TERMINAL EACH TIME, BUT NOT CONVENIENT TO BE HARDWIRED.)
C     0'S IN A FIELD ALLOW PROGRAM DEFAULTS TO TAKE OVER, EXCEPT
C     FOR ELASTIC CONSTANTS.  THERE, EITHER
C        (A)  ALL 3 ARE ZERO (DEFAULTS WILL BE USED)
C        (B)  ANY ONE IS ZERO (AND IS COMPUTED FROM OTHER TWO)
C        (C)  ALL 3 ARE NON-ZERO.  (IN THIS CASE, POISSONS RATIO
C             IS MODIFIED FOR CONSISTENCY.)
C     ****************************************************************
C
      IMPLICIT REAL*8(A-H), REAL*8(O-Z)
      REAL*4 A(5)
C
      COMMON /UNIT/ NPRT,NDBUG,NPLOT,NSTRS,NIN,NOUT,NDBASE
C
      COMMON /SOIL/ EMOD,GMOD,PR,DNSITY,VOIDR,CSFT,PRESSC
C
      REAL*4 ALPHA
      COMMON /HYS/ ALPHA(5)
C
      COMMON /CMPCTR/ DLNGTH,CWIDTH,RADIUS,WBASE,FWGHT,DWGHT,
     1                ECCENT,FREQH,DAMP,STIFF,SPEED
C
      COMMON /EFFECT/ FRAMEW,FRAMEM,DRUMW,DRUMM
C
      DATA IY /1HY/, IN /1HN/
C
      OPEN(7,FILE='DBASE.DAT',STATUS='OLD')
C
      PRINT 999
  999 FORMAT(' ENTER FREQUENCY IN HZ')
      READ(NIN,*) FREQH
C
      READ(NDBASE,1000)
 1000 FORMAT(A1)
      READ(NDBASE,*) R,D,C
      IF(R .NE. 0.D0) RADIUS = R
      IF(D .NE. 0.D0) DLNGTH = D
      IF(C .NE. 0.D0) CWIDTH = C
      WRITE(NPRT,1100) CWIDTH,DLNGTH,RADIUS
 1100 FORMAT(' CONTACT AREA GEOMETRY:',
     1 /,5X,'HALF-WIDTH:',T20,G15.5,' IN.',
     2 /,5X,'LENGTH:',T20,G15.5,' IN.',
```

```
     3 /,5X,'DRUM RADIUS:',T20,G15.5,' IN.')
C
      READ(NDBASE,1000)
      READ(NDBASE,*) STF,DMP,WF,WD,EC,SPD
      IF(STF .NE. 0.D0) STIFF = STF
      IF(DMP .NE. 0.D0) DAMP = DMP
      IF(WF .NE. 0.D0) FWGHT = WF
      IF(WD .NE. 0.D0) DWGHT = WD
      IF(EC .NE. 0.D0) ECCENT = EC
      IF(SPD.NE. 0.D0) SPEED = SPD
      WRITE(NPRT,1200) STIFF,DAMP
 1200 FORMAT(' SUSPENSION:',/,5X,'K:',D15.7,' LB/IN.',
     1                      /,5X,'C:',D15.7,' LB/IN. (STRUCTURAL)')
      WRITE(NPRT,1300) FWGHT,DWGHT,ECCENT
 1300 FORMAT(' COMPONENT WEIGHTS:',/,5X,'FRAME:',D15.7,' LB',
     1                              /,5X,'DRUM: ',D15.7,' LB',
     2                              /,5X,'M-E:  ',D15.7,' LB-IN.')
C
C     EFFECTIVE WEIGHTS AND INERTIAS
      DRUMW = DWGHT
      DRUMM = DRUMW
      FRAMEW = FWGHT/3.D0
      FRAMEM = 0.25D0*FWGHT
      PRINT 1400,FWGHT,DWGHT
 1400 FORMAT(' FRAME WEIGHT:',T30,G15.7,' LB F',
     1 /,    ' DRUM WEIGHT:',T30,G15.7,' LB F')
      PRINT 1500,FRAMEW,FRAMEM
      WRITE(NPRT,1500) FRAMEW,FRAMEM
 1500 FORMAT(' FRAME WEIGHT AND MASS REFLECTED TO DRUM:',
     1 /,5X,'WEIGHT OF FRAME AT DRUM:',T30,G15.7,' LB F',
     2 /,5X,'INERTIA OF FRAME AT DRUM:',T30,G15.7,' LB M')
      PRINT 1600
 1600 FORMAT(' ENTER FRACTION OF TOTAL FRAME MASS TO BE TRANSFERRED',
     1 /,' FROM TIRES TO BACK END')
      READ(NIN,*) FRACM
      IF(FRACM .EQ. 0.D0) GO TO 100
      FRAMEM = (0.25D0 + FRACM)*FWGHT
      PRINT 1700
 1700 FORMAT(' ADJUST DEADWEIGHT? (Y/N)')
      READ(NIN,1800) IYN
 1800 FORMAT(A1)
      IF(IYN .EQ. IY) FRAMEW = FRAMEW + FRACM*FWGHT
 100  CONTINUE
      WRITE(NPRT,1900) FRACM,FRAMEW,FRAMEM
      PRINT 1900,FRACM,FRAMEW,FRAMEM
 1900 FORMAT(' FRACTION OF FRAME MASS MOVED TO DRUM-END',G10.3,
```

```
     1 /,5X,' EFFECTIVE FRAME WEIGHT:',T30,G12.5,' LB F',
     2 /,5X,' EFFECTIVE FRAME INERTIA:',T30,G12.5,' LB M')
C
      READ(NDBASE,1000)
      READ(NDBASE,*)E,G,P,D,VR
      IF(P.NE.0.D0) PR = P
      IF(D.NE.0.D0) DNSITY = D
      IF(VR.NE.0.D0) VOIDR = VR
      WRITE(NPRT,2000) DNSITY,VOIDR
 2000 FORMAT(' SOIL PARAMETERS:',
     1 /,5X,'DENSITY:',T20,G15.4,' PCI',
     2 /,5X,'VOID RATIO:',T20,G15.4)
C
      IF(E.EQ.0.D0 .AND. G.EQ.0.D0)GO TO 200
      IF(E.NE.0.D0) EMOD = E
      IF(G.NE.0.D0) GMOD = G
      IF(E.NE.0.D0 .AND. G.NE.0.D0) PR = 0.5*E/G - 1.
      DENOM = 2.D0*(1.D0+PR)
      IF(EMOD .EQ. 0.D0) EMOD = GMOD*DENOM
      IF(GMOD .EQ. 0.D0) GMOD = EMOD/DENOM
      GO TO 300
C
 200  CONTINUE
      COEF = PR/(1.D0 - PR)
      PRINT 2100
 2100 FORMAT(' ENTER AVERAGE CONFINING STRESS IN SOIL MASS FOR',
     1 /,' ESTIMATING SHEARING MODULUS.  (SUGGEST 3. PSI)')
      READ(NIN,*) PRESSC
      WRITE(NPRT,2200) PRESSC
 2200 FORMAT(' AVG CONFINING STRESS:',T30,G15.6,' PSI')
      GMOD = 1230.D0*(2.97 - VOIDR)**2
      GMOD = GMOD*DSQRT(PRESSC)/(1.D0 + VOIDR)
      EMOD = 2.D0*(1.D0 + PR)*GMOD
C
 300  CONTINUE
      CSFT = DSQRT(GMOD*386.088D0/DNSITY)/12.D0
      WRITE(NPRT,3000) EMOD,GMOD,PR,CSFT
 3000 FORMAT(' INITIAL ELASTIC CONSTANTS:',
     1 /,5X,'E:  ',D12.3,' PSI',
     2 /,5X,'G:  ',D12.3,' PSI',
     3 /,5X,'v:  ',D12.3,
     4 /,' SHEAR WAVE VELOCITY:',G14.7,' FT/SEC')
C
C
C     HYSTERETIC CONSTANTS
      READ(NDBASE,1000)
```

```
      READ(NDBASE,*) (A(I),I=1,5)
      DO 400 I = 1,5
 400  IF(A(I) .NE. 0.) ALPHA(I) = A(I)
      WRITE(NPRT,4000) (ALPHA(I),I=1,5)
 4000 FORMAT(' HYSTERETIC AND RESIDUAL STRESS COEFFICIENTS:',
     1 /,1X,5G15.7)
C
      RETURN
      END
```

```
      SUBROUTINE DYNMCS(NPASS)
C
C     ***************************************************************
C     DETERMINE THE DYNAMIC CONTACT STRESS DISTRIBUTION AND SURFACE
C     MOTION.  ASSUME THAT THE DYNAMIC CONTACT STRESS IS DISTRIBUTED
C     OVER THE STATIC CONTACT AREA (WHICH IS THE MEAN CONTACT AREA
C     OVER ONE CYCLE).
C         THE MAGNITUDES OF THE STRESSES ARE UNKNOWN. HOWEVER, THE
C     DISTRIBUTION MUST CONFORM TO THAT PRODUCING UNIFORM DISPLACEMENT
C     OF POINTS ON THE CONTACT SURFACE, SINCE THE DRUM IS RIGID, AND
C     THIS DISPLACEMENT MUST EQUAL THE DRUM DISPLACEMENT.  MOREOVER,
C     THE INTEGRAL OF THE CONTACT STRESS OVER THE CONTACT AREA GIVES
C     THE SOIL REACTION SEEN BY THE DRUM.  THEREFORE WE MUST ASSEMBLE
C     EQUATIONS DESCRIBING THE COUPLED DYNAMICS OF SOIL AND COMPACTOR.
C         THE METHOD THAT FOLLOWS IS ESENTIALLY THAT OF WONG AND LUCO
C     (1975), EXCEPT THAT SIMPLIFYING ASSUMPTIONS OF PLANE STRAIN ARE
C     INVOKED TO REDUCE THE NUMBER OF INTEGRAL EVALUATIONS.  THE
C     CONTACT AREA IS DIVIDED INTO ELEMENTAL STRIPS.  THE STRESS IN
C     EACH STRIP IS ASSUMED UNIFORM.  THE INFLUENCE OF EACH ELEMENTAL
C     LOAD ON THE DISPLACEMENT OF EVERY OTHER STRIP IS FIRST
C     DETERMINED, USING THE INTEGRATION METHOD OF    THOMSON AND
C     KOBORI (JAM, 1963).  THESE EFFECTS ARE SUPERIMPOSED IN AN
C     OVERALL COMPLIANCE MATRIX.  THIS MATRIX IS AUGMENTED BY TWO
C     OTHER COMPLEX EQUATIONS DESCRIBING THE FRAME AND DRUM DYNAMICS.
C     ***************************************************************
C
      IMPLICIT REAL*8 (A-H), REAL*8(O-Z)
      EXTERNAL G1,H1,APPRX1
C
      DIMENSION AMP(10), PHASE(10), F(24), CR(20), CI(20)
      DIMENSION IPIVOT(24)
C
      COMMON /UNIT/ NPRT,NDBUG,NPLOT,NSTRS,NIN,NOUT,NDBASE
C
      COMMON /SOIL/ EMOD,GMOD,PR,DNSITY,VOIDR,CSFT,PRESSC
C
      COMMON /EFFECT/ FRAMEW,FRAMEM,DRUMW,DRUMM
C
      COMMON /CMPCTR/ DLNGTH,CWIDTH,RADIUS,WBASE,FWGHT,DWGHT,
     1                ECCENT,FREQH,DAMP,STIFF,SPEED
C
      COMMON /TRIGD/ PI,TWOPI,DTR
C
      REAL*4 RANGE,DEPTH
      COMMON /MESH/ HALF,FULL,RANGE(40),DEPTH(15),N,KVAR,NR,NZ
C
```

```
C     U IS THE PARTITIONED VECTOR OF UNKNOWN FORCES AND DISPLACEMENTS
      COMMON /STRDAT/ FSR,FSI,S(20),W(4),G(24,25),DUMMY(300)
      DIMENSION U(24)
      EQUIVALENCE (U(1),S(1))
C
      DATA NMAX /10/, NMX /24/
      DATA GRVITY /386.044/
C
C     NO. ELEMENTS TO ONE SIDE OF DRUM CENTERLINE:
      IF(NPASS .NE. 1) GO TO 50
      PRINT 1000
 1000 FORMAT(' ENTER NO. ELEMENTS PER HALF-WIDTH OF CONTACT AREA')
      READ(NIN,*) N
      N = MIN0(N,NMAX)
      N2 = 2*N
      N2 = MAX0(N2,1)
      HALF = CWIDTH/DFLOAT(N2)
      FULL = 2.D0*HALF
      WRITE(NPRT,1100) N,FULL
 1100 FORMAT(' NO. ELEMENTS PER HALF-WIDTH:  ',T40,I5,
     1     /,' ELEMENT WIDTH:',T40,G20.10)
 50   CONTINUE
C
C     SET UP FOR INFLUENCE FACTORS
      CALL INFL0(HALF)
C
      WRITE(NPRT,1300) NPASS
 1300 FORMAT(1H1,' CONTACT STRESSES AND SURFACE DISPLACEMENTS',
     1 ' FOR PASS NO.',I3)
C
C     COMPUTE INFLUENCE COEFFICIENTS
      DO 200 J = 1,N2
      X = FULL*DFLOAT(J-1)
      Y = 0.D0
      KVAR = 1
      CALL INFLNC(FREQH,X,Y,KVAR,G1,H1,APPRX1,CR(J),CI(J))
 200  CONTINUE
C
C     FORM COEFFICIENT MATRIX G FOR SOLVING
C        G*U = F
C     FOR U, WHERE
C        U = [ S | W | WF ]-TRANSPOSE
C        F = [ 0 | FA| 0  ]-TRANSPOSE
C     HERE, THE (COMPLEX) UNKNOWNS ARE
C        S:  CONTACT FORCE/UNIT LENGTH ON EACH STRIP ELEMENT
C            (SCALED BY GMOD)
```

```
C        W:  CONTACT SURFACE DISPLACEMENT
C       WF:  FRAME DISPLACEMENT
C     FA IS THE KNOWN DYNAMIC FORCE APPLIED TO THE DRUM (ALSO SCALED
C     BY GMOD.)
C          FOR N ELEMENTS, WE HAVE N UNKNOWN FORCES, PLUS TWO UNKOWN
C     DISPLACEMENTS (DRUM AND FRAME).  SINCE ALL QUANTITIES ARE
C     COMPLEX, WE HAVE 2*(N+2) UNKNOWNS.  IN THE FOLLOWING,
C          I1 AND J1 INDEX REAL PARTS
C          I2 AND J2 INDEX IMAGINARY PARTS.
C
C     1.  FIRST 2*N EQNS RELATE ELEMENT LOADS/UNIT LENGTH S(J)
C     TO SURFACE DISPLACEMENTS, WHICH ARE ALL EQUAL TO THE DRUM
C     DISPLACEMENT.  THE COEFFICIENTS OF THE UNKNOWN LOADS ARE
C     THE APPROPRIATE COMPLIANCE FUNCTIONS.  NOTE THAT, IN ORDER
C     TO REDUCE THE NUMBER OF EQUATIONS, WE HAVE USED SYMMETRY TO
C     SOLVE ONLY FOR THE LOADS ON THE RIGHT-HALF OF THE CONTACT
C     AREA (X.GT.0).  HOWEVER, DISPLACEMENTS THERE ARE ALSO
C     INFLUENCED BY LOADS ON THE LEFT SIDE OF THE SAME MAGNITUDE
C     BUT AT GREATER DISTANCE.  OVERALL INFLUENCE FOR AN ELEMENTAL
C     LOAD IS THE SUM OF INFLUENCES FROM BOTH SIDES.  IN THE FOLLOWING
C         IJ1 INDEXES INFLUENCE FROM RIGHT
C         IJ2 INDEXES INFLUENCE FROM LEFT.
      I1 = -1
      DO 400 I = 1,N
      I1 = I1 + 2
      I2 = I1 + 1
C
      J1 = -1
      DO 300 J = 1,N
      J1 = J1 + 2
      J2 = J1 + 1
      IJ1 = IABS(I-J) + 1
      IJ2 = IABS(I+J)
      GR = CR(IJ1) + CR(IJ2)
      GI = CI(IJ1) + CI(IJ2)
C
      G(I1,J1) = GR
      G(I1,J2) = -GI
      G(I2,J1) = GI
      G(I2,J2) = GR
  300 CONTINUE
C
C     COEFFICIENTS OF DRUM AND FRAME DISPLACEMENT.  ONLY THE
C     DRUM DISPLACEMENT (EQUAL TO THE CONTACT AREA DISPLACEMENT)
C     ENTERS INTO THESE EQUATIONS.
      N21 = N2 + 1
```

```
      N24 = N2 + 4
      DO 350 J = N21,N24
      G(I1,J) = 0.D0
      G(I2,J) = 0.D0
  350 CONTINUE
      G(I1,N2+1) = -1.D0
      G(I2,N2+2) = -1.D0
C
  400 CONTINUE
C
C     2.  NOW ADD 2 MORE ROWS TO G TO DESCRIBE DRUM DYNAMICS.
C     TOTAL CONTACT FORCE ON DRUM PER UNIT LENGTH IS
C        FS = SUMj( S(J) )
C     (OVER BOTH SIDES -- HENCE, FACTOR OF 2. BELOW).
C     WE DIVIDE THE OTHER FORCE TERMS-- STIFFNESS, DAMPING, AND
C     APPLIED FORCE -- BY THE OVERALL DRUM LENGTH, FOR A 2-D
C     FORMULATION.
C          AS BEFORE, WE NORMALIZE ALL FORCES BY GMOD.
      I1 = N2 + 1
      I2 = I1 + 1
      J1 = -1
      DO 410 J = 1,N
      J1 = J1+2
      J2 = J1+1
      G(I1,J1) = -2.D0
      G(I1,J2) = 0.D0
      G(I2,J1) = 0.D0
      G(I2,J2) = -2.D0
  410 CONTINUE
C
C     NEXT TWO ENTRIES GIVE INERTIA AND SUSPENSION FORCES ON DRUM
C     NOTE THAT THE SUSPENSION DAMPING IS STRUCTURAL, NOT VISCOUS,
C     SO THAT THE DAMPING IS INDEPENDENT OF FREQUENCY:
C            F = (K1 + j*K2)*X
      J1 = N2 + 1
      J2 = J1 + 1
      OMEGA = TWOPI*FREQH
      A = STIFF/(GMOD*DLNGTH)
      B = DAMP/(GMOD*DLNGTH)
      C = -(DRUMM/GRVITY)*OMEGA*OMEGA/(GMOD*DLNGTH)
      G(I1,J1) = A + C
      G(I1,J2) = -B
      G(I2,J1) =  B
      G(I2,J2) =  A + C
C
C     LAST TWO ENTRIES REDUCE SUSPENSION FORCE DUE TO MOTION OF FRAME
```

```
      J1 = J1+2
      J2 = J1+1
      G(I1,J1) = -A
      G(I1,J2) = B
      G(I2,J1) = -B
      G(I2,J2) = -A
C
C     3.  FINALLY, ADD TWO ROWS FOR FRAME MOTION.  ONLY FORCE
C     IS SUSPENSION FORCE.
      I1 = I1 + 2
      I2 = I1+1
      DO 420 J = 1,N2
      G(I1,J) = 0.D0
      G(I2,J) = 0.D0
 420  CONTINUE
      J1 = N2 + 1
      J2 = J1 + 1
      D = -(FRAMEM/GRVITY)*OMEGA*OMEGA/(GMOD*DLNGTH)
      G(I1,J1) = -A
      G(I1,J2) = B
      G(I2,J1) = -B
      G(I2,J2) = -A
      J1 = J1 + 2
      J2 = J1 + 1
      G(I1,J1) = A+D
      G(I1,J2) = -B
      G(I2,J1) = B
      G(I2,J2) = A+D
C
C
C     FORM THE VECTOR OF APPLIED FORCES.  THE ONLY NON-ZERO ENTRY IS
C     THE REAL PART OF THE APPLIED DYNAMIC FORCE, WHICH IS
C     APPLIED TO THE DRUM.
      N3 = N2 + 1
      N6 = N2 + 4
      DO 450 J = 1,N6
 450  F(J) = 0.D0
      FA = ECCENT*OMEGA*OMEGA/GRVITY
      F(N3) = FA/(GMOD*DLNGTH)
C
C     SOLVE FOR THE UNKNOWNS:
      NEQS = N2 + 4
      GNORM = ANORM1(G,NEQS,NMX)
      CALL FACTOR(G,IPIVOT,NEQS,NMX,IFLAG)
      CONNUM = AKAPPA(G,GNORM,IPIVOT,S,NEQS,NMX)
 3000 FORMAT(' CONDITION NUMBER',G20.10)
```

```
      WRITE(NPRT,3000) CONNUM
      CALL SOLVE(G,U,F,IPIVOT,NEQS,NMX)
      WRITE(NPRT,4000)
 4000 FORMAT(' CONTACT STRESS (PSI):',
     1 /,'  (J)',4X,'(+/-) X',11X,'RE',13X,'IM',13X,'AMP',11X,'PHASE')
      SUMR = 0.D0
      SUMI = 0.D0
      K1 = -1
      X = -HALF
      DO 500 K = 1,N
      K1 = K1 + 2
      K2 = K1 + 1
      X = X + FULL
      SUMR = SUMR + S(K1)
      SUMI = SUMI + S(K2)
      S(K1) = S(K1)/FULL
      S(K2) = S(K2)/FULL
      AMP(K) = DSQRT( S(K1)**2 + S(K2)**2 )
      PHASE(K) = DATAN(S(K2)/S(K1))/DTR
      S(K1) = S(K1)*GMOD
      S(K2) = S(K2)*GMOD
      AMP(K) = AMP(K)*GMOD
 4100 FORMAT(1X,I4,5G15.5)
      WRITE(NPRT,4100) K,X,S(K1),S(K2),AMP(K),PHASE(K)
 500  CONTINUE
C
      FSR = 2.D0*SUMR*DLNGTH
      FSI = 2.D0*SUMI*DLNGTH
      FSA = DSQRT(FSR*FSR + FSI*FSI)
      FSP = DATAN(FSI/FSR) / DTR
      FSR = FSR*GMOD
      FSI = FSI*GMOD
      FSA = FSA*GMOD
C
      DO 520 I = 1,4
 520  W(I) = U(N2 + I)
C
      WDA = DSQRT(W(1)*W(1) + W(2)*W(2))
      WDP = DATAN(W(2)/W(1))/DTR
      WFA = DSQRT(W(3)*W(3) + W(4)*W(4))
      WFP = DATAN(W(4)/W(3))/DTR
      WRITE(NPRT,5000) FA,FSR,FSI,FSA,FSP,W(1),W(2),WDA,WDP,
     1                 W(3),W(4),WFA,WFP
 5000 FORMAT(/,' DYNAMIC FORCE:',T66,G15.5,' LB  @ ',3X,'0.',9X,
     1 ' DEG',
     1       /,' SOIL REACTION:',T30,'(',G15.5,',',G15.5,') = ',G15.5,
```

```
     1         ' LB  @ ',G14.5,' DEG',
     2       /,' DRUM DISPLACEMENT:',T30,'(',G15.5,',',G15.5,') = ',
     2         G15.5,' IN. @ ',G14.5,' DEG',
     3       /,' FRAME DISPLACEMENT;',T30,'(',G15.5,',',G15.5,') = ',
     3         G15.5,' IN. @ ',G14.5,' DEG')
      CALL CDIV(FSR,FSI,W(1),W(2),SSTIFF,SDAMP)
      SSTIFF = -SSTIFF
      SDAMP = -SDAMP/OMEGA
      WRITE(NPRT,5100) SSTIFF,SDAMP
 5100 FORMAT(' SOIL STIFFNESS:  ',T25,G20.5,' LB/IN.',
     1  /,   '         DAMPING:  ',T25,G20.5,' LB-SEC/IN.')
      WRITE(NPLOT) FREQH,FA,FSA,FSP,FSR,FSI,WDA,WDP,WFA,WFP
      WRITE(NPLOT) FREQH,N2,(S(K),K=1,N2)
C
 800  CONTINUE
C
      RETURN
      END
```

```
      SUBROUTINE FIELD (NPASS)
C
C     ***************************************************************
C     GENERATE STRESS AND STRAIN FIELDS FROM LINEAR MODEL.
C     ***************************************************************
C
      IMPLICIT REAL*8 (A-H),REAL*8(O-Z)
      EXTERNAL G2,H2,APPRX2
C
      DIMENSION LABL1(3),LABL2(2,2)
      DIMENSION CR(50),CI(50)
C
      COMMON /UNIT/ NPRT,NDBUG,NPLOT,NSTRS,NIN,NOUT,NDBASE
C
      COMMON /SOIL/ EMOD,GMOD,PR,DNSITY,VOIDR,CSFT,PRESSC
C
      COMMON /CMPCTR/ DLNGTH,CWIDTH,RADIUS,WBASE,FWGHT,DWGHT,
     1                ECCENT,FREQH,DAMP,STIFF,SPEED
C
      COMMON /EFFECT/ FRAMEW,FRAMEM,DRUMW,DRUMM
C
      COMMON /TRIGD/ PI,TWOPI,DTR
C
      REAL*4 RANGE,DEPTH
      COMMON /MESH/ HALF,FULL,RANGE(40),DEPTH(15),N,KVAR,NR,NZ
C
      REAL*4 FR,FI,FST
      COMMON /STRDAT/ FSR,FSI,S(20),W(4),FR(15,40),FI(15,40),FST(15,40)
C
      DATA LABL1/4H STR,4HAIN ,4HESS /
      DATA LABL2/4HuIN.,4H/IN.,4HPSI ,4H     /
C
C
      KVAR = 2
      LVAR = 1
C     WRITE(NPRT,1030) LABL1(1),LABL1(KVAR),FREQH
 1030 FORMAT(1H1,/,' FIELD GENERATION:  ',2A4,' AT ',F15.5,' HZ')
C
C
C     LOOP ON DEPTH
      NZ = 0
  100 CONTINUE
      NZ = NZ + 1
      IF(NZ .EQ. 16) GO TO 600
      IF(NPASS .NE. 1) GO TO 110
      PRINT 1100
```

```
 1100 FORMAT(' ENTER DEPTH IN FEET.  ENTER NEGATIVE DEPTH TO QUIT.')
      READ(NIN,*) DEPTH(NZ)
 110  CONTINUE
      DEP = DEPTH(NZ)*12.
      IF(DEP .LT. 0.D0) GO TO 600
C
C     1.  NEAR FIELD--GENERATE ON ORIGINAL SURFACE MESH
      N2 = 2*N
      N3 = 3*N
      N4 = 4*N
      CALL INFLO(HALF)
      DO 200 J = 1,N3
      X = FULL*DFLOAT(J-1)
      CALL INFLNC(FREQH,X,DEP,KVAR,G2,H2,APPRX2,CR(J),CI(J))
 200  CONTINUE
C
C     SUPERIMPOSE THE DYNAMIC EFFECTS
      FACT = 1.D0
      IF(KVAR .EQ. 2) FACT = GMOD
      PRINT 3010,DEPTH(NZ),LABL1(1),LABL1(KVAR),LABL2(1,LVAR),
     1 LABL2(2,LVAR)
C     WRITE(NPRT,3010) DEPTH(NZ),LABL1(1),LABL1(KVAR),LABL2(1,LVAR),
C    1 LABL2(2,LVAR)
 3010 FORMAT(' FOR ',G15.6,' FT DEPTH:  ',
     1     '  X (IN.), DYNAMIC',2A4,'IN ',2A4,'(AMP AND PHASE)')
C     WRITE(NPRT,3020)
 3020 FORMAT(' NEAR FIELD:')
      X = -HALF
      I1 = -1
      DO 400 I = 1,N2
      I1 = I1 + 2
      I2 = I1 + 1
      X = X + FULL
      RANGE(I) = X/12.D0
      J1 = -1
      SUMR = 0.D0
      SUMI = 0.D0
      DO 300 J = 1,N
      J1 = J1 + 2
      J2 = J1 + 1
      IJ1 = IABS(I-J) + 1
      IJ2 = IABS(I+J)
      GR = CR(IJ1) + CR(IJ2)
      GI = CI(IJ1) + CI(IJ2)
      SUMR = SUMR + (GR*S(J1) - GI*S(J2))*2.D0
      SUMI = SUMI + (GI*S(J1) + GR*S(J2))*2.D0
```

```
 300  CONTINUE
      AMP = DSQRT(SUMR*SUMR + SUMI*SUMI)
      PHASE = DATAN(SUMI/SUMR)/DTR
      AMP = AMP/FACT
      IF(KVAR .EQ. 2) AMP = AMP*1.D6
      PRINT 3100,X,AMP,PHASE
 3100 FORMAT(1X,3G20.10)
C     WRITE(NPRT,3100) X,AMP,PHASE
      FR(NZ,I) = SUMR/FACT
      FI(NZ,I) = SUMI/FACT
 400  CONTINUE
C
C     FAR FIELD
C     2.  FAR FIELD--INVOKE ST VENANTS PRINCIPLE AND SAY THE HELL WITH
C     IT, WAY OUT THERE, IT LOOKS LIKE A UNIFORM LOAD.
      CALL INFLO(CWIDTH)
C     WRITE(NPRT,4000)
 4000 FORMAT(' FAR FIELD:')
      PRINT 4000
C
C     REPEAT THE LAST POINT, FOR COMPARISON OF NEAR- AND FAR-FIELD
C     RESULTS
      X = X - CWIDTH
      DO 500 I = N2,N3
      X = X + CWIDTH
      RANGE(I) = X/12.D0
      CALL INFLNC(FREQH,X,DEP,KVAR,G2,H2,APPRX2,GR,GI)
      STR = (GR*FSR - GI*FSI)/(CWIDTH*DLNGTH)
      STI = (GI*FSR + GR*FSI)/(CWIDTH*DLNGTH)
      AMP = DSQRT(STR*STR + STI*STI)
      PHASE = DATAN(STI/STR)/DTR
      AMP = AMP/FACT
      IF(KVAR .EQ. 2) AMP = 1.D6*AMP
      PRINT 3100,X,AMP,PHASE
C     WRITE(NPRT,3100) X,AMP,PHASE
      IF( I.NE.N2) FR(NZ,I) = STR/FACT
      IF( I.NE.N2) FI(NZ,I) = STI/FACT
 500  CONTINUE
C
      GO TO 100
C
 600  CONTINUE
      NZ = NZ - 1
      NR = N3
C
C     STATIC EFFECT
```

```
      DEADWT = (FRAMEW + DRUMW) / DLNGTH
      Q0 = 2.D0*DEADWT/(PI*CWIDTH)
C     WRITE(NPRT,6000) LABL1(1),LABL1(KVAR),LABL2(1,LVAR),LABL2(2,LVAR)
 6000 FORMAT(/,'  X(IN.), STATIC',2A4,'IN ',2A4)
      DO 700 I = 1,NZ
C     WRITE(NPRT,6010) DEPTH(I)
 6010 FORMAT(' DEPTH:  ',G20.10)
      DO 700 J = 1,NR
      X1 = RANGE(J)*12.
      DEP = DEPTH(I)*12.
      SUM = 0.D0
      X2 = -(DFLOAT(N)*FULL + HALF)
      DO 670 K = 1,N2
      X2 = X2 + FULL
      XB = X2/CWIDTH
      Q = Q0*DSQRT( DABS(1.D0-XB*XB) )/PI
      X = DABS(X1-X2)
      D = PI/2.D0
      IF(X .LT. HALF) D = -D
      IF(DEP .NE. 0.D0) D = DATAN( (X-HALF)/DEP)
      E = PI/2.D0
      IF(DEP .NE. 0.D0) E = DATAN( (X+HALF)/DEP)
      A = E - D
      CY = A + DSIN(A)*DCOS(A + 2.D0*D)
      CX = A - DSIN(A)*DCOS(A + 2.D0*D)
      SX = CX*Q
      SY = CY*Q
      EY = (1.D0+PR)*( (1.D0-PR)*SY - PR*SX)*(1.D6/EMOD)
      DF = EY
      IF(KVAR .EQ. 3) DF = SY
      SUM = SUM + DF
 670  CONTINUE
      XINCH = RANGE(J)*12.D0
      FST(I,J) = SUM/1.D6
C     WRITE(NPRT,3100) XINCH,SUM
 700  CONTINUE
C
 800  CONTINUE
      RETURN
      END
```

```
      SUBROUTINE STRESS(NPASS)
C
C     ****************************************************************
C     THIS ROUTINE INTEGRATES THE NONLINEAR CONSTITUTIVE EQUATIONS
C     THAT GENERATE RESIDUAL STRESSES
C     ****************************************************************
C
      DIMENSION STATE1(30),STATE2(30),WORK(300)
      DIMENSION SPAVG(15,11)
C
      COMMON /HYS/ ALPHA(5)
C
      REAL*8 EMOD,GMOD,PR,DNSITY,VOIDR,CSFT,PRESSC
      COMMON /SOIL/ EMOD,GMOD,PR,DNSITY,VOIDR,CSFT,PRESSC
C
      COMMON /UNIT/ NPRT,NDBUG,NPLOT,NSTRS,NIN,NOUT,NDBASE
C
      REAL*8 DLNGTH,CWIDTH,RADIUS,WBASE,FWGHT,DWGHT,
     1       ECCENT,FREQH,DAMP,STIFF,SPEED
      COMMON /CMPCTR/ DLNGTH,CWIDTH,RADIUS,WBASE,FWGHT,DWGHT,
     1                ECCENT,FREQH,DAMP,STIFF,SPEED
C
      REAL*8 FRAMEW,FRAMEM,DRUMW,DRUMM
      COMMON /EFFECT/ FRAMEW,FRAMEM,DRUMW,DRUMM
C
      REAL*8 PI,TWOPI,DTR
      COMMON /TRIGD/ PI,TWOPI,DTR
C
      REAL*8 HALF,FULL
      COMMON /MESH/ HALF,FULL,RANGE(40),DEPTH(15),N,KVAR,NR,NZ
C
      REAL*8 DUMMY
      COMMON /STRDAT/DUMMY(26),FR(15,40),FI(15,40),FST(15,40)
C
      COMMON /INTEG/ T1,T2,X1,X2,OMEGA,AVGP(15),EMODZ(15),SE(15),
     1               E(15),EDOT(15),SP(15)
C
C
C       INITIALIZE THE COMPACTION.  STORE THE DEPTH-DEPENDENT VALUES
C       OF THE AVERAGE CONFINING PRESSURE AND ELASTIC MODULUS IN
C       AVGP AND EMODZ.  NOTE THAT AVGP CONTAINS THE CONTRIBUTIONS
C       OF THE WEIGHT OF THE SOIL COLUMN AND THE RESIDUAL STRESSES,
C       BUT NOT THE EFFECT DUE TO THE COMPACTOR DEADWEIGHT.  THIS
C       MUST BE ADDED IN SEPARATELY (AT EACH RANGE) TO THE
C       CONFINING PRESSURE USED TO ESTIMATE THE LOCAL STIFFNESS.
        IF(NPASS .GT. 1) GO TO 150
```

```
      NSTATE = NZ
      POIS = PR
      WIDTH = CWIDTH
      PCMPCT = (FRAMEW + DRUMW)/(DLNGTH*2.D0*CWIDTH)
      OMEGA = TWOPI*FREQH
      DIST = 12.*RANGE(NR)
      GEO = (1. + POIS)/(3.*(1. - POIS))
      RICHRT = (1230.*(2.97 - VOIDR)**2)/(1. + VOIDR)
      CALL RK0
      T2 = 0.
      KAVG = 0
      DO 110 I = 1,NZ
      DEP = 12.*DEPTH(I)
      SZ = DNSITY*DEP
      AVGP(I) = GEO*SZ
      P1 = AVGP(I)
      CALL SINFL(DIST,DEP,WIDTH,POIS,SX,SY,SZ)
      P2 = (SX + SY + SZ)*PCMPCT/3.
      EMODZ(I) = 2.*(1. + POIS)*RICHRT*SQRT(P1 + P2)
C
      DO 105 J = 1,10
 105  SPAVG(I,J) = 0.
C
      SP(I) = 0.
      STATE2(I) = SP(I)
 110  CONTINUE
C
      CALL INTERP(T2,RANGE(NR))
      WRITE(NSTRS) NZ,(DEPTH(I),I=1,NZ)
      WRITE(NSTRS) T2,X2,NPASS,NZ,(AVGP(I),EMODZ(I),SE(I),E(I),SP(I),
     1          SPAVG(I,11),        I = 1,NZ)
C
C     INITIALIZE FOR THIS PASS--
 150  CONTINUE
      DT = 0.1/FREQH
      DTOMIN = DT/50.
      JFLAG = 0
      SMAX = -1.E6
      X2 = -RANGE(NR)
      DX = SPEED*DT
C
      DO 170 I = 1,NZ
 170  STATE2(I) = SP(I)
C
 200  CONTINUE
      T1 = T2
```

```
      X1 = X2
      X2 = X1 + DX
      X2 = AMIN1(X2,RANGE(NR))
      T2 = T1 + (X2 - X1)/SPEED
      KAVG = KAVG + 1
      IF(KAVG .GT. 10) KAVG = 1
C
      DO 210 I = 1,NSTATE
 210  STATE1(I) = STATE2(I)
C
      CALL RK1(T1,T2,DTOMIN,STATE1,STATE2,NSTATE,WORK,1.E-4,IFLAG)
C
      IF(IFLAG .NE. 0) GO TO 220
      JFLAG = JFLAG + 1
      IF(JFLAG .LT. 5) GO TO 230
      JFLAG = 0
      DTOMIN = DTOMIN*2.
      DTOMIN = AMIN1(DTOMIN,DT/20.)
      GO TO 230
C
 220  CONTINUE
      JFLAG = 0
      DTOMIN = DTOMIN/2.
      DTOMIN = AMAX1(DT/200.,DTOMIN)
C
 230  CONTINUE
C
      DO 240 I = 1,NZ
      SP(I) = STATE2(I)
      SPAVG(I,KAVG) = SP(I)
      SMAX = AMAX1(SMAX,SP(I))
      SUM = 0.
      DO 235 J = 1,10
 235  SUM = SUM + SPAVG(I,J)
      SPAVG(I,11) = SUM/10.
 240  CONTINUE
C
C     OUTPUT QUANTITIES FOR THIS STEP
      CALL INTERP(T2,X2)
      WRITE(NSTRS) T2,X2,NPASS,NZ,(AVGP(I),EMODZ(I),SE(I),E(I),SP(I),
     1            SPAVG(I,11),      I = 1,NZ)
C
C     UPDATE THE CONFINING PRESSURES AND STIFFNESS MODULI
      DIST = 12.*X2
      DO 250 I = 1,NZ
      P1 = AVGP(I)
```

```
      DEP = 12.*DEPTH(I)
      CALL SINFL(DIST,DEP,WIDTH,POIS,SX,SY,SZ)
      P2 = (SX + SY + SZ)*PCMPCT/3.
      EMODZ(I) = 2.*(1. + POIS)*RICHRT*SQRT(P1 + P2)
 250  CONTINUE
C
      IF(X2 .LT. RANGE(NR)) GO TO 200
C
C     AVERAGE THE RESIDUAL STRESS OVER DEPTH--
      SUM = 0.
      DO 500 I = 1,NZ
      AVGP(I) = AVGP(I) + SPAVG(I,11)/3.
 500  SUM = SUM + SPAVG(I,11)
      SUM = SUM/FLOAT(NZ)
C
C     AUGMENT THE ESTIMATED PRESSURE
      PCON = PRESSC + SUM/3.
      GMOD = RICHRT*SQRT(PCON)
      EMOD = 2.*(1. + PR)*GMOD
      CSFT = DSQRT(GMOD*386.088D0/DNSITY)/12.
      WRITE(NPRT,5000) EMOD,GMOD,PR,CSFT,PRESSC
 5000 FORMAT(' UPDATED ELASTIC PARAMETERS:',
     1 /,5X,'E:  ',D12.3,' PSI',
     2 /,5X,'G:  ',D12.3,' PSI',
     3 /,5X,'v:  ',D12.3,
     4 /,' SHEAR WAVE VELOCITY:',3X,G14.7,' FT/SEC',
     5 /,' AVG CONFINING PRESSURE:',G14.7,' PSI')
C
C     DETERMINE RATIO OF PLASTIC STRESS TO OVERBURDEN
      WRITE(NPRT,5300)
 5300 FORMAT(/,' PASS NO., DEPTH(FT), SP (PSI), SZ, KX + KY')
      PRINT 5300
      DO 600 I = 1,NZ
      SZ = 12.*DNSITY*DEPTH(I)
      SPSZ = SPAVG(I,11)/SZ
      SXSYSZ = 2.*POIS/(1. - POIS)
      SUM = SPSZ + SXSYSZ
      WRITE(NPRT,5400) NPASS,DEPTH(I),SPAVG(I,11),SZ,SUM
 5400 FORMAT(1X,I3,4D15.6)
      PRINT 5400,NPASS,DEPTH(I),SPAVG(I,11),SZ,SUM
 600  CONTINUE
C
      RETURN
      END
```

```
      SUBROUTINE SYSDE(T,STATE,DERIV,NS)
C
C     ******************************************************************
C     DIFFERENTIAL EQUATIONS FOR STRAIN AND PLASTIC STRESS
C     ******************************************************************
C
      DIMENSION STATE(NS),DERIV(NS)
      DIMENSION SLOPE(15)
C
      COMMON /HYS/ ALPHA(5)
C
      COMMON /INTEG/ T1,T2,X1,X2,OMEGA,AVGP(15),EMODZ(15),SE(15),
     1               E(15),EDOT(15),SP(15)
C
      REAL*8 DLNGTH,CWIDTH,RADIUS,WBASE,FWGHT,DWGHT,
     1       ECCENT,FREQH,DAMP,STIFF,SPEED
      COMMON /CMPCTR/ DLNGTH,CWIDTH,RADIUS,WBASE,FWGHT,DWGHT,
     1                ECCENT,FREQH,DAMP,STIFF,SPEED
C
C     DETERMINE POSITION X AT TIME T.
      X = X1 + SPEED*(T - T1)
C
C     OBTAIN ELASTIC STRAINS AND STRESSES AT ALL DEPTHS--
      CALL INTERP(T,X)
C
C     PLASTIC STRESS --
      DO 200 I = 1,NS
  200 DERIV(I) = ALPHA(4)*EDOT(I)*( SE(I) - EMODZ(I)*E(I) )
C
      RETURN
      END
```

```
      SUBROUTINE INTERP(T,X)
C
C     ****************************************************************
C     INTERPOLATE THE ELASTIC STRESS AND STRAIN FIELD AT TIME T AND
C     DISTANCE X  FROM THE COMPACTOR, FOR ALL NZ DEPTHS.
C     ****************************************************************
C
      COMMON /INTEG/ T1,T2,X1,X2,OMEGA,AVGP(15),EMODZ(15),SE(15),
     1               E(15),EDOT(15),SP(15)
C
      COMMON /HYS/ ALPHA(5)
C
      REAL*8 HALF,FULL
      COMMON /MESH/ HALF,FULL,RANGE(40),DEPTH(15),N,KVAR,NR,NZ
C
      REAL*8 DUMMY
      COMMON /STRDAT/DUMMY(26),FR(15,40),FI(15,40),FST(15,40)
C
      ABSX = ABS(X)
      WT = OMEGA*T
      COSWT = COS(WT)
      SINWT = SIN(WT)
      IF(ABSX .GT. RANGE(1)) GO TO 20
C
      DO 10 I = 1,NZ
      E(I) = FR(I,1)*COSWT - FI(I,1)*SINWT + FST(I,1)
      EDOT(I) = -OMEGA*( FR(I,1)*SINWT + FI(I,1)*COSWT)
 10   CONTINUE
      GO TO 100
C
 20   CONTINUE
      IF(ABSX .LT. RANGE(NR)) GO TO 40
      DO 30 I = 1,NZ
      E(I) = FR(I,NR)*COSWT - FI(I,NR)*SINWT + FST(I,NR)
      EDOT(I) = -OMEGA*( FR(I,NR)*SINWT + FI(I,NR)*COSWT)
 30   CONTINUE
      GO TO 100
C
 40   CONTINUE
      DO 50 J2 = 2,NR
 50   IF(ABSX .LT. RANGE(J2)) GO TO 60
 60   CONTINUE
      J1 = J2 - 1
      DXDR = (ABSX - RANGE(J1)) /(RANGE(J2) - RANGE(J1))
      DO 70 I = 1,NZ
      ER = FR(I,J1) + (FR(I,J2) - FR(I,J1))*DXDR
```

```
      EI = FI(I,J1) + (FI(I,J2) - FI(I,J1))*DXDR
      ES = FST(I,J1) + (FST(I,J2) - FST(I,J1))*DXDR
      E(I) = ER*COSWT - EI*SINWT + ES
      EDOT(I) = -OMEGA*(ER*SINWT + EI*COSWT)
 70   CONTINUE
C
 100  CONTINUE
C
C     CLIP THE ELASTIC STRESS TO PREVENT UNREALISTIC TENSION EFFECTS
      DO 150 I = 1,NZ
      SE(I) = EMODZ(I)*E(I)*EXP(ALPHA(3)*EDOT(I))
      SE(I) = AMAX1(SE(I),0.)
 150  CONTINUE
C
      RETURN
      END
```

```
      SUBROUTINE SINFL(X,Z,B,PR,SX,SY,SZ)
C
C     ***************************************************************
C     COMPUTE STATIC INFLUENCE COEFFICIENTS FOR INFINITE STRIP
C     LOADING.
C        X,Z          COORDINATES OF A POINT RELATIVE TO THE
C                     CENTER OF THE STRIP (X .GT. 0)
C        B            STRIP HALF-WIDTH
C        PR           POISSONS RATIO
C        SX,SY,SZ     STRESSES AT (X,Z), NORMALIZED BY CONTACT PRESSURE
C      ***************************************************************
C
      DATA PI /3.14159/
C
      ABSX = ABS(X)
      D = PI/2.
      IF(ABSX .LT. B) D = -D
      IF(Z .NE. 0.) D = ATAN( (ABSX-B)/Z)
      E = PI/2.
      IF(Z .NE. 0.) E = ATAN( (ABSX+B)/Z)
      A = E - D
      TERM = SIN(A)*COS(A+2.*D)
      SX = (A - TERM)/PI
      SZ = (A + TERM)/PI
      SY = PR*(SX + SZ)
      RETURN
      END
```

```
      SUBROUTINE RKO
C
C     ******************************************************************
C     RKO INITIALIZES A RUNGE-KUTTA INTEGRATION SCHEME
C     ******************************************************************
C
      COMMON /ZRK/ ARK(6), BRK(6,6), CRK(6), DRK(6), DTSUM, NSTEP
C
      DTSUM = 0.
      NSTEP = 0
C
      ARK(1) = 0.
      ARK(2) = 1./4.
      ARK(3) = 3./8.
      ARK(4) = 12./13.
      ARK(5) = 1.
      ARK(6) = 1./2.
C
      BRK(1,1) = 0.
      BRK(2,1) = 1./4.
      BRK(3,1) = 3./32.
      BRK(3,2) = 9./32.
      BRK(4,1) = 1932./2197.
      BRK(4,2) = -7200./2197.
      BRK(4,3) = 7296./2197.
      BRK(5,1) = 439./216.
      BRK(5,2) = -8.
      BRK(5,3) = 3680./513.
      BRK(5,4) = -845./4104.
      BRK(6,1) = -8./27.
      BRK(6,2) = 2.
      BRK(6,3) = -3544./2565.
      BRK(6,4) = 1859./4104.
      BRK(6,5) = -11./40.
C
      CRK(1) = 25./216.
      CRK(2) = 0.
      CRK(3) = 1408./2565.
      CRK(4) = 2197./4104.
      CRK(5) = -1./5.
      CRK(6) = 0.
C
      DRK(1) = 1./360.
      DRK(2) = 0.
      DRK(3) = -128./4275.
      DRK(4) = -2197./75240.
```

```
      DRK(5) = 1./50.
      DRK(6) = 2./55.
C
      RETURN
      END
```

```
      SUBROUTINE RK1(T0,TF,DTOMIN,X0,XF,N,WORK,EPS,IFLAG)
C
C     ***************************************************************
C     RK1 PERFORMS A RUNGE-KUTTA INTEGRATION ON AN INTERVAL FROM
C     (T0,TF) OF THE (VECTOR) DIFFERENTIAL EQUATION:
C         dX/dt = F(X,t)
C     THE METHOD IS 4-TH ORDER, WITH A 6-TH ORDER CHECK TO DETERMINE
C     THE RELATIVE ERROR AND ADJUST THE STEP SIZE ACCORDINGLY.
C     SUBROUTINE RK0 MUST BE CALLED PRIOR TO ANY STEPS, FOR
C     INITIALIZATION OF CONSTANTS.
C     ARGUMENTS:
C
C         T0                  VALUE OF THE INDEPENDENT VARIABLE (t)
C                             AT THE BEGINNING OF THE INTERVAL
C         TF                  VALUE OF THE INDEPENDENT VARIABLE (t)
C                             AT THE END OF THE INTERVAL.
C         DTOMIN              MINIMUM ACCEPTABLE STEP SIZE IN INDEPENDENT
C                             VARIABLE t.
C         X0                  VALUE(S) OF THE DEPENDENT VARIABLE(S)
C                             (VECTOR X) AT t = T0.  N-VECTOR.
C         XF                  VALUE(S) OF THE DEPENDENT VARIABLE(S)
C                             AT t = TF.  RETURNED BY THIS ROUTINE.
C                             N VECTOR.
C         N                   VECTOR DIMENSION
C         WORK                WORK-SPACE VECTOR.  THE VECTOR LENGTH MUST
C                             BE AT LEAST 9*N
C         EPS                 RELATIVE ERROR CRITERION.
C         IFLAG               INITIALIZED TO 0, BUT SET TO 1 IF ERROR
C                             CRITERION IS NOT MET.
C
C     NOTE THAT THE FOLLOWING SUBROUTINE MUST BE SUPPLIED:
C         SUBROUTINE SYSDE (T,X,XDOT,N)
C     SYSDE PROVIDES THE SYSTEM DIFFERENTIAL EQUATIONS.  FOR
C     INPUTS:
C         T                   INDEPENDENT VARIABLE
C         X                   DEPENDENT VARIABLE [VECTOR]
C         N                   VECTOR LENGTH
C     SYSDE MUST RETURN:
C         XDOT                VECTOR DERIVATIVE dX/dT.
C     ***************************************************************
C
      DIMENSION X0(N), XF(N), WORK(N,9)
C
      COMMON / ZRK/ ARK(6), BRK(6,6), CRK(6), DRK(6), DTSUM,NSTEP,NDUM
C
      LOGICAL DONE
```

```
      LOGICAL STEP
      DATA NDBUG / 2 /
C
C     INITIALIZE STEP QUANTITIES--FIRST TRY FULL STEP (TF - T0)
      IFLAG = 0
      DONE = .FALSE.
      DTSUM = 0.
      NSTEP = 0
      T1 = T0
      DT0 = TF - T0
      DT1 = DT0
      DO 10 I = 1,N
 10   WORK(I,7) = X0(I)
C
C     OUTERMOST LOOP ON FULL STEPS
 100  CONTINUE
C
C     FORM AND SAVE DERIVATIVES AT INITIAL POINT
      CALL SYSDE (T1, WORK(1,7),WORK(1,1),N)
C
C     IF LAST STEP WAS UNSUCCESSFUL, RETURN HERE--NO NEED TO
C     RECOMPUTE INITIAL DERIVATIVES
 200  CONTINUE
C
C     1.  EVALUATE DERIVATIVES AT 5 OTHER POINTS
      DO 300 K = 2,6
      KM1 = K-1
      TK = T1 + ARK(K)*DT1
C
      DO 250 I = 1,N
      WORK(I,8) = WORK(I,1)*BRK(K,1)
      IF(K .EQ. 2) GO TO 250
C
      DO 220 J = 2,KM1
 220  WORK(I,8) = WORK(I,8) + WORK(I,J)*BRK(K,J)
 250  WORK(I,8) = WORK(I,8)*DT1 + WORK(I,7)
C
      CALL SYSDE(TK,WORK(1,8),WORK(1,K),N)
C
 300  CONTINUE
C
C     2.  FORM ESTIMATE AT STEP ENDPOINT
      DO 320 I =1,N
 320  XF(I) = WORK(I,7) + DT1*(  CRK(1)*WORK(I,1)
     1                         + CRK(3)*WORK(I,3)
     2                         + CRK(4)*WORK(I,4)
```

```
     3                        + CRK(5)*WORK(I,5) )
C
      IF (DONE) GO TO 800
C
C     3.  ESTIMATE ERROR BY TAKING DIFFERENCE WITH 6-TH ORDER FORM
      DO 360 I = 1,N
      WORK(I,9) = WORK(I,1) / 360.
      DO 340 J = 3,6
 340  WORK(I,9) = WORK(I,9) + WORK(I,J)*DRK(J)
 360  CONTINUE
C
C     4.  COMPUTE OPTIMUM STEP SIZE
C     IF ALL COMPONENTS OF COL 9 ARE ZERO, SET STEP TO MAX SIZE.
      DTMIN = 0.1*DT1
      DTMAX = 5.0*DT1
C
      DO 370 I = 1,N
 370  IF(WORK(I,9) .NE. 0.) GO TO 375
      GAMMA = 6.25
      GO TO 400
C
 375  CONTINUE
       I1 = I
       GMIN = XF(I1)/WORK(I1,9)
       IF(GMIN .EQ. 0.) GMIN = EPS/WORK(I1,9)
       GMIN = ABS(GMIN)
       GMIN = (EPS*GMIN/DT0)**0.25
       IF( I1 .EQ. N) GO TO 390
       I2 = I1 + 1
       DO 380 I = I2,N
       IF(WORK(I,9) .EQ. 0.) GO TO 380
       G = XF(I)/WORK(I,9)
       IF(G .EQ. 0.) GO TO 380
       G = ABS(G)
       G = (EPS*G/DT0)**0.25
       GMIN = AMIN1 (GMIN,G)
 380   CONTINUE
C
 390   CONTINUE
       GAMMA = GMIN
C
C      DETERMINE WHETHER STEP WAS ACCEPTABLE
 400   CONTINUE
       STEP = GAMMA .GE. 1.
       DT2  = 0.8*GAMMA*DT1
       DT2 = AMAX1(DT2,DTMIN)
```

```
      DT2 = AMIN1(DT2,DTMAX)
      IF(DT2  GE. DTOMIN) GO TO 500
C
      PRINT 4000
 4000 FORMAT(' WARNING--ERROR CRITERION VIOLATED. REDUCE STEP SIZE.')
      DT2 = DTOMIN
      IFLAG = 1
      IF(DT1 .LE. DTOMIN) STEP = .TRUE.
C
 500  CONTINUE
      T2 = T1 + DT1
      DT1 = DT2
      IF(.NOT. STEP) GO TO 200
      IF(T2 .GE. TF) GO TO 600
      T1 = T2
      DO 510 I = 1,N
 510  WORK(I,7) = XF(I)
      NSTEP = NSTEP + 1
      DTSUM = DTSUM + DT1
      GO TO 100
C
C     ONE LAST STEP
 600  CONTINUE
      DONE = .TRUE.
      DT1 = TF - T1
      IF(DT1 .GT. 0.) GO TO 200
C
 800  CONTINUE
      DTSUM = DTSUM + DT1
      NSTEP = NSTEP + 1
      DTAVG = DTSUM / FLOAT(NSTEP)
      RETURN
      END
```

```
      SUBROUTINE INFLO(HALF)
C
C     ***************************************************************
C     SET INFLUENCE-FACTOR PARAMETERS
C     ***************************************************************
C
      IMPLICIT REAL*8 (A-H), REAL*8 (O-Z)
C
      COMMON /INFL/ AO,AN,AN2,B,CS,ZO
C
      COMMON /SOIL/ EMOD,GMOD,PR,DNSITY,VOIDR,CSFT,PRESSC
C
      COMMON /UNIT/ NPRT,NDBUG,NPLOT,NSTRS,NIN,NOUT,NDBASE
C
      COMMON /TRIGD/ PI,TWOPI,DTR
C
      PI = 4.DO*DATAN(1.DO)
      TWOPI = 2.DO*PI
      DTR = TWOPI/360.DO
C
C     SHEAR WAVE VELOCITY
      CS = CSFT*12.DO
  100 CONTINUE
C
C     ELEMENT WIDTH
      B = HALF
C
      AN2 = 0.5*(1.DO -2.DO*PR) / (1.DO - PR)
      AN = DSQRT(AN2)
C
      CALL POLE(ZO)
C
      RETURN
      END
```

```
      SUBROUTINE INFLNC(FHZ,X,Y,KVAR,G,H,APPROX,COMPR,COMPI)
C
C     **********************************************************************
C     INTEGRATION TO OBTAIN THE RESPONSE OF A UNIFORMLY-LOADED
C     INFINITE STRIP ON A HALF-SPACE.
C           FHZ IS THE EXCITATION FREQUENCY, IN HZ.
C           X GIVES THE DISTANCE IN THE X DIRECTION FROM THE
C        CENTER OF THE STRIP TO THE POINT WHOSE DISPLACEMENT
C        IS SOUGHT;  Y IS THE DEPTH.
C           KVAR = 1  FOR SURFACE DISPLACEMENT
C                = 2  FOR SUBSURFACE STRAIN
C                = 3  FOR SUBSURFACE STRESS
C           G,H,APPROX ARE THE APPROPRIATE SUBROUTINES FOR THE
C        FUNCTIONS BEING INTEGRATED.
C           COMPR AND COMPI ARE THE REAL AND IMAGINARY PARTS
C        OF THE COMPLIANCE (SCALED DISPLACEMENT).
C     **********************************************************************
C
      IMPLICIT REAL*8 (A-H), REAL*8 (O-Z)
      EXTERNAL G,H,APPROX
      LOGICAL LINFLG,STPFLG,DONE3
      DIMENSION ZINT(4),ZA(5),HA(5)
C
      COMMON /INFL/ A0,AN,AN2,B,CS,Z0
C
      COMMON /POINT/ XB,YB,ZB
C
      COMMON /TRIGD/ PI,TWOPI,DTR
C
      COMMON /UNIT/ NPRT,NDBUG,NPLOT,NSTRS,NIN,NOUT,NDBASE
C
      DATA STPMAX /5.D-3/
C
C     INITIALIZE COMMON--
      XB = X/B
      YB = Y/B
      ZB = 0.D0
      A0 = (TWOPI*FHZ)*B/CS
C
C     DETERMINE SYMMETRIC INTERVAL ABOUT POLE FOR REDUCED
C     STEP SIZE.  TOWARDS THE CENTER OF THIS REGION, F(Z)
C     WILL BE LINEARIZED FOR IMPROVED ACCURACY.
C     WE USE THE TAYLOR POLYNOMIAL RESIDUAL TO ESTIMATE THE
C     ERROR ASSOCIATED WITH LINEARIZATION--
C          E = (F''(a) * (z-z0)**2)/2!
C     WHERE  a IS BETWEEN z0 and z.  WE ASSUME F''(a) = F''(z0)
```

```
C       AND INVERT THE EXPRESSION FOR THE APPROPRIATE RADIUS RLIN
C       FOR SPECIFIED ACCURACY.
        CALL DERIVS(Z0,DFDZ,D2FDZ2)
        CONSYM = 0.0001
        ARG = DABS(2.D0*CONSYM/D2FDZ2)
        RLIN = DSQRT( ARG )
        SYM = Z0 - 1.D0
        ZSYM1 = 1.D0
        ZSYM2 = Z0 + SYM
C
C       INTEGRATION:
C       WRITE(NDBUG,1400) A0,XB,YB
 1400   FORMAT(//,' A0 = ',D20.10,/,' XB = ',D20.10,' YB = ',D20.10)
C
C       FIRST INTERVAL: (0.,1.).
        ZINT(1) = 0.99*AN
        ZINT(2) = 0.02*AN
        ZINT(3) = 1.D0 - (ZINT(1) + ZINT(2) + 0.01)
        ZINT(4) = 0.01
        NSTEP1 = 50
        NSTEP2 = 100
        Z = 0.D0
        DCR1 = 0.D0
        DCI1 = 0.D0
C
C       INITIALIZE INTEGRAND FOR APPROPRIATE FUNCTION
        LVAR = KVAR - 2
        IF(LVAR) 10,20,30
C
C       DISPLACEMENT
 10     CONTINUE
        DR = 0.D0
        DI = AN*A0
        GO TO 50
C
C       STRAIN
 20     CONTINUE
        FACT = A0*AN2
        ARG = A0*AN*YB
        DR = FACT*DCOS(ARG)
        DI = -FACT*DSIN(ARG)
        GO TO 50
C
C       STRESS
 30     CONTINUE
        FACT = A0
```

```
      ARG = A0*AN*YB
      DR = DCOS(ARG)*FACT
      DI = -DSIN(ARG)*FACT
 50   CONTINUE
C
      DO 200 INT = 1,4
      IF(ZINT(INT) .EQ. 0.) GO TO 200
      ISIMPZ = 2
      NSTEP = NSTEP1
      IF( ((INT/2)*2) .EQ. INT) NSTEP = NSTEP2
      DZ = ZINT(INT)/DFLOAT(NSTEP)
      SUMR = DR
      SUMI = DI
C
      DO 100 ISTEP = 1,NSTEP
      ISIMPZ = 6 - ISIMPZ
      IF(ISTEP .EQ. NSTEP) ISIMPZ = 1
      Z = Z + DZ
      CALL F(Z,FR,FI)
      CALL G (Z,GR,GI)
      CALL CDIV(GR,GI,FR,FI,DR,DI)
      SUMR = SUMR + DR*DFLOAT(ISIMPZ)
      SUMI = SUMI + DI*DFLOAT(ISIMPZ)
 100  CONTINUE
      DCR1 = DCR1 + SUMR*DZ/3.D0
      DCI1 = DCI1 + SUMI*DZ/3.D0
      NS = NS + NSTEP
 200  CONTINUE
C
C
C     SECOND INTERVAL.  INTEGRATE "AROUND" POLE.
C     ACTUALLY, WE TRANSLATE THE ORIGIN OF THE Z AXIS TO Z0,
C     THEN WE EXPRESS THE INTEGRAND AS THE SUM OF EVEN AND
C     ODD COMPONENTS.  THE INTEGRAL OF THE ODD COMPONENT ON A
C     SYMMETRIC INTERVAL VANISHES.  THE INTEGRAL OF THE EVEN
C     COMPONENT IS TWICE THE VALUE OF THE INTEGRAL OF EITHER
C     SIDE.  THEREFORE THE PROBLEM OF DETERMINING THE CAUCHY
C     PRINCIPLE VALUE OF AN INTEGRAL IS REDUCED TO THE EVALUATION
C     OF THE INTEGRAL OF A FUNCTION THAT IS UNBOUNDED AT ONE LIMIT.
C     WE WILL INTEGRATE TOWARDS THE POLE, DECREASING OUR STEP SIZE
C     BY HALF AS WE APPROACH IT.  THUS, WHILE [G(Z)/F(Z)] INCREASES,
C     dZ DECREASES.  WE HOPE THAT THE PRODUCT OF THE TWO IS
C     DIMINISHING.  MOREOVER, NOTE THAT WE LINEARIZE F(Z) FOR
C     IMPROVED ACCURACY IN ITS EVALUATION CLOSE TO THE POLE.
C          THE EVEN-ODD SEPARATION IS GIVEN BY WRITING, FOR THE
C     INTEGRAND H(Z),
```

```
C           H(Z) = [ H(Z0+U) + H(Z0-U) ] / 2
C                + [ H(Z0+U) - H(Z0-U) ] / 2
C      WHERE THE FIRST TERM IS SYMMETRIC AROUND Z0 AND THE SECOND IS
C      ANTI-SYMMETRIC ABOUT Z0.  HERE,
C          U = Z - Z0 = DISTANCE FROM POLE
C      IN THE FOLLOWING,
C          Z1L,Z2L,Z3L     ARE INTERPOLATION POINTS TO LEFT OF POLE
C                          (FOR SIMPSON'S 1-4-1 RULE)
C          Z1R,Z2R,Z3R     ARE THEIR REFLECTIONS ABOUT Z0
C          G1,G2,G3        ARE THE INTEGRANDS:
C                          G1 = G(Z1L)/F(Z1L) + G(Z1R)/F(G1R) ETC.
       NSTEP = 0
       Z3L = ZSYM1
       U3 = Z3L - Z0
       Z3R = Z0 - U3
       FL = 1.D0
       CALL F(Z3R,FR,FI)
       CALL G (Z3L,GL,GI)
       CALL G (Z3R,GR,GI)
       G3 = GL/FL + GR/FR
       DCR2 = 0.D0
       DCI2 = 0.D0
       LINFLG = .FALSE.
C
 400   CONTINUE
       NSTEP = NSTEP + 1
       Z1L = Z3L
       Z1R = Z3R
       U1 = U3
       G1 = G3
       Z3L = (Z0 + Z1L)/2.D0
       Z3L = DMIN1(Z3L,Z1L + STPMAX)
       Z2L = (Z3L + Z1L)/2.D0
       U3 = Z3L -Z0
       U2 = Z2L - Z0
       Z3R = Z0 - U3
       Z2R = Z0 - U2
       STEP = Z3L - Z1L
       IF((-U2) .LE. RLIN) LINFLG = .TRUE.
       IF(LINFLG) GO TO 405
       CALL F(Z2L,FL,FI)
       CALL F(Z2R,FR,FI)
       GO TO 410
 405   FL = DFDZ*U2
       FR = -FL
 410   CONTINUE
```

```
      CALL G(Z2L,GL,GI)
      CALL G(Z2R,GR,GI)
      G2 = GL/FL + GR/FR
      IF(LINFLG) GO TO 415
      CALL F(Z3L,FL,FI)
      CALL F(Z3R,FR,FI)
      GO TO 420
 415  CONTINUE
      FL = DFDZ*U3
      FR = - FL
 420  CONTINUE
      CALL G(Z3L,GL,GI)
      CALL G(Z3R,GR,GI)
      G3 = GL/FL + GR/FR
      SUM = (G1 + 4.D0*G2 + G3) * STEP / 6.D0
      IF(NSTEP .NE. 1) GO TO 430
      DCR2 = SUM
      GO TO 400
C
 430  CONTINUE
      DDCR = DABS(SUM/DCR2)
      DCR2 = DCR2 + SUM
      IF(DDCR .GT. 1.D-4) GO TO 400
      NS = NS + NSTEP
C
C     THIRD INTERVAL (Z0 + SYM, Z1)
C     SELECT Z1 DEPENDING ON HOW WE INTEGRATE THE FOURTH INTERVAL
C     FROM Z1 TO INFINITY.
      DCR3 = 0.D0
      DCI3 = 0.D0
      DCR4 = 0.D0
      DCI4 = 0.D0
      NINTEG = 2
      IF(KVAR .EQ. 1) NINTEG = 1
      IF(XB .EQ. 1.D0) NINTEG = 1
C
      DO 600 INT = 1,NINTEG
      Z1 = 10.D0
      TSIGN = 1.D0
      IF(KVAR .EQ. 1) GO TO 510
C
      W0 = A0*(1.D0 + XB)
      IF(INT .EQ. 2) W0 = A0*(1.D0 - XB)
      IF(W0 .LT. 0.) TSIGN = -1.D0
      W0 = DABS(W0)
      P = PI/W0
```

```
      Z1 = 0.D0
      Z2 = ZSYM2
 505  CONTINUE
      Z1 = Z1 + P
      IF(Z1 .LT. Z2) GO TO 505
C     WRITE(NDBUG,5000) W0,P,Z1
 5000 FORMAT(' W0,P,Z1',3D20.7)
C
C     USE FAIRLY SMALL STEPS NEAR THE POLE BUT ADAPT WITH DISTANCE.
C     (ADAPTIVE INTEGRATION SCHEME FROM JOHNSON AND RIESS,
C     "NUMERICAL ANALYSIS", CH. 5.)
 510  CONTINUE
      NSTEP = 0
      ZA(5) = ZSYM2
      STEP = STPMAX
      STPMIN = STPMAX
      STPFLG = .TRUE.
      DONE3 = .FALSE.
      CALL F(ZA(5),FR,FI)
      CALL H(ZA(5),W0,GR,GI)
      HA(5) = GR/FR
C
C     LAST STEP WAS SUCCESSFUL
 516  CONTINUE
      ZA(1) = ZA(5)
      HA(1) = HA(5)
      GO TO 518
C
C     LAST STEP WAS TOO LARGE.
 517  CONTINUE
      ZA(5) = ZA(3)
      HA(5) = HA(3)
      ZA(3) = ZA(2)
      HA(3) = HA(2)
C
 518  CONTINUE
      NSTEP = NSTEP + 1
      NSIMP= 4
      IF(STPFLG) NSIMP= 5
      DO 519 I = 2,NSIMP
      IF( (.NOT. STPFLG) .AND. I.EQ.3) GO TO 519
      ZA(I) = ZA(1) + DFLOAT(I-1)*0.25D0*STEP
      CALL F(ZA(I),FR,FI)
      CALL H(ZA(I),W0,GR,GI)
      HA(I) = GR/FR
 519  CONTINUE
```

```
C
      S1 = HA(1) + 4.D0*HA(3) + HA(5)
      S2 = HA(1) + HA(5) + 4.D0*(HA(2) + HA(4)) + 2.D0*HA(3)
      S1 = S1*STEP/6.D0
      S2 = S2*STEP/12.D0
      IF(S2 .EQ. 0.D0) GO TO 600
      IF(DONE3) GO TO 535
      ERRTOL = DABS(1.D-3 * S2)
      ERR = DABS( (S2 - S1) /  15.D0)
      STPFLG = .FALSE.
      IF(ERR .LE. ERRTOL) STPFLG = .TRUE.
      IF(STEP .LT. 1.001D0*STPMIN) STPFLG = .TRUE.
C     IF(KVAR .NE. 1) WRITE(NDBUG,1234) STPFLG,ZA(5),HA(5),STPMIN
 1234 FORMAT(' STPFLG,ZA(5),HA(5),STPMIN',L2,1X,4D15.5)
      IF(STPFLG) GO TO 520
      STEP = 0.5D0*STEP
      STEP = DMAX1(STEP,STPMIN)
      GO TO 517
C
 520  CONTINUE
      IF(ZA(5) .GE. Z1) GO TO 530
      IF(ERR .LT. 0.5D0*ERRTOL) STEP = 2.D0*STEP
      STEP = DMAX1(STEP,STPMIN)
      DCR3 = DCR3 + TSIGN*S2
      GO TO 516
 530  CONTINUE
      STEP = Z1 - ZA(1)
      STPFLG = .TRUE.
      DONE3 = .TRUE.
      NSTEP = NSTEP - 1
      GO TO 518
 535  DCR3 = DCR3 + TSIGN*S2
C
      NS = NS + NSTEP
C
C     FOURTH INTERVAL:  (Z1,INFINITY)
C     APPROXIMATE EXPRESSIONS USING QUADRATIC APPROX TO F(Z)
      CALL APPROX(Z1,H,W0,DDCR4)
      DCR4 = DCR4 + TSIGN*DDCR4
C
 600  CONTINUE
C
C     END OF INTEGRATION OVER Z.
C     SUBTRACT RESIDUE TERM.
      CALL G(Z0,GR,GI)
      DRESI = PI*GR/DFDZ
```

```
C       WRITE(NDBUG,5780) DCR1,DCR2,DCR3,DCR4,
C     1            DCI1,DCI2,DCI3,DCI4,DRESI
C5780   FORMAT(' DCR 1,2,3,4    ',1X,4D11.4,
C     1 /,      ' DCI 1,2,3,4,RES',1X,5D11.4)
C
        COMPR = DCR1 + DCR2 + DCR3 + DCR4
        COMPI = DCI1 + DCI2 + DCI3 + DCI4 - DRESI
C
        FACT = PI*A0
        IF(KVAR .NE. 1) FACT = PI
        COMPR = COMPR/FACT
        COMPI = COMPI/FACT
C       WRITE(NDBUG,6000) A0,COMPR,COMPI
C6000   FORMAT(' FOR A0 = ',G15.7,1X,'Re C, Im C =' ,
C     1 2G15.7)
C
C
        RETURN
C
        END
```

```
      SUBROUTINE POLE(Z0)
C
C     **********************************************************************
C     LOCATE ZERO OF RAYLEIGH FUNCTION F(Z) BY INTERVAL BISECTION.
C     **********************************************************************
C
      IMPLICIT REAL*8 (A-H),REAL*8(O-Z)
      DATA TOL /1.D-8/
C
      A = 1.D0 + TOL
      B = 2.D0 - TOL
      CALL F (A,FA,FI)
C
 10   Z0 = (A+B)/2.D0
      CALL F (Z0,FM,FI)
      IF(FA*FM .LT. 0.D0) GO TO 20
C
      A = Z0
      FA = FM
      GO TO 30
C
 20   B = Z0
C
 30   CONTINUE
      IF( (B-A) .LE. TOL) GO TO 40
      GO TO 10
C
 40   Z0 = (A+B)/2.D0
      RETURN
      END
```

```
      SUBROUTINE F (Z,FR,FI)
C
C     ***************************************************************
C     COMPUTE THE RAYLEIGH FUNCTION FOR AN ELASTIC HALF-SPACE
C     ***************************************************************
C
      IMPLICIT REAL*8 (A-H), REAL*8 (O-Z)
C
      COMMON /INFL/ AO,AN,AN2,B,CS,ZO
C
      COMMON /TRIGD/ PI,TWOPI,DTR
C
      COMMON /UNIT/ NPRT,NDBUG,NPLOT,NSTRS,NIN,NOUT,NDBASE
C
      FI = 0.DO
      Z2 = Z*Z
      IF(Z .GT. 1.D2) GO TO 100
C
      FR = (2.DO*Z2 - 1.DO)
      FR = FR*FR
      TERM = (Z2 - AN2)*(Z2 - 1.DO)
      IF(TERM) 10,20,20
C
 10   FI = - 4.DO*Z2*DSQRT(-TERM)
      RETURN
C
 20   PART = 4.DO*Z2*DSQRT(TERM)
      IF(Z .LT. AN) PART = -PART
      FR = FR - PART
      RETURN
C
 100  CONTINUE
      FR = 1.DO -2.DO*(1.DO-AN2)*Z2
      RETURN
C
      END
```

```
      SUBROUTINE DERIVS(Z,FP,FPP)
C
C     **********************************************************************
C     COMPUTE FIRST AND SECOND DERIVATIVES OF THE RAYLEIGH FUNCTION
C     F(Z).
C     **********************************************************************
C
      IMPLICIT REAL*8 (A-H), REAL*8 (O-Z)
C
      COMMON /INFL/ A0,AN,AN2,B,CS,Z0
C
      Z2 = Z*Z
      R1 = DSQRT( DABS(Z2 - AN2) )
      R2 = DSQRT( DABS(Z2 - 1.D0) )
      FP = 4.D0*Z*(  2.D0*(2.D0*Z2 - 1.D0)
     1                - (4.D0*Z2*Z2 - 3.D0*(1.D0+AN2)*Z2 + 2.D0*AN2)
     2                    /   (R1*R2)                                  )
      Z4 = Z2*Z2
      AN21 = AN2 + 1.D0
      DENOM1 = R1*R2
      DENOM2 = DENOM1*DENOM1*DENOM1
      FPP = 4.D0*( 12.D0*Z2-2.D0 - (20.D0*Z4-9.D0*AN21*Z2+2.D0*AN2)
     1 /DENOM1 + (4.D0*Z4-3.D0*AN21*Z2 + 2.D0*AN2)*(2.D0*Z4-AN21*Z2)
     2 /DENOM2 )
      RETURN
      END
```

```
      SUBROUTINE CDIV(A,B,C,D,E,F)
C
C     ***********************************************************
C     COMPLEX DIVISION:
C         (A + jB)/(C + jD) = E + jF
C     ***********************************************************
C
      REAL*8 A,B,C,D,E,F,DENOM
C
      DENOM = C*C + D*D
      E = (A*C + B*D)/DENOM
      F = (B*C - A*D)/DENOM
C
      RETURN
      END
```

```
      SUBROUTINE G1(Z,GR,GI)
C
C     ***************************************************************
C     EVALUATE THE REST OF THE INTEGRAND MULTIPLYING 1./F(Z)
C     FOR SURFACE DISPLACEMENTS.
C     ***************************************************************
C
      IMPLICIT REAL*8 (A-H), REAL*8 (O-Z)
C
      COMMON /INFL/ A0,AN,AN2,B,CS,Z0
C
      COMMON /POINT/ XB,YB,ZB
C
      GR = 0.D0
      GI = 0.D0
      ARG1 = A0*Z
      ARG2 = ARG1*XB
      T1 = DSIN(ARG1)*DCOS(ARG2)
C
      Z2 = Z*Z
      T2 = DSQRT( DABS(Z2-AN2) ) /Z
      IF(Z .LT. AN) GI = T1*T2
      IF(Z .GT. AN) GR = T1*T2
C
      RETURN
      END
```

```
      SUBROUTINE H1(Z,W0,GR,GI)
C
C     **********************************************************************
C     DUMMY ROUTINE TO PASS CALL TO G1 FOR DISPLACEMENTS
C     **********************************************************************
C
      IMPLICIT REAL*8(A-H),REAL*8(O-Z)
C
      CALL G1(Z,GR,GI)
      RETURN
      END
```

```
      SUBROUTINE APPRX1(Z1,H,W0,DCR4)
C
C     ***************************************************************
C     APPROXIMATE EXPRESSION FOR INTEGRAL FROM Z1 TO INFINITY
C     USING QUADRATIC F(Z).
C     ***************************************************************
C
      IMPLICIT REAL*8(A-H), REAL*8(O-Z)
      EXTERNAL H
C
      COMMON /INFL/ A0,AN,AN2,B,CS,Z0
C
      COMMON /POINT/ XB,YB,ZB
C
      COMMON /TRIGD/ PI,TWOPI,DTR
C
      DCI4 = 0.D0
      DENOM = -4.D0*(1.D0 - AN2)
      W1 = A0*(1.D0 + XB)
      W2 = A0*(1.D0 - XB)
      ARG1 = W1*Z1
      ARG2 = W2*Z1
      DCR4 = (DSIN(ARG1) + DSIN(ARG2))/Z1
      IF(W1 .EQ. 0.D0) GO TO 100
      ARG1 = DABS(ARG1)
      DCR4 = DCR4 - W1*CI(ARG1)
  100 CONTINUE
      IF(W2 .EQ. 0.D0) GO TO 200
      ARG2 = DABS(ARG2)
      DCR4 = DCR4 - W2*CI(ARG2)
  200 CONTINUE
      DCR4 = DCR4/DENOM
C
      RETURN
      END
```

```
      REAL FUNCTION SI*8(X)
C
C     ******************************************************************
C     SINE INTEGRAL
C
C            X
C           $       SIN(T)/T DT
C          0
C
C     ******************************************************************
C
      IMPLICIT REAL*8(A-H), REAL*8(O-Z)
C
      DATA TOL /1.D-6/
      DATA PI/3.14159265359/
C
      SI = 0.D0
      IF ( X .EQ. 0.D0) RETURN
      IF(DABS(X) .GT. 15.D0) GO TO 100
C
      SUM = X
      TERM = X
      N = 1
C
 10   CONTINUE
      N = N + 2
      TERM1 = -DFLOAT(N-2)/DFLOAT(N-1)
      TERM2 = X/DFLOAT(N)
      TERM = TERM1*TERM2*TERM2*TERM
      EPS = DABS(TERM/SUM)
      SUM = SUM + TERM
      IF(EPS .GT. TOL) GO TO 10
      SI = SUM
C
      RETURN
C
C     ASYMPTOTIC EXPANSION FOR LARGE X
 100  CONTINUE
      SUMF = 1.D0
      TERM = 1.D0
      Z = DABS(X)
      Z2 = Z*Z
      N = 0
      ANTERM = (DSQRT(1.D0 + 4.D0*Z2) - 3.D0)/4.D0
      NTERM = ANTERM - 1.D0
      DO 150 I = 1,NTERM
```

```
      N = N + 2
      TERM1 = N*(N-1)
      TERM = -TERM1*TERM/Z2
      SUMF = SUMF + TERM
  150 CONTINUE
      SUMF = SUMF/Z
      SUMG = 1.D0
      TERM = 1.D0
      N = 0
      NTERM = ANTERM - 2.75
      DO 200 I = 1,NTERM
      N = N + 2
      TERM1 = N*(N+1)
      TERM = -TERM1*TERM/Z2
      SUMG = SUMG + TERM
  200 CONTINUE
      SUMG = SUMG/Z2
      SI = PI/2.D0 - SUMF*DCOS(Z) - SUMG*DSIN(Z)
      SI = DSIGN(SI,X)
C
      RETURN
      END
```

```
      REAL FUNCTION CI*8(X)
C
C     ******************************************************************
C     COSINE INTEGRAL:
C
C        INFINITY
C         -  $     COS(T)/T  DT
C           X
C
C     ******************************************************************
C
      IMPLICIT REAL*8(A-H), REAL*8(O-Z)
C
      DATA GAMMA/0.5772156649/, TOL/1.D-6/
C
      Z = DABS(X)
      IF(Z .GT. 15.D0) GO TO 100
C
      SUM = GAMMA + DLOG(Z)
      TERM = -Z*Z/4.D0
      SUM = SUM + TERM
      N = 2
C
 10   CONTINUE
      TERM1 = N
      TERM2 = N+1
      N = N+2
      TERM3 = N
      TERM3 = Z/TERM3
      TERM = -TERM1*TERM3*TERM3*TERM/TERM2
      EPS = DABS(TERM/SUM)
      SUM = SUM + TERM
      IF(EPS .GT. TOL) GO TO 10
C
      CI = SUM
      RETURN
C
C     ASYMPTOTIC EXPANSION FOR LARGE Z
 100  CONTINUE
      SUMF = 1.D0
      TERM = 1.D0
      Z2 = Z*Z
      N = 0
      ANTERM = (DSQRT(1.D0 + 4.D0*Z2) - 3.D0)/4.D0
      NTERM = ANTERM - 1.D0
      DO 150 I = 1,NTERM
```

```
      N = N + 2
      TERM1 = N*(N-1)
      TERM = -TERM1*TERM/Z2
      SUMF = SUMF + TERM
  150 CONTINUE
      SUMF = SUMF/Z
      SUMG = 1.D0
      TERM = 1.D0
      N = 0
      NTERM = ANTERM - 2.75
      DO 200 I = 1,NTERM
      N = N + 2
      TERM1 = N*(N+1)
      TERM = -TERM1*TERM/Z2
      SUMG = SUMG + TERM
  200 CONTINUE
      SUMG = SUMG/Z2
      CI = SUMF*DSIN(Z) - SUMG*DCOS(Z)
C
      RETURN
      END
```

```
      SUBROUTINE G2(Z,GR,GI)
C
C     ***************************************************************
C     EVALUATE THE TERMS IN THE STRAIN AND STRESS INTEGRANDS
C     MULTIPLYING 1./F(Z)
C     ***************************************************************
C
      IMPLICIT REAL*8(A-H), REAL*8(O-Z)
C
      COMMON /INFL/ A0,AN,AN2,B,CS,Z0
C
      REAL*4 DUMMY
      COMMON /MESH/ DUM1,DUM2,DUMMY(55),IDUM,KVAR,JDUM,KDUM
C
      COMMON /POINT/ XB,YB,ZB
C
      GR = 0.D0
      GI = 0.D0
      TERM0 = DSIN(A0*Z)*DCOS(XB*A0*Z) / Z
      Z2 = Z*Z
      T1 = Z2 - AN2
      T2 = DSQRT( DABS(T1) )
      T3 = 2.D0*Z2 - 1.D0
      T3A = T1
      IF(KVAR .EQ. 3) T3A = T3
      T3 = T3*T3A
      ARG = YB*A0*T2
      IF(Z .GE. AN) GO TO 20
C
      GR = T3*DCOS(ARG)
      GI = -T3*DSIN(ARG)
      GO TO 50
C
 20   CONTINUE
      GR = T3*DEXP(-ARG)
      GI = 0.D0
C
 50   CONTINUE
      T4 = DSQRT( DABS(Z2 - 1.D0) )
      T5 = 2.D0*Z2*T2*T4
      IF(KVAR .EQ. 3) T5 = 2.D0*T5
      ARG = YB*A0*T4
      IF(Z .GE. AN) GO TO 70
      GR = GR + T5*DCOS(ARG)
      GI = GI - T5*DSIN(ARG)
      GO TO 100
```

```
C
 70   CONTINUE
      IF(Z .GE. 1.D0) GO TO 90
      GR = GR - T5*DSIN(ARG)
      GI = GI - T5*DCOS(ARG)
      GO TO 100
C
 90   CONTINUE
      GR = GR - T5*DEXP(-ARG)
      GI = 0.D0
C
 100  CONTINUE
      GR = GR*TERM0
      GI = GI*TERM0
      RETURN
      END
```

```
      SUBROUTINE H2(Z,W0,GR,GI)
C
C     ***************************************************************
C     COMPUTE THE INTEGRAND TERMS MULTIPLYING 1./F(Z) FOR USE BY
C     LONGMAN'S METHOD IN COMPUTING STESS AND STRAIN.  NOTE THAT
C     WE HAVE HAD THE BREAK THE PRODUCT OF SIN AND COS INTO THE
C     SUM OF TWO SINES.
C     ***************************************************************
C
      IMPLICIT REAL*8 (A-H), REAL*8(O-Z)
C
      COMMON /INFL/ A0,AN,AN2,B,CS,Z0
C
      COMMON /POINT/ XB,YB,ZB
C
      COMMON /TRIGD/ PI,TWOPI,DTR
C
      REAL*4 DUMMY
      COMMON /MESH/ DUM1,DUM2,DUMMY(55),IDUM,KVAR,JDUM,KDUM
C
      GI = 0.D0
      TERM0 = 0.5*DSIN(W0*Z) / Z
      Z2 = Z*Z
      T1 = Z2 - AN2
      T2 = DSQRT(T1)
      T3 = DSQRT(Z2 - 1.D0)
      T4 = 2.D0*Z2 - 1.D0
      T4A = T1
      IF(KVAR .EQ. 3) T4A = T4
      T5 = T4*T4A
      T6 = T5*DEXP(-YB*A0*T2)
      T7 = -2.D0*Z2*T2*T3*DEXP(-YB*A0*T3)
      IF(KVAR .EQ. 3) T7 = 2.D0*T7
      GR = TERM0*(T6 + T7)
      RETURN
      END
```

```
      SUBROUTINE APPRX2(Z1,H,W0,DDCR4)
C
C     ***************************************************************
C     FOR INTRACTABLE INTEGRANDS (STRAIN AND STRESS) USE LONGMAN'S
C     FORWARD DIFFERENCE SCHEME TO ESTIMATE THE INTEGRAL ON THE
C     INTERVAL Z1 TO INFINITY.  TREAT THE INTEGRAL AS A SUM
C      OF INTEGRALS OVER HALF-CYCLES (BETWEEN ZEROES).  SINCE
C      THE INTEGRAND IS OSCILLATORY, THIS SUM REPRESENTS AN
C      ALTERNATING SERIES.  USE OF FORWARD DIFFERENCES PERMITS
C      EXPRESSION OF THE SUM IN ANOTHER, MORE RAPIDLY CONVERGING
C      FORM.
C      ***************************************************************
C
       IMPLICIT REAL*8(A-H),REAL*8(O-Z)
       EXTERNAL H
       DIMENSION V(20,20)
C
       COMMON /UNIT/ NPRT,NDBUG,NPLOT,NSTRS,NIN,NOUT,NDBASE
C
       COMMON /TRIGD/ PI,TWOPI,DTR
C
       Z2 = Z1
       P = PI/W0
       NSTEP = 10
       DZ = P/DFLOAT(NSTEP)
       NCY = 0
       VSIGN = -1.D0
       DENOM = -1.D0
       VSUM = 0.D0
C
C      LOOP ON HALF-CYCLES.  FOR EACH HALF-CYCLE:
C         (A)  INTEGRATE
C         (B)  ADD A NEW ROW TO THE DIFFERENCE TABLE.
C         (C)  ADD A TERM TO THE DIFFERENCE SERIES AND CHECK FOR
C              ADEQUATE CONVERGENCE.
  540  CONTINUE
       NCY = NCY + 1
       IF(NCY .GT. 20) GO TO 575
       VSIGN = -VSIGN
       DENOM = -DENOM/2.D0
       ISIMPZ = 2
       Z = Z2
       Z2 = Z2 + P
       CALL F(Z,FR,FI)
       CALL H(Z,W0,GR,GI)
       SUM = GR/FR
```

```
C
      DO 550 ISTEP = 1,NSTEP
      ISIMPZ = 6 - ISIMPZ
      IF(ISTEP .EQ. NSTEP) ISIMPZ = 1
      Z = Z + DZ
      CALL F(Z,FR,FI)
      CALL H(Z,W0,GR,GI)
      DSUM = GR/FR
      SUM = SUM + DFLOAT(ISIMPZ)*DSUM
 550  CONTINUE
      V(NCY,1) = VSIGN*SUM * DZ/3.D0
C
C     UPDATE DIFFERENCE TABLE
      NS = NS + NSTEP
      IF(NCY .NE. 1) GO TO 567
      VSUM = V(1,1)*DENOM
      GO TO 540
C
 567  CONTINUE
      DO 570 JTAB = 2,NCY
      ITAB = NCY + 1 - JTAB
      V1 = V(ITAB  ,JTAB-1)
      V2 = V(ITAB+1,JTAB-1)
      V(ITAB,JTAB) = V2 - V1
 570  CONTINUE
C
      TERM = DENOM*V(1,NCY)
      IF(VSUM .EQ. 0.D0) GO TO 575
      DSUM = DABS(TERM/VSUM)
      VSUM = VSUM + TERM
      IF(DSUM .GT. 1.E-4) GO TO 540
C
 575  CONTINUE
      DDCR4 = VSUM
C     WRITE(NDBUG,1000) NCY,Z1,Z2,VSUM
 1000 FORMAT(' NCY,Z1,Z2,VSUM',I3,3D20.7)
      RETURN
      END
```

The vita has been removed from the scanned document

COMPACTION OF SOIL BY A VIBRATORY ROLLER: A THEORETICAL DESCRIPTION

by

David Towery

(ABSTRACT)

This study models the compaction of soil by a vibratory roller compactor and examines changes to current designs that may provide more efficient compaction. The modeling of the soil differs from previous analyses of the compaction process in its use of a distributed-parameter characterization of the soil mass and in the application of nonlinear constitutive relations that predict the continuous evolution of residual stresses in the soil.

The model was used to determine whether compactor performance might be improved by changes in the forward speed of the compactor or by redistribution of the weight of the frame. No improvement was found to occur. The model was also used to estimate the effects of varying the frequency of vibration to match the evolutionary changes in soil properties during compaction. Hardly any improvement over operation at constant frequency was indicated, but this finding may reflect the tendency of the model to underestimate the rate of stiffening in the soil.